# Preparation of Stepwise Tissue Development-Mimicking ECM-Deposited PLGA-Collagen Hybrid Meshes and Their Influence on Stem Cell Functions

Yazhou CHEN

February 2020

# Preparation of Stepwise Tissue Development-Mimicking ECM-Deposited PLGA-Collagen Hybrid Meshes and Their Influence on Stem Cell Functions

Yazhou CHEN

Doctoral Program in Materials Science and Engineering

Submitted to the Graduate School of

Pure and Applied Sciences

in Partial Fulfillment of the Requirements

for the Degree of Doctor of Philosophy in

Engineering

at the

University of Tsukuba

# Content

# List of abbreviations

| | |
|---|---|
| ECM | Extracellular matrix |
| hMSCs | Human mesenchymal stem cells |
| RGD | Arg-Gly-Asp |
| 2D | Two-dimensional |
| 3D | Three-dimensional¥ |
| PLLA | Poly-L-lactic acid |
| FABP4 | Fatty acid binding protein 4 |
| FASN | Fatty acid synthase |
| CEBPA | CCAAT/enhancer binding protein |
| LPL | Lipoprotein lipase |
| ALP | Alkaline phosphatase |
| RT-PCR | Real-time polymerase chain reaction |
| GAPDH | Glyceraldehyde-3-phosphate dehydrogenase |
| IBSP | Bone sialoprotein 2 |
| SPP1 | Secreted phosphoprotein 1 |
| SP7 | Osterix |
| RUNX2 | Runt-related transcription factor-2 |
| IHC | Immunohistochemical staining |
| OM | Osteogenic medium |
| AM | Adipogenic medium |
| SEM | Scanning electron microscope |
| DMEM | Dulbecco's modified Eagle's medium |
| FBS | Fetal bovine serum |
| SC | Stem cell stage |
| EA | Early stage of adipogenesis |
| LA | Late stage of adipogenesis |
| EO | Early stage of osteogenesis |
| LO | Late stage of osteogenesis |
| GAG | Glycosaminoglycans |
| FGF | Fibroblast growth factor |
| S.D. | Standard deviation |
| HUVECs | Standard deviation |
| cDNA | Complementary DNA |

# Chapter 1

# General introduction

Resident cells are surrounded by extracellular matrix (ECM), cells continually read environment cues and respond during the tissue development.[1-3] ECM has an important role in regulating cell behaviors, including cell migration,[4] proliferation[5] and differentiation,[6-8] thus ECM possess a great potential as next generation materials for tissue engineering (Figure 1.1). Understanding the precise roles of ECM-cell interactions could facilitate its application on tissue engineering. A major obstacle in defining the exact role of ECM on stem cell functions is lack of suitable ECM models.

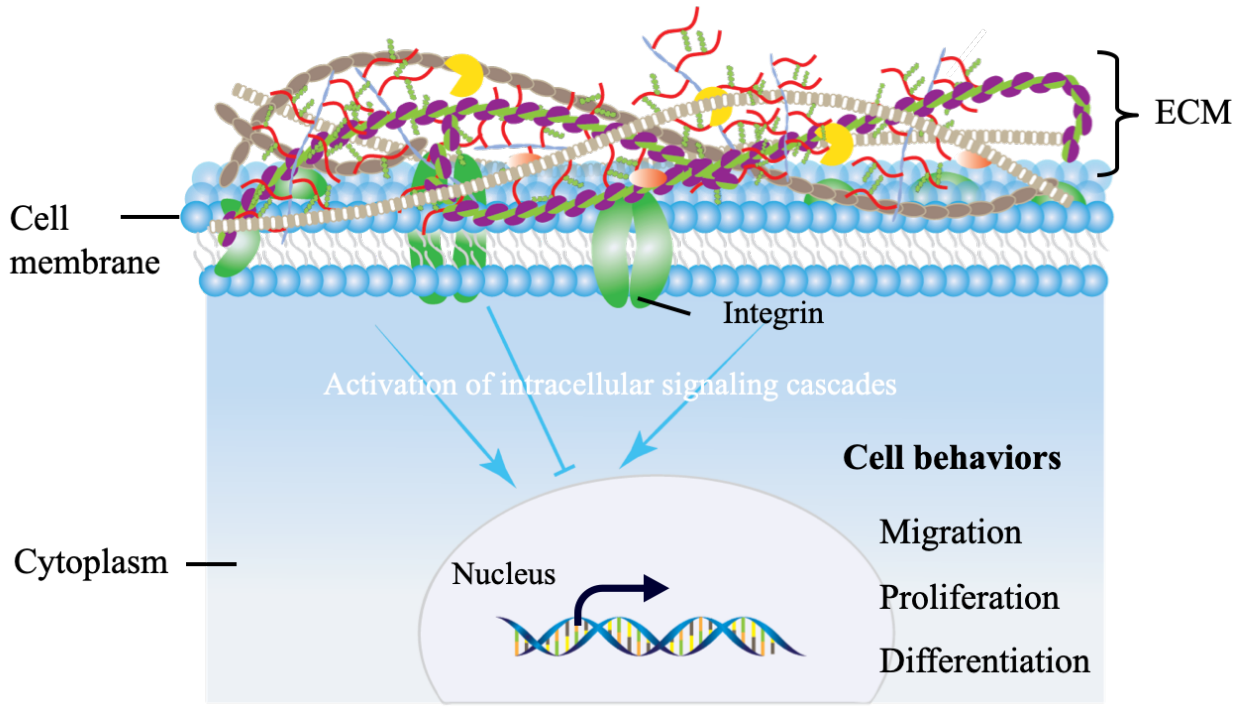


Figure 1.1. The interactions of ECM and cell. The biological activity of ECM was realized through binding and activation of integrin receptors.

## 1.1 ECM based materials

The best way to investigate interactions of ECM-cell is to mimic the ECM microenvironment. Until now, there are many methods have been introduced to generate biomimicking ECM models,[9-12] including the chemical coating of ECM proteins, tissue derived decellularized ECM and cell derived decellularized ECM. All the ECM based materials have facilitated the development of tissue engineering due to their desirable characters. As for mimicking the ECM microenvironment, there are still some limitations.[13, 14] Based on the concept of establishing an ECM-mimicking scaffold, the advantages and disadvantages of each ECM based materials are compared.

### 1.1.1 The coating of ECM proteins

A monolayer coated with ECM proteins can provide a microenvironment partially mimicking the components of native ECM.[6, 15-17] The ECM components regulate cell behaviors through the interaction with cell receptors.[18] Among them, integrin receptors are the most investigated.[19-21] (Figure 1.2).

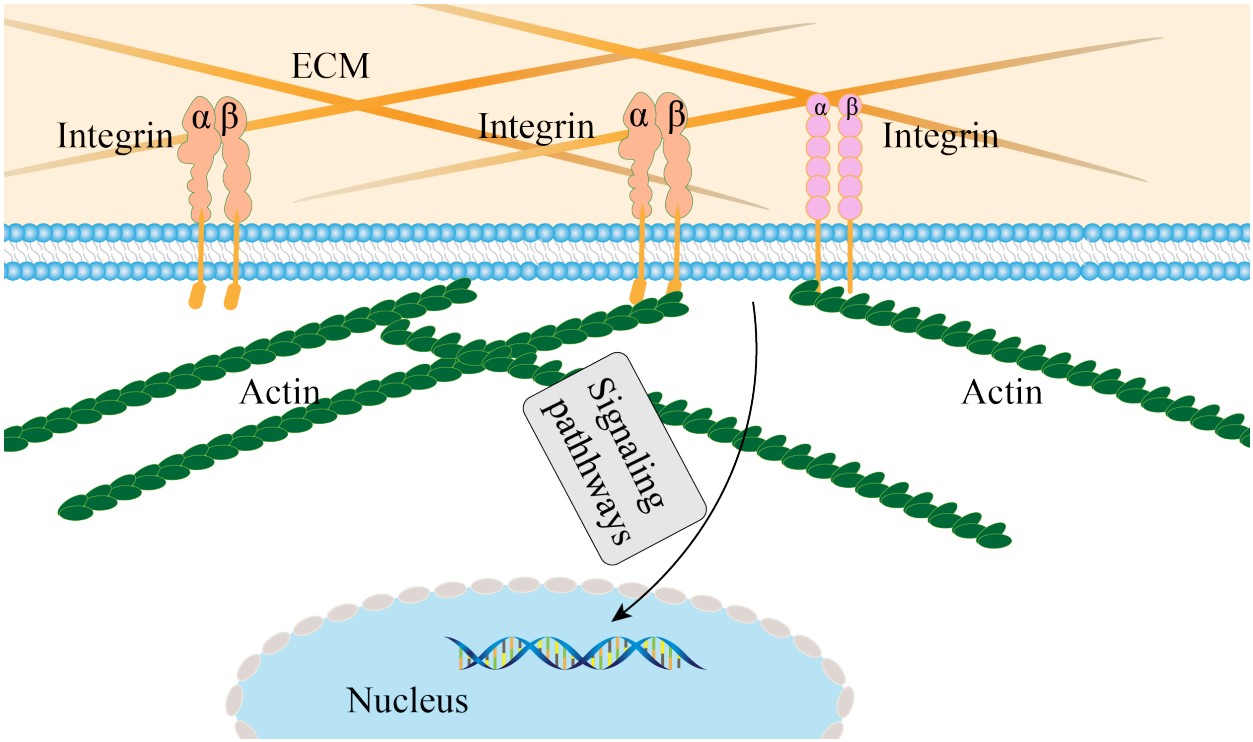


Figure 1.2. ECM-cell interactions and associated intracellular structures.

Chemical coating ECM has been widely investigated in recent years. A variety types of ECM molecules are used for investigating the influences of ECM components on cell functions.[22] The most used ECM proteins are commonly depended on the three constituents: collagen, fibronectin and laminin. Collagens are the major structure protein in ECM, they have made up from 25% to 35% of the whole-body protein content.[23, 24] Collagen superfamily comprises 28 members ordered by roman numerals, among them, collagen type I, collagen type II and collagen type X are the most common components of the collagen family.[24-26] Many studies have demonstrated that coating of collagens contribute to cell functions.[27, 28] For instance, collagen type II can promote glycosaminoglycans (GAG) deposition in a dose-dependent

manner.[29] Fibronectin is another type of adhesive protein that can assemble into fibrous network in the ECM.[30] In fibronectin, the Arg-Gly-Asp (RGD) has a high affinity binding with integrin α5β1.[31-33] This interaction can promote the cell adhesion and spreading. Researches have shown that fibronectin can inhibit adipogenic differentiation by decreasing the synthesis of cytoskeletal proteins.[34, 35] Laminins are multidomain proteins composed of thee subchains, α, β and γ chains.[36-39] The laminins are large proteins (from 400 to 900 KDa), that is present in all basement membranes. Diversity of biological activities has been reported in the multifunctional proteins. It can influence cell adhesion, growth, morphology and differentiation. Previous study has shown that laminin α4 can inhibit the adipogenic differentiation by binding to fibroblast growth factors that have a promotive effect on adipogenesis of stem cells, or by binding to integrins.[40] Here, the main ECM components and their effects on differentiation of hMSCs were summarized in Table 1.1.

Table 1.1.
The effects of main ECM components on cell differentiation

| ECM components | Influences | Mechanism |
|---|---|---|
| Collagen I[41] | Promotive effect on osteogenesis | Through ERK signaling pathway |
| Fibronectin[42] | Gradient effect on osteogenesis | Lower fibronectin-density elicited stronger osteogenic expression |
| Biglycan[43, 44] | Inhibitory effect on osteogenesis | 1. Binding with BMP-2 to inhibit activation of the following signaling pathway<br>2. Increasing the inhibitory activity of chordin |
| Decorin[45, 46] | Promotive effect on osteogenesis | 1. Through Wnt/β-catenin signaling pathway<br>2. A high attraction for calcium phosphate formation |
| Versican[47] | Promotive effect on chondrogenesis | Interaction with chondroitin sulfate chains |
| Laminin α4[40] | Inhibitory effect on adipogenesis | 1. Blocking the interaction of fibroblast growth factor with cells<br>2. Interacting with integrin receptor family |

It is a useful tool to investigate the influence of single ECM protein on cells functions by coating ECM. However, it is impossible to use the ECM coating method to mimic the complex components of ECM. Replication of the ECM components need fabricate a more complicated ECM system.

### 1.1.2 Tissue decellularized ECM

Decellularized ECMs from tissues and organs have been broadly explored in previous work, they have showed a great promise in tissue engineering due to their similar characteristics with the *in vivo* ECM microenvironment, such as the complex components, structures and mechanical properties.[48-52] The decellularized ECM from tissues or organs can be fabricated as a ECM sheet or ECM hydrogel for implantation, they also can be served as templates for whole organ engineering (Figure 1.3).

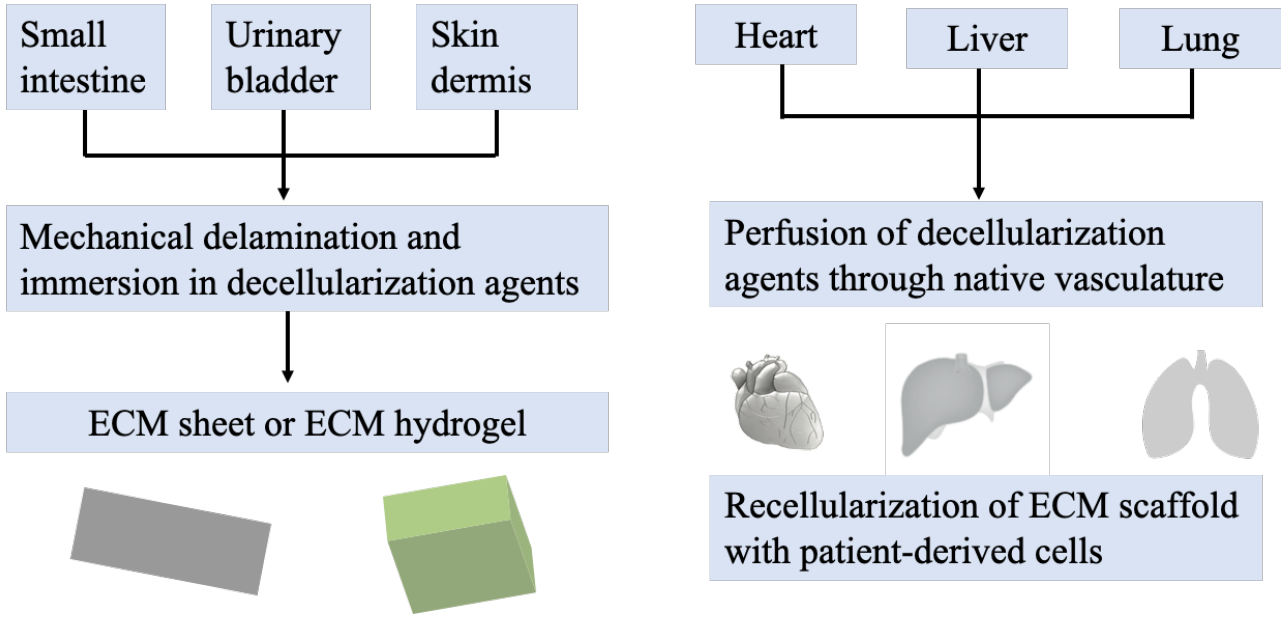


Figure 1.3. Production of ECM scaffolds from tissues and whole organs for tissue regeneration.

Recently, many studies describing the preparation of organ- or tissue-derived ECM scaffolds have been published.[53-58] For instance, cartilage is an avascular tissue, once damaged, it is very hard to repair by itself. Preparation of long-lasting implantable cartilage with a biological function still remains a big challenge. This problem can be solved by using the cartilage derived ECM with a porous property.[59-61] The cartilage construct has been gone through shatter, homogenization, freeze-drying, and the further crosslinking. In this case, the cartilage ECM can be processed into a porous scaffold for engineering tissue or organ (Figure 1.4).

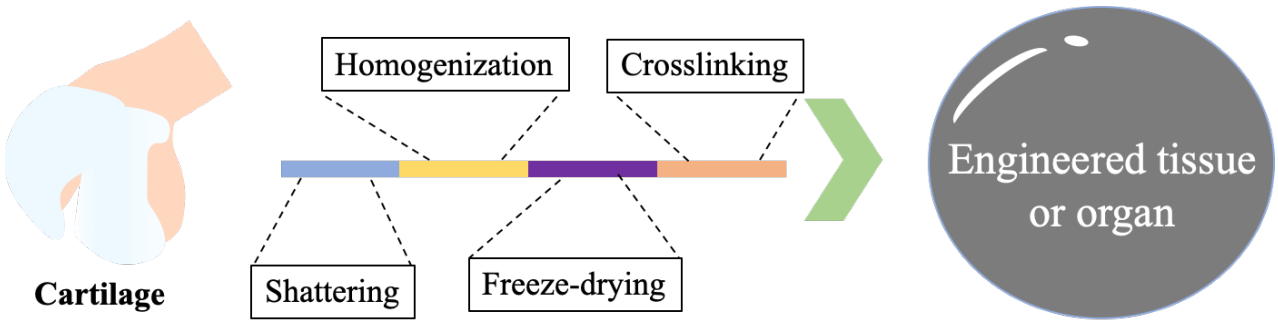


Figure 1.4. Reconstruction of cartilage ECM. Decellularized ECM scaffold from cartilage tissue can be used for tissue engineering.

Tissue-derived ECM hold very high promise for tissue engineering. While ECM compositions are

dynamically changed during tissue development. As for mimicking the stepwise development of ECM, the limited source is a hard problem.

### 1.1.3 Cell decellularized ECM

Except decellularized tissues and organs ECM, decellularized ECM biomaterials have also been prepared from cell culture.[8, 62-64] Cell-derived ECM is more readily customizable through the use of different types of cells,[65-67] thereby avoiding the problem of donor shortage of decellularized tissues and organs. Cell-derived ECM has another advantage to dynamically mimic the remodeling ECM components. Their composition can be adjusted thorough controlling the differentiation conditions and different differentiation stages. Therefore, cell-derived ECM can resume the dynamic change or remodeling of ECMs during stepwise differentiation of stem cells that mimicking the stepwise development of tissues and organs.[68] The capacities of stem cells including the self-renewal, multi-lineage differentiation potential have made them possess a great potential in tissue regeneration.[69, 70] Moreover, the surrounded ECM components are remolded during the stepwise differentiation of the stem cells. Based on this, our previous studies have created 2D ECM models to mimic the stepwise ECM changing (Figure 1.5). The matrixes are prepared from in vitro cultured human mesenchymal stem cells (hMSCs) controlled at different stages of osteogenesis,[45] adipogenesis[71] or osteogenesis-co-adipogenesis.[72] The cellular components are selectively removed after decellularization. The deposited ECM on the cell culture plate can mimic the dynamically changed ECM components. Furthermore, the sufficient cell types have ensured the sources of ECM. Therefore, this is a good in vitro method to mimic dynamical ECM components.

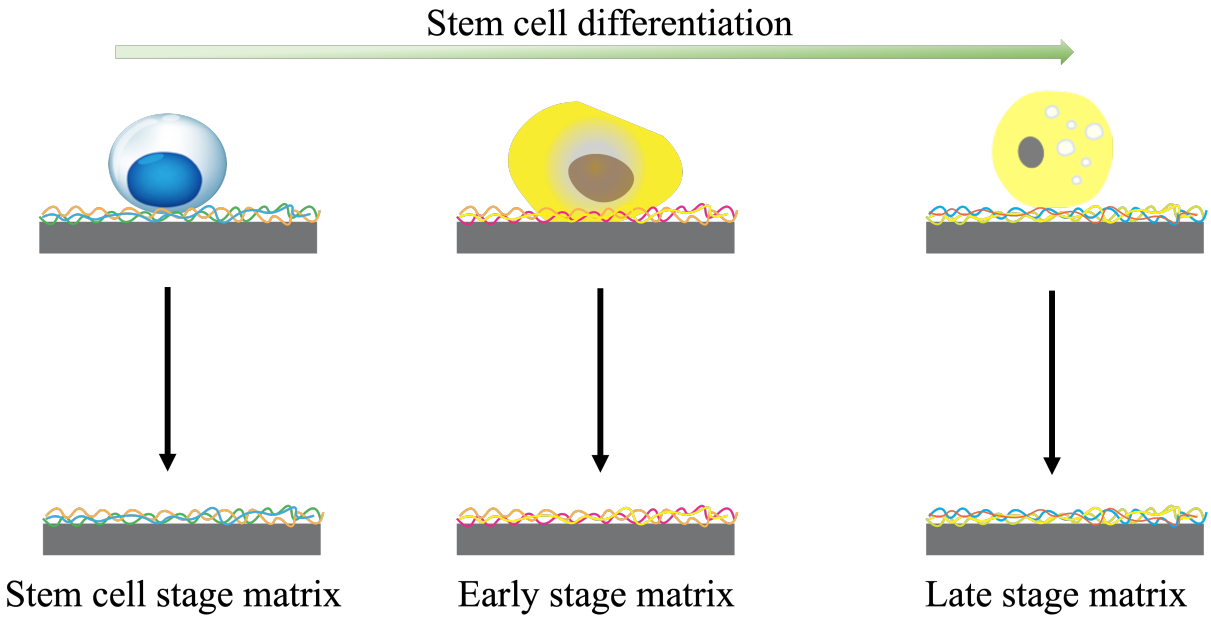


Figure 1.5. Cell-derived decellularized ECM model on 2D culture plate. ECM components were remolded during the stem cell differentiation.

The previous researches have shown that 2D substrates are good for cell expansion culture.[73-75] When cells cultured on 2D plastic substrates, the high stiffness surface promotes monolayer cell spreading. However, the soluble factors secreted by cells will be diffused in the culture medium with the culture, the restricted cell-cell interactions will be formed on 2D culture surfaces. When the cells are cultured on three-dimensional (3D) microenvironment, the interactions between each cell are from multiple direction, the adhesion of cells is

through integrin-matrix binding, which are similar with the in vivo cell microenvironment. Therefore, it is necessary to prepare 3D ECM scaffolds for tissue engineering applications and investigation of 3D ECM-cell interactions. Until now, researchers have established pure 3D ECM scaffolds.[49, 76] However, when the cells are cultured in the pure 3D ECM scaffolds, the cells/ECM constructs are curled and shrunk by cells to form pellets (Figure 1.6).[49, 76, 77] This is caused by the low mechanical strength of the scaffolds. While scaffolds should provide mechanical strength to withstand physiological loads. Therefore, to enhance mechanical property of ECM, other materials should be introduced to the ECM scaffold system to form hybrid constructs. These materials should have such characteristics, including high mechanical property, biocompatibility and shapeability. The materials can be devided into inorganic materials and organic materials. By combination of these materials, their mechanical property can be enhanced.

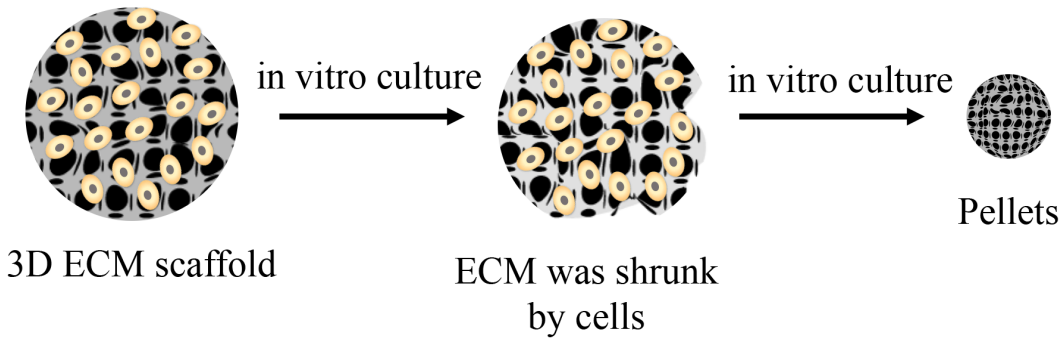


Figure 1.6. Culture of cells in the pure 3D ECM scaffold. The ECM scaffold was curled and shrunk by the cells with increase of culture time.

## 1.2 Scaffolds

### 1.2.1 Inorganic-material based scaffolds

The high mechanical properties of inorganic materials that have endowed them with high potential for scaffold preparation. In recent years, advances in bioengineering technology have facilitated the development of implant materials. Inorganic materials including mesoporous silica,[78, 79] metals,[80] and metal oxides[81] have been widely explored. Among them, hydroxylapatite (HA)-based material has emerged as a good candidate for scaffold preparation owing to its economic and biocompatible properties. Their widely used in clinical applications are reported in previous work.[82-84] The advantage of these materials is their similar chemical components with the components of bone mineral. Porous structure is another essential factor for cell proliferation, differentiation and scaffold integration.[85, 86] Various processes have been implemented to produce porous structures with differentiation pore size, pore type and pore interconnectivity.[87-89] Polymer replication is one of the methods that commonly used for preparing a tailored scaffold with controllable pore.[90] The porous scaffold should allow cell migration as well as flow of body fluids, the porous diameters usually lay between 150 ~ 500 μm.[91, 92] HA-scaffold is a good model for bone regeneration, but it is not good to be used as a 3D system for mimicking tissue development because of their poor cellular responsive properties. The pore interconnective porous structure is another limitation for cell penetration and distribution.

### 1.2.2 Organic-material based scaffolds

Organic materials can be divided into native derived polymers and synthetic derived polymers. Native derived polymers including collagen, gelatin and polyglutamic acid have shown a good affinity with cells, facilitating cell attachment, growth, differentiation, migration and tissue regeneration. They have been widely used as scaffolds for culture of cells.[93-97] Even though, there are still some shortcomings such as low mechanic properties, rapid biodegradation, which have limited their further clinical implantation. On the other hand, synthetic polymers are very attractive candidates as their material properties are higher mechanical strength and more flexible than those of natural materials. The synthetic biodegradable polymers such as polycaprolactone (PCL), poly (lactic acid-co-glycolic acid) (PLGA), poly-L-lactic acid (PLLA) and etc.[98] can provide structural requirements for the target tissue but they lack the biological cues inherent in many native derived polymers that can promote desirable cell responses. Such polymers of PLGA and PLLA have been used as mechanical skeletons to provide high mechanical strength for the scaffolds.[98, 99] Hybrid scaffolds of PLGA, PLLA and collagen, gelatin have been reported by using the hybridization method.[100-102] In particular, PLGA-collagen hybrid mesh has been shown high good mechanical property and good biocompatibility.[103, 104] Combination of synthetic and natural biomaterials can improve relevant issues associated with hydrophobic property, cell attachment and proliferation. As shown in Figure 1.7, the hybridization of PLGA mesh and collagen polymer are prepared for cell culture in our previous work, the surface of mesh scaffold is functionalized with collagen proteins that is helpful for enhancing cellular responses.[105-108]

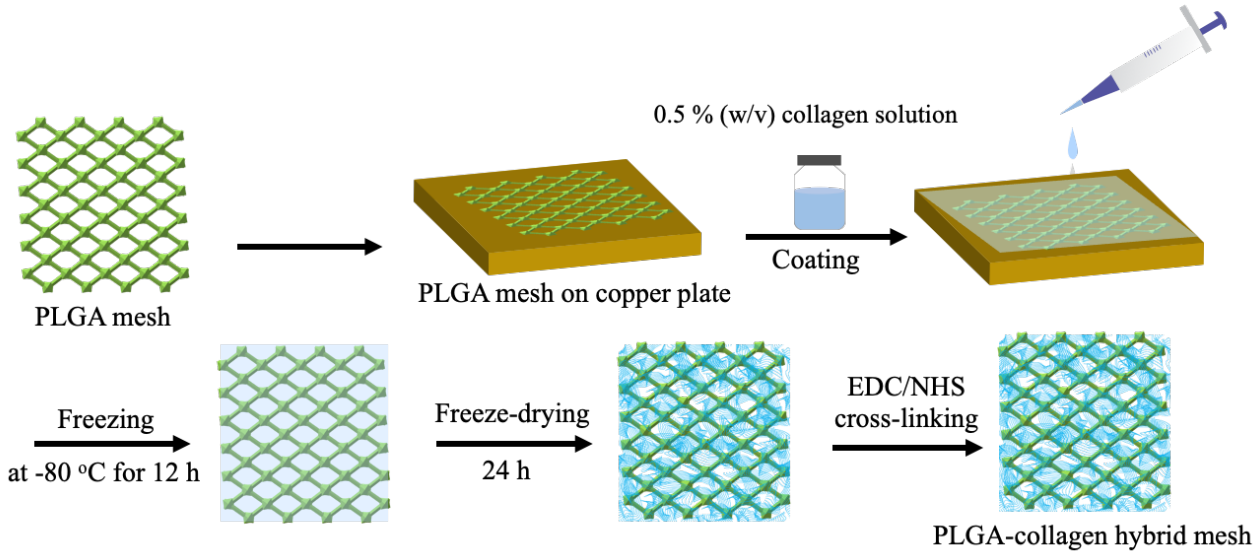


Figure 1.7. Preparation of PLGA-collagen hybrid mesh. Schematic illustration of the hybridization of collagen and PLGA mesh.

## 1.3 ECM decellularization techniques

Decellularization methods have been through chemical and enzymatic method, Physical method, biological method. The decellularization efficiency is evaluated by measuring the removal of cellular cytoskeleton and cellular nuclei. Here we compare each method in table 1.3.

Table 1.3.
Comparation of decellularization methods

| Method | Description | Decellularization effect |
|---|---|---|
| **(1) Chemical and enzymatic method** | | |
| Surfactants | The cell membrane is disarranged by the reagents to lyse cells. | |
| SDS (Sodium dodecyl sulfate) | Ion solvent | Cytotoxic: requires extensive wash process[109] |
| Triton X-100 | Moderate differentiation effect leads to be used with additional reagent such as 1.5M KCl. | Less damaging to structure of tissue than ionic surfactants[110, 111] |
| Enzymes<br>Deoxyribonuclease (DNase)<br>Ribonuclease (RNase) | <br>Destroy the fragments of DNA<br>Destroy the fragments of RNA | Used as a supplementary after other chemical treatments[112] |
| **(2) Physical method** | | |
| Freeze-thaw cycling | Freeze at -80 $^{o}$C and thaw at biological temperature (~ 37 $^{o}$C) | Remnant DNA fragments[113, 114] |
| High hydrostatic pressure | More than 600 MPa pressure was applied to lyse cells | Denatures ECM proteins[115, 116] |
| **(3) Biological method** | | |
| Apoptosis-Induction | Activate the apoptosis pathway through the dimerization of the modified caspase 9 | Remnant DNA fragments[117] |

Except for these methods as shown above, the combinative method is an alternate solution. Our previous work has reported the a combinative decellularization approach combined the chemical and physical methods. 3D ECM scaffold from cell culture are prepared after decellularization.[118] By comparison, the methods of freeze-thaw cycling with $NH_4OH$ and TX100 with 1.5M KCl have shown a better effect on removal of cellular components.

## 1.4 Motivation and objectives

Our motivation is stem from the ECM microenvironment during bone tissue development. hMSCs have a potential to differentiate into osteoblasts and adipocytes, the differentiation ratio between osteogenesis and adipogenesis are kept in a balance. Furthermore, the different types of differentiation pass through a stepwise manner into mature cells, ECM components are dynamically changed during the stepwise differentiation. On the other hand, once differentiation balance is disordered, diseases will be happened. A shift in osteogenesis toward adipogenesis of human bone marrow-derived MSCs is a crucial pathological factor in the progression of osteoporosis. To understand the relationship between ECM of bone and hMSCs are important for guiding

tissue regeneration and 3D ECM scaffolds are required. As we mentioned above, 3D ECM scaffolds need reinforcement by other biomaterials. Synthetic polymer has been used as mechanical skeletons to provide high mechanical strength to the scaffolds. In previous work, we have prepared the PLGA-collagen hybrid mesh using hybridization method. They have been widely applied for tissue engineering, including culture of skin bone and cartilage cells. They have exhibited high mechanical property and good biocompatibility. It is anticipated that the PLGA-collagen hybrid mesh can be used as a good mechanical supporting skeleton for the deposition of cell-derived ECM components to prepare tissue development-mimicking 3D ECM scaffolds. Our objectives are firstly preparing the PLGA-collagen-ECM hybrid mesh as a 3D ECM scaffold model. After that, we will investigate the influence of the biomimetic 3D ECM scaffolds on hMSCs functions.

In chapter 2, the stepwise adipogenesis-mimicking ECM-deposited PLGA-collagen hybrid meshes were prepared, their influences on adipogenic differentiation of hMSCs were investigated.

In chapter 3, the stepwise osteogenesis-mimicking ECM were induced in vitro and the secreted ECMs were deposited in 3D the PLGA-collagen hybrid mesh to create a 3D ECM scaffold. After decellularization, the hMSCs were reseeded in the 3D ECM scaffolds, their osteogenic differentiation ability was further evaluated.

In chapter 4, PLGA-collagen meshes were functionalized with the ECM secreted from hMSCs undergoing osteogenesis-co-adipogenesis to mimic the ECM microenvironment during the development of osteoporosis. Understanding the relationship between osteoporosis-related ECM and stem cells are important for the therapy of this disease. Therefore, an in vitro 3D ECM model that reflects the remodeling of ECMs during osteogenesis-co-adipogenesis of hMSCs was prepared, their influences on stem cell differentiation were investigated.

## 1.5 Reference

[1] G.S. Hussey, J.L. Dziki, S.F. Badylak, Extracellular matrix-based materials for regenerative medicine, Nature Reviews Materials 3(7) (2018) 159-173.

[2] J.D. Humphrey, E.R. Dufresne, M.A. Schwartz, Mechanotransduction and extracellular matrix homeostasis, Nat Rev Mol Cell Biol 15(12) (2014) 802-12.

[3] J.K. Mouw, G. Ou, V.M. Weaver, Extracellular matrix assembly: a multiscale deconstruction, Nat Rev Mol Cell Biol 15(12) (2014) 771-85.

[4] J. Lou, R. Stowers, S. Nam, Y. Xia, O. Chaudhuri, Stress relaxing hyaluronic acid-collagen hydrogels promote cell spreading, fiber remodeling, and focal adhesion formation in 3D cell culture, Biomaterials 154 (2018) 213-222.

[5] M. An, K. Kwon, J. Park, D.R. Ryu, J.A. Shin, J. Lee Kang, J.H. Choi, E.M. Park, K.E. Lee, M. Woo, M. Kim, Extracellular matrix-derived extracellular vesicles promote cardiomyocyte growth and electrical activity in engineered cardiac atria, Biomaterials 146 (2017) 49-59.

[6] X. Wang, Z. Chen, B. Zhou, X. Duan, W. Weng, K. Cheng, H. Wang, J. Lin, Cell-Sheet-Derived ECM Coatings and Their Effects on BMSCs Responses, ACS applied materials & interfaces 10(14) (2018) 11508-11518.

[7] C. Bonnans, J. Chou, Z. Werb, Remodelling the extracellular matrix in development and disease, Nat Rev Mol Cell Biol 15(12) (2014) 786-801.

[8] H. Ragelle, A. Naba, B.L. Larson, F. Zhou, M. Prijic, C.A. Whittaker, A. Del Rosario, R. Langer, R.O. Hynes, D.G. Anderson, Comprehensive proteomic characterization of stem cell-derived extracellular matrices, Biomaterials 128 (2017) 147-159.

[9] R.G. LeBaron, K.A. Athanasiou, Extracellular Matrix Cell Adhesion Peptides: Functional Applications in Orthopedic Materials, Tissue engineering 6(2) (2000) 85-103.
[10] T.G. Kim, T.G. Park, Biomimicking Extracellular Matrix: Cell Adhesive RGD Peptide Modified Electrospun Poly(D,L-lactic-co-glycolic acid) Nanofiber Mesh, Tissue engineering 12(2) (2006) 221-233.
[11] T.M. Blanco, A. Mantalaris, A. Bismarck, N. Panoskaltsis, The development of a three-dimensional scaffold for ex vivo biomimicry of human acute myeloid leukaemia, Biomaterials 31(8) (2010) 2243-2251.
[12] A.S. Pellowe, A.L. Gonzalez, Extracellular matrix biomimicry for the creation of investigational and therapeutic devices, WIREs Nanomedicine and Nanobiotechnology 8(1) (2016) 5-22.
[13] H. Itoh, Y. Aso, M. Furuse, Y. Noishiki, T. Miyata, A Honeycomb Collagen Carrier for Cell Culture as a Tissue Engineering Scaffold, Artificial Organs 25(3) (2001) 213-217.
[14] E. Knight, S. Przyborski, Advances in 3D cell culture technologies enabling tissue-like structures to be created in vitro, Journal of Anatomy 227(6) (2015) 746-756.
[15] G.A. Silva, C. Czeisler, K.L. Niece, E. Beniash, D.A. Harrington, J.A. Kessler, S.I. Stupp, Selective differentiation of neural progenitor cells by high-epitope density nanofibers, Science 303(5662) (2004) 1352-5.
[16] S. Zhang, Fabrication of novel biomaterials through molecular self-assembly, Nature biotechnology 21(10) (2003) 1171-8.
[17] Z. Tong, K. Martyn, A. Yang, X. Yin, B.E. Mead, N. Joshi, N.E. Sherman, R.S. Langer, J.M. Karp, Towards a defined ECM and small molecule based monolayer culture system for the expansion of mouse and human intestinal stem cells, Biomaterials 154 (2018) 60-73.
[18] J.D. Humphrey, E.R. Dufresne, M.A. Schwartz, Mechanotransduction and extracellular matrix homeostasis, Nature Reviews Molecular Cell Biology 15(12) (2014) 802-812.
[19] J.D. Humphrey, E.R. Dufresne, M.A. Schwartz, Mechanotransduction and extracellular matrix homeostasis, Nat Rev Mol Cell Biol 15(12) (2014) 802-812.
[20] P. Moreno-Layseca, J. Icha, H. Hamidi, J. Ivaska, Integrin trafficking in cells and tissues, Nature Cell Biology 21(2) (2019) 122-132.
[21] R. Milner, I.L. Campbell, The integrin family of cell adhesion molecules has multiple functions within the CNS, Journal of Neuroscience Research 69(3) (2002) 286-291.
[22] E. Elagamey, K. Narula, N. Chakraborty, S. Chakraborty, Extracellular Matrix Proteome: Isolation of ECM Proteins for Proteomics Studies, Methods in molecular biology (Clifton, N.J.) 2057 (2020) 155-172.
[23] M.E. Lukashev, Z. Werb, ECM signalling: orchestrating cell behaviour and misbehaviour, Trends in Cell Biology 8(11) (1998) 437-441.
[24] S. Ricard-Blum, The collagen family, Cold Spring Harb Perspect Biol 3(1) (2011) a004978.
[25] S. Ricard-Blum, The collagen family, Cold Spring Harb Perspect Biol 3(1) (2011) a004978-a004978.
[26] X. Liu, H. Wu, M. Byrne, S. Krane, R. Jaenisch, Type III collagen is crucial for collagen I fibrillogenesis and for normal cardiovascular development, Proceedings of the National Academy of Sciences 94(5) (1997) 1852-1856.
[27] C.L. Hall, J. Dai, K.L. van Golen, E.T. Keller, M.W. Long, Type I collagen receptor (alpha 2 beta 1) signaling promotes the growth of human prostate cancer cells within the bone, Cancer research 66(17) (2006) 8648-54.
[28] O. Olivares, J.R. Mayers, V. Gouirand, M.E. Torrence, T. Gicquel, L. Borge, S. Lac, J. Roques, M.N. Lavaut, P. Berthezene, M. Rubis, V. Secq, S. Garcia, V. Moutardier, D. Lombardo, J.L. Iovanna, R. Tomasini, F. Guillaumond, M.G. Vander Heiden, S. Vasseur, Collagen-derived proline promotes pancreatic ductal adenocarcinoma cell survival under nutrient limited conditions, Nature communications 8 (2017) 16031.
[29] S. Claus, N. Mayer, E. Aubert-Foucher, H. Chajra, E. Perrier-Groult, J. Lafont, M. Piperno, O. Damour,

F. Mallein-Gerin, Cartilage-characteristic matrix reconstruction by sequential addition of soluble factors during expansion of human articular chondrocytes and their cultivation in collagen sponges, Tissue engineering. Part C, Methods 18(2) (2012) 104-12.
[30] A.J. Zollinger, M.L. Smith, Fibronectin, the extracellular glue, Matrix Biology 60-61 (2017) 27-37.
[31] F. Kuonen, I. Surbeck, K.Y. Sarin, M. Dontenwill, C. Ruegg, M. Gilliet, A.E. Oro, O. Gaide, TGFbeta, Fibronectin and Integrin alpha5beta1 Promote Invasion in Basal Cell Carcinoma, The Journal of investigative dermatology 138(11) (2018) 2432-2442.
[32] T. Tao, Y. Li, C. Gui, Y. Ma, Y. Ge, H. Dai, K. Zhang, J. Du, Y. Guo, Y. Jiang, J. Gui, Fibronectin Enhances Cartilage Repair by Activating Progenitor Cells Through Integrin alpha5beta1 Receptor, Tissue engineering. Part A 24(13-14) (2018) 1112-1124.
[33] X. Yu, Q.Q. Zhang, B. Wang, L. Sun, [Expression and significance of integrin alpha5beta1 and fibronectin in atherosclerotic plaques from autopsy specimens], Zhonghua bing li xue za zhi = Chinese journal of pathology 46(3) (2017) 182-186.
[34] B.M. Spiegelman, C.A. Ginty, Fibronectin modulation of cell shape and lipogenic gene expression in 3T3-adipocytes, Cell 35(3 Pt 2) (1983) 657-66.
[35] D.B. Bosco, M.D. Roycik, Y. Jin, M.A. Schwartz, T.J. Lively, D.A. Zorio, Q.A. Sang, A new synthetic matrix metalloproteinase inhibitor reduces human mesenchymal stem cell adipogenesis, PloS one 12(2) (2017) e0172925.
[36] M. Aumailley, L. Bruckner-Tuderman, W.G. Carter, R. Deutzmann, D. Edgar, P. Ekblom, J. Engel, E. Engvall, E. Hohenester, J.C.R. Jones, H.K. Kleinman, M.P. Marinkovich, G.R. Martin, U. Mayer, G. Meneguzzi, J.H. Miner, K. Miyazaki, M. Patarroyo, M. Paulsson, V. Quaranta, J.R. Sanes, T. Sasaki, K. Sekiguchi, L.M. Sorokin, J.F. Talts, K. Tryggvason, J. Uitto, I. Virtanen, K. von der Mark, U.M. Wewer, Y. Yamada, P.D. Yurchenco, A simplified laminin nomenclature, Matrix Biology 24(5) (2005) 326-332.
[37] R. Stick, A. Peter, Evolution of the lamin protein family at the base of the vertebrate lineage, Cell and tissue research (2019).
[38] J.M. Urbano, C.N. Torgler, C. Molnar, U. Tepass, A. Lopez-Varea, N.H. Brown, J.F. de Celis, M.D. Martin-Bermudo, Drosophila laminins act as key regulators of basement membrane assembly and morphogenesis, Development (Cambridge, England) 136(24) (2009) 4165-76.
[39] D. Hollfelder, M. Frasch, I. Reim, Distinct functions of the laminin beta LN domain and collagen IV during cardiac extracellular matrix formation and stabilization of alary muscle attachments revealed by EMS mutagenesis in Drosophila, BMC developmental biology 14 (2014) 26.
[40] H. Yamashita, C. Goto, R. Tajima, A.T. Koparal, M. Kobori, Y. Ohki, K. Shitara, R. Narita, K. Toriyama, S. Torii, T. Niimi, Y. Kitagawa, Cryptic fragment alpha4 LG4-5 derived from laminin alpha4 chain inhibits de novo adipogenesis by modulating the effect of fibroblast growth factor-2, Development, growth & differentiation 50(2) (2008) 97-107.
[41] S. Viale-Bouroncle, M. Gosau, C. Morsczeck, Collagen I induces the expression of alkaline phosphatase and osteopontin via independent activations of FAK and ERK signalling pathways, Archives of oral biology 59(12) (2014) 1249-55.
[42] A.B. Faia-Torres, T. Goren, T.O. Ihalainen, S. Guimond-Lischer, M. Charnley, M. Rottmar, K. Maniura-Weber, N.D. Spencer, R.L. Reis, M. Textor, N.M. Neves, Regulation of human mesenchymal stem cell osteogenesis by specific surface density of fibronectin: a gradient study, ACS applied materials & interfaces 7(4) (2015) 2367-75.
[43] A.M. Hocking, T. Shinomura, D.J. McQuillan, Leucine-rich repeat glycoproteins of the extracellular matrix, Matrix biology : journal of the International Society for Matrix Biology 17(1) (1998) 1-19.
[44] M. Moreno, R. Munoz, F. Aroca, M. Labarca, E. Brandan, J. Larrain, Biglycan is a new extracellular

component of the Chordin-BMP4 signaling pathway, The EMBO journal 24(7) (2005) 1397-405.
[45] T. Hoshiba, N. Kawazoe, T. Tateishi, G. Chen, Development of stepwise osteogenesis-mimicking matrices for the regulation of mesenchymal stem cell functions, The Journal of biological chemistry 284(45) (2009) 31164-73.
[46] X.G. Han, D.K. Wang, F. Gao, R.H. Liu, Z.G. Bi, Bone morphogenetic protein 2 and decorin expression in old fracture fragments and surrounding tissues, Genetics and molecular research : GMR 14(3) (2015) 11063-72.
[47] N. Kamiya, H. Watanabe, H. Habuchi, H. Takagi, T. Shinomura, K. Shimizu, K. Kimata, Versican/PG-M regulates chondrogenesis as an extracellular matrix molecule crucial for mesenchymal condensation, The Journal of biological chemistry 281(4) (2006) 2390-400.
[48] J.W. Lee, S. Chae, S. Oh, S.H. Kim, K.H. Choi, M. Meeseepong, J. Chang, N. Kim, K. Yong Ho, N.E. Lee, J.H. Lee, J.Y. Choi, Single-Chain Atomic Crystals as Extracellular Matrix-Mimicking Material with Exceptional Biocompatibility and Bioactivity, Nano letters 18(12) (2018) 7619-7627.
[49] H. Lu, T. Hoshiba, N. Kawazoe, G. Chen, Autologous extracellular matrix scaffolds for tissue engineering, Biomaterials 32(10) (2011) 2489-99.
[50] A.E. Jakus, M.M. Laronda, A.S. Rashedi, C.M. Robinson, C. Lee, S.W. Jordan, K.E. Orwig, T.K. Woodruff, R.N. Shah, "Tissue Papers" from Organ-Specific Decellularized Extracellular Matrices, Adv Funct Mater 27(3) (2017).
[51] T. Rezaei Topraggaleh, M. Rezazadeh Valojerdi, L. Montazeri, H. Baharvand, A testis-derived macroporous 3D scaffold as a platform for the generation of mouse testicular organoids, Biomaterials science 7(4) (2019) 1422-1436.
[52] S.R. Cerqueira, Y.S. Lee, R.C. Cornelison, M.W. Mertz, R.A. Wachs, C.E. Schmidt, M.B. Bunge, Decellularized peripheral nerve supports Schwann cell transplants and axon growth following spinal cord injury, Biomaterials 177 (2018) 176-185.
[53] V.E. Getova, J.A. van Dongen, L.A. Brouwer, M.C. Harmsen, Adipose tissue-derived ECM hydrogels and their use as 3D culture scaffold, Artificial cells, nanomedicine, and biotechnology 47(1) (2019) 1693-1701.
[54] P. Morissette Martin, A. Shridhar, C. Yu, C. Brown, L.E. Flynn, Decellularized Adipose Tissue Scaffolds for Soft Tissue Regeneration and Adipose-Derived Stem/Stromal Cell Delivery, Methods in molecular biology (Clifton, N.J.) 1773 (2018) 53-71.
[55] T. Ansari, A. Southgate, I. Obiri-Yeboa, L.G. Jones, A. Olayanju, K. Greco, L. Mbundi, M. Somasundaram, B. Davidson, P.D. Sibbons, Development and characterisation of a Porcine Liver Scaffold, Stem cells and development (2019).
[56] I. Rosadi, K. Karina, I. Rosliana, S. Sobariah, I. Afini, T. Widyastuti, A. Barlian, In vitro study of cartilage tissue engineering using human adipose-derived stem cells induced by platelet-rich plasma and cultured on silk fibroin scaffold, Stem Cell Res Ther 10(1) (2019) 369.
[57] D. Choudhury, H.W. Tun, T. Wang, M.W. Naing, Organ-Derived Decellularized Extracellular Matrix: A Game Changer for Bioink Manufacturing?, Trends in biotechnology 36(8) (2018) 787-805.
[58] E. Lih, W. Park, K.W. Park, S.Y. Chun, H. Kim, Y.K. Joung, T.G. Kwon, J.A. Hubbell, D.K. Han, A Bioinspired Scaffold with Anti-Inflammatory Magnesium Hydroxide and Decellularized Extracellular Matrix for Renal Tissue Regeneration, ACS central science 5(3) (2019) 458-467.
[59] H. Kang, J. Peng, S. Lu, S. Liu, L. Zhang, J. Huang, X. Sui, B. Zhao, A. Wang, W. Xu, Z. Luo, Q. Guo, In vivo cartilage repair using adipose-derived stem cell-loaded decellularized cartilage ECM scaffolds, Journal of Tissue Engineering and Regenerative Medicine 8(6) (2014) 442-453.
[60] A. Moradi, F. Ataollahi, K. Sayar, S. Pramanik, P.-P. Chong, A.A. Khalil, T. Kamarul, B. Pingguan-Murphy, Chondrogenic potential of physically treated bovine cartilage matrix derived porous scaffolds on

human dermal fibroblast cells, Journal of Biomedical Materials Research Part A 104(1) (2016) 245-256.
[61] H.V. Almeida, G.M. Cunniffe, T. Vinardell, C.T. Buckley, F.J. O'Brien, D.J. Kelly, Coupling Freshly Isolated CD44+ Infrapatellar Fat Pad-Derived Stromal Cells with a TGF-β3 Eluting Cartilage ECM-Derived Scaffold as a Single-Stage Strategy for Promoting Chondrogenesis, Advanced healthcare materials 4(7) (2015) 1043-1053.
[62] T. Hoshiba, Cultured cell-derived decellularized matrices: a review towards the next decade, Journal of Materials Chemistry B 5(23) (2017) 4322-4331.
[63] Y. Teng, X. Li, Y. Chen, H. Cai, W. Cao, X. Chen, Y. Sun, J. Liang, Y. Fan, X. Zhang, Extracellular matrix powder from cultured cartilage-like tissue as cell carrier for cartilage repair, Journal of Materials Chemistry B 5(18) (2017) 3283-3292.
[64] B. Nyambat, C.-H. Chen, P.-C. Wong, C.-W. Chiang, M.K. Satapathy, E.-Y. Chuang, Genipin-crosslinked adipose stem cell derived extracellular matrix-nano graphene oxide composite sponge for skin tissue engineering, Journal of Materials Chemistry B 6(6) (2018) 979-990.
[65] C.-Y. Gao, Z.-H. Huang, W. Jing, P.-F. Wei, L. Jin, X.-H. Zhang, Q. Cai, X.-L. Deng, X.-P. Yang, Directing osteogenic differentiation of BMSCs by cell-secreted decellularized extracellular matrixes from different cell types, Journal of Materials Chemistry B 6(45) (2018) 7471-7485.
[66] T. Urooj, B. Wasim, S. Mushtaq, S.N.N. Shah, M. Shah, Cancer Cell-Derived Secretory Factors in Breast Cancer-Associated Lung Metastasis: their Mechanism and Future Prospects, Current cancer drug targets (2019).
[67] X. Xiong, X. Yang, H. Dai, G. Feng, Y. Zhang, J. Zhou, W. Zhou, Extracellular matrix derived from human urine-derived stem cells enhances the expansion, adhesion, spreading, and differentiation of human periodontal ligament stem cells, Stem Cell Res Ther 10(1) (2019) 396.
[68] W. Zhang, Y. Zhu, J. Li, Q. Guo, J. Peng, S. Liu, J. Yang, Y. Wang, Cell-Derived Extracellular Matrix: Basic Characteristics and Current Applications in Orthopedic Tissue Engineering, Tissue engineering. Part B, Reviews 22(3) (2016) 193-207.
[69] A.M. Yousefi, P.F. James, R. Akbarzadeh, A. Subramanian, C. Flavin, H. Oudadesse, Prospect of Stem Cells in Bone Tissue Engineering: A Review, Stem cells international 2016 (2016) 6180487.
[70] J. Jang, H.J. Park, S.W. Kim, H. Kim, J.Y. Park, S.J. Na, H.J. Kim, M.N. Park, S.H. Choi, S.H. Park, S.W. Kim, S.M. Kwon, P.J. Kim, D.W. Cho, 3D printed complex tissue construct using stem cell-laden decellularized extracellular matrix bioinks for cardiac repair, Biomaterials 112 (2017) 264-274.
[71] T. Hoshiba, N. Kawazoe, T. Tateishi, G. Chen, Development of extracellular matrices mimicking stepwise adipogenesis of mesenchymal stem cells, Advanced materials (Deerfield Beach, Fla.) 22(28) (2010) 3042-7.
[72] R. Cai, T. Nakamoto, T. Hoshiba, N. Kawazoe, G. Chen, Matrices secreted during simultaneous osteogenesis and adipogenesis of mesenchymal stem cells affect stem cells differentiation, Acta biomaterialia 35 (2016) 185-93.
[73] I. Hilmi, A. Lotnyk, J.W. Gerlach, P. Schumacher, B. Rauschenbach, Influence of substrate dimensionality on the growth mode of epitaxial 3D-bonded GeTe thin films: From 3D to 2D growth, Materials & Design 168 (2019) 107657.
[74] F.C. Paccola Mesquita, C. Hochman-Mendez, J. Morrissey, L.C. Sampaio, D.A. Taylor, Laminin as a Potent Substrate for Large-Scale Expansion of Human Induced Pluripotent Stem Cells in a Closed Cell Expansion System, Stem cells international 2019 (2019) 9704945.
[75] D. Kong, L. Peng, S. Di Cio, P. Novak, J.E. Gautrot, Stem Cell Expansion and Fate Decision on Liquid Substrates Are Regulated by Self-Assembled Nanosheets, ACS nano 12(9) (2018) 9206-9213.
[76] H. Lu, T. Hoshiba, N. Kawazoe, I. Koda, M. Song, G. Chen, Cultured cell-derived extracellular matrix scaffolds for tissue engineering, Biomaterials 32(36) (2011) 9658-66.

[77] R. Cai, T. Nakamoto, N. Kawazoe, G. Chen, Influence of stepwise chondrogenesis-mimicking 3D extracellular matrix on chondrogenic differentiation of mesenchymal stem cells, Biomaterials 52 (2015) 199-207.
[78] N. Shadjou, M. Hasanzadeh, Silica-based mesoporous nanobiomaterials as promoter of bone regeneration process, Journal of biomedical materials research. Part A 103(11) (2015) 3703-16.
[79] Y. Wang, Q. Zhao, N. Han, L. Bai, J. Li, J. Liu, E. Che, L. Hu, Q. Zhang, T. Jiang, S. Wang, Mesoporous silica nanoparticles in drug delivery and biomedical applications, Nanomedicine : nanotechnology, biology, and medicine 11(2) (2015) 313-27.
[80] N. Lu, T. Hu, Y. Zhai, H. Qin, J. Aliyeva, H. Zhang, Fungal cell with artificial metal container for heavy metals biosorption: Equilibrium, kinetics study and mechanisms analysis, Environmental research 182 (2019) 109061.
[81] L. Bergamonti, C. Bergonzi, C. Graiff, P.P. Lottici, R. Bettini, L. Elviri, 3D printed chitosan scaffolds: A new TiO2 support for the photocatalytic degradation of amoxicillin in water, Water research 163 (2019) 114841.
[82] H. Oonishi, H. Oonishi, S.C. Kim, L.L. Hench, J. Wilson, E. Tsuji, H. Fujita, H. Oohashi, K. Oomamiuda, 27 - Clinical application of hydroxyapatite, in: T. Kokubo (Ed.), Bioceramics and their Clinical Applications, Woodhead Publishing2008, pp. 606-687.
[83] E. Mazzoni, A. D'Agostino, M.R. Iaquinta, I. Bononi, L. Trevisiol, J.C. Rotondo, S. Patergnani, C. Giorgi, M.J. Gunson, W. Arnett, P.F. Nocini, M. Tognon, F. Martini, Hydroxylapatite-collagen hybrid scaffold induces human adipose-derived mesenchymal stem cells to osteogenic differentiation in vitro and bone regrowth in patients, Stem cells translational medicine (2019).
[84] P. Kazimierczak, A. Benko, M. Nocun, A. Przekora, Novel chitosan/agarose/hydroxyapatite nanocomposite scaffold for bone tissue engineering applications: comprehensive evaluation of biocompatibility and osteoinductivity with the use of osteoblasts and mesenchymal stem cells, International journal of nanomedicine 14 (2019) 6615-6630.
[85] S.J. Hollister, Porous scaffold design for tissue engineering, Nature Materials 4(7) (2005) 518-524.
[86] E. Magrofuoco, M. Flaibani, M. Giomo, N. Elvassore, Cell culture distribution in a three-dimensional porous scaffold in perfusion bioreactor, Biochemical Engineering Journal 146 (2019) 10-19.
[87] G. Li, S. Qin, X. Liu, D. Zhang, M. He, Structure and properties of nano-hydroxyapatite/poly(butylene succinate) porous scaffold for bone tissue engineering prepared by using ethanol as porogen, Journal of biomaterials applications 33(6) (2019) 776-791.
[88] J. Zhang, D. Xiao, X. He, F. Shi, P. Luo, W. Zhi, K. Duan, J. Weng, A novel porous bioceramic scaffold by accumulating hydroxyapatite spheres for large bone tissue engineering. III: Characterization of porous structure, Materials science & engineering. C, Materials for biological applications 89 (2018) 223-229.
[89] Z. Zhang, J. Du, Z. Wei, Z. Wang, M. Li, J. Ni, A 3D computational model of perfusion seeding for investigating cell transport and adhesion within a porous scaffold, Biomechanics and modeling in mechanobiology (2020).
[90] G. Tripathi, B. Basu, A porous hydroxyapatite scaffold for bone tissue engineering: Physico-mechanical and biological evaluations, Ceramics International 38(1) (2012) 341-349.
[91] B. Bhaskar, R. Owen, H. Bahmaee, Z. Wally, P. Sreenivasa Rao, G.C. Reilly, Composite porous scaffold of PEG/PLA support improved bone matrix deposition in vitro compared to PLA-only scaffolds, Journal of biomedical materials research. Part A 106(5) (2018) 1334-1340.
[92] X. Mendibil, R. Ortiz, V.S. Viteri, J.M. Ugartemendia, J.R. Sarasua, I. Quintana, High Throughput Manufacturing of Bio-Resorbable Micro-Porous Scaffolds Made of Poly(L-lactide-co-epsilon-caprolactone) by Micro-Extrusion for Soft Tissue Engineering Applications, Polymers 12(1) (2019).
[93] M. Montgomery, S. Ahadian, L. Davenport Huyer, M. Lo Rito, R.A. Civitarese, R.D. Vanderlaan, J. Wu,

L.A. Reis, A. Momen, S. Akbari, A. Pahnke, R.-K. Li, C.A. Caldarone, M. Radisic, Flexible shape-memory scaffold for minimally invasive delivery of functional tissues, Nature Materials 16(10) (2017) 1038-1046.
[94] A. Berner, J. Henkel, M.A. Woodruff, S. Saifzadeh, G. Kirby, S. Zaiss, J. Gohlke, J.C. Reichert, M. Nerlich, M.A. Schuetz, D.W. Hutmacher, Scaffold–cell bone engineering in a validated preclinical animal model: precursors vs differentiated cell source, Journal of Tissue Engineering and Regenerative Medicine 11(7) (2017) 2081-2089.
[95] X.-B. Hu, Y.-L. Liu, W.-J. Wang, H.-W. Zhang, Y. Qin, S. Guo, X.-W. Zhang, L. Fu, W.-H. Huang, Biomimetic Graphene-Based 3D Scaffold for Long-Term Cell Culture and Real-Time Electrochemical Monitoring, Analytical Chemistry 90(2) (2018) 1136-1141.
[96] Z. Atoufi, P. Zarrintaj, G.H. Motlagh, A. Amiri, Z. Bagher, S.K. Kamrava, A novel bio electro active alginate-aniline tetramer/ agarose scaffold for tissue engineering: synthesis, characterization, drug release and cell culture study, Journal of Biomaterials Science, Polymer Edition 28(15) (2017) 1617-1638.
[97] C. Drieschner, M. Minghetti, S. Wu, P. Renaud, K. Schirmer, Ultrathin Alumina Membranes as Scaffold for Epithelial Cell Culture from the Intestine of Rainbow Trout, ACS applied materials & interfaces 9(11) (2017) 9496-9505.
[98] F. Pu, N.P. Rhodes, Y. Bayon, J.A. Hunt, In vitro cellular response to oxidized collagen-PLLA hybrid scaffolds designed for the repair of muscular tissue defects and complex incisional hernias, J Tissue Eng Regen Med 10(10) (2016) E454-e466.
[99] G. Chen, T. Ushida, T. Tateishi, Hybrid Biomaterials for Tissue Engineering: A Preparative Method for PLA or PLGA–Collagen Hybrid Sponges, Advanced Materials 12(6) (2000) 455-457.
[100] X. He, H. Lu, N. Kawazoe, T. Tateishi, G. Chen, A novel cylinder-type poly(L-lactic acid)-collagen hybrid sponge for cartilage tissue engineering, Tissue engineering. Part C, Methods 16(3) (2010) 329-38.
[101] H. Lu, H.H. Oh, N. Kawazoe, K. Yamagishi, G. Chen, PLLA–collagen and PLLA–gelatin hybrid scaffolds with funnel-like porous structure for skin tissue engineering, Science and technology of advanced materials 13(6) (2012) 064210.
[102] G. Chen, T. Ushida, T. Tateishi, Poly(DL-lactic-co-glycolic acid) sponge hybridized with collagen microsponges and deposited apatite particulates, Journal of Biomedical Materials Research 57(1) (2001) 8-14.
[103] G. Chen, T. Sato, T. Ushida, R. Hirochika, Y. Shirasaki, N. Ochiai, T. Tateishi, The use of a novel PLGA fiber/collagen composite web as a scaffold for engineering of articular cartilage tissue with adjustable thickness, Journal of biomedical materials research. Part A 67(4) (2003) 1170-80.
[104] G. Chen, T. Sato, H. Ohgushi, T. Ushida, T. Tateishi, J. Tanaka, Culturing of skin fibroblasts in a thin PLGA–collagen hybrid mesh, Biomaterials 26(15) (2005) 2559-2566.
[105] G. Chen, T. Sato, H. Ohgushi, T. Ushida, T. Tateishi, J. Tanaka, Culturing of skin fibroblasts in a thin PLGA-collagen hybrid mesh, Biomaterials 26(15) (2005) 2559-66.
[106] W. Dai, N. Kawazoe, X. Lin, J. Dong, G. Chen, The influence of structural design of PLGA/collagen hybrid scaffolds in cartilage tissue engineering, Biomaterials 31(8) (2010) 2141-52.
[107] N. Kawazoe, C. Inoue, T. Tateishi, G. Chen, A cell leakproof PLGA-collagen hybrid scaffold for cartilage tissue engineering, Biotechnology progress 26(3) (2010) 819-26.
[108] G. Chen, T. Sato, T. Ushida, R. Hirochika, T. Tateishi, Redifferentiation of dedifferentiated bovine chondrocytes when cultured in vitro in a PLGA-collagen hybrid mesh, FEBS letters 542(1-3) (2003) 95-9.
[109] O. Syed, N.J. Walters, R.M. Day, H.W. Kim, J.C. Knowles, Evaluation of decellularization protocols for production of tubular small intestine submucosa scaffolds for use in oesophageal tissue engineering, Acta biomaterialia 10(12) (2014) 5043-5054.
[110] D.C. Sullivan, S.H. Mirmalek-Sani, D.B. Deegan, P.M. Baptista, T. Aboushwareb, A. Atala, J.J. Yoo, Decellularization methods of porcine kidneys for whole organ engineering using a high-throughput system,

Biomaterials 33(31) (2012) 7756-64.
[111] B. Mendoza-Novelo, E.E. Avila, J.V. Cauich-Rodriguez, E. Jorge-Herrero, F.J. Rojo, G.V. Guinea, J.L. Mata-Mata, Decellularization of pericardial tissue and its impact on tensile viscoelasticity and glycosaminoglycan content, Acta biomaterialia 7(3) (2011) 1241-8.
[112] W.C. Chen, Z. Wang, M.A. Missinato, D.W. Park, D.W. Long, H.J. Liu, X. Zeng, N.A. Yates, K. Kim, Y. Wang, Decellularized zebrafish cardiac extracellular matrix induces mammalian heart regeneration, Science advances 2(11) (2016) e1600844.
[113] Q. Xing, K. Yates, M. Tahtinen, E. Shearier, Z. Qian, F. Zhao, Decellularization of fibroblast cell sheets for natural extracellular matrix scaffold preparation, Tissue engineering. Part C, Methods 21(1) (2015) 77-87.
[114] B.D. Elder, D.H. Kim, K.A. Athanasiou, Developing an articular cartilage decellularization process toward facet joint cartilage replacement, Neurosurgery 66(4) (2010) 722-7; discussion 727.
[115] S. Funamoto, K. Nam, T. Kimura, A. Murakoshi, Y. Hashimoto, K. Niwaya, S. Kitamura, T. Fujisato, A. Kishida, The use of high-hydrostatic pressure treatment to decellularize blood vessels, Biomaterials 31(13) (2010) 3590-5.
[116] Y. Hashimoto, S. Funamoto, S. Sasaki, T. Honda, S. Hattori, K. Nam, T. Kimura, M. Mochizuki, T. Fujisato, H. Kobayashi, A. Kishida, Preparation and characterization of decellularized cornea using high-hydrostatic pressurization for corneal tissue engineering, Biomaterials 31(14) (2010) 3941-8.
[117] P.E. Bourgine, E. Gaudiello, B. Pippenger, C. Jaquiery, T. Klein, S. Pigeot, A. Todorov Jr, S. Feliciano, A. Banfi, I. Martin, Engineered Extracellular Matrices as Biomaterials of Tunable Composition and Function, Advanced Functional Materials 27(7) (2017) 1605486.
[118] H. Lu, T. Hoshiba, N. Kawazoe, G. Chen, Comparison of decellularization techniques for preparation of extracellular matrix scaffolds derived from three-dimensional cell culture, Journal of biomedical materials research. Part A 100(9) (2012) 2507-16.

# Chapter 2

# Preparation of stepwise adipogenesis-mimicking ECM-deposited PLGA-collagen hybrid meshes and their influence on adipogenic differentiation of hMSCs

## 2.1 Abstract

Extracellular matrixes (ECMs) play a vital role in controlling cell functions because of their similarity to the in vivo microenvironment. The composition of ECMs is not constant but dynamically remolded during stem cell differentiation and tissue development. Development of three-dimensional (3D) biomimetic ECM scaffolds is desirable for investigation of ECM−cell interactions and tissue engineering applications. Here, 3D ECM scaffolds that mimicked the dynamic ECM remodeling during stepwise adipogenesis of human mesenchymal stem cells (hMSCs) were developed. A biodegradable hybrid mesh of poly-(DL-lactic-co-glycolic acid) and collagen was used as a template for cell culture. hMSCs were cultured in the hybrid mesh, and their adipogenic differentiation was controlled at early, late, and undifferentiated stages. Three types of stepwise 3D ECM hybrid scaffolds were prepared from the cultured cells after decellularization. They are mesenchymal stem cell ECM scaffold (SC-ECM scaffold), early-stage adipogenesis-mimicking ECM scaffold (EA-ECM scaffold), and late-stage adipogenesis-mimicking ECM scaffold (LA-ECM scaffold). The stepwise 3D ECM scaffolds had a different composition that was dependent on the differentiation stage of hMSCs. They also showed a different effect on the adipogenic differentiation of hMSCs. The EA-ECM scaffold promoted, while the SC-ECM and LA-ECM scaffolds inhibited the adipogenic differentiation of hMSCs.

## 2.2 Introduction

Extracellular matrixes (ECMs) are a supramolecular network that consists of a variety of proteins, proteoglycans, and glycosaminoglycans. .[1] Cellular interaction with ECMs can directly or indirectly regulate cellular behaviors such as cell proliferation,[2] migration[3] and stem cell differentiation.[4-6] It is important to investigate the interactions between ECMs and cells because *in vivo* cells are always surrounded and interact with ECMs.

Biomimetic matrices and materials have been designed for investigation of ECM roles in the regulation of stem cell functions and tissue engineering.[7-9] Some in vitro ECM models have been developed by isolated

ECM components or decellularized ECMs.[10-12] Isolated ECMs components such as collagen, laminin, fibronectin and so on have been coated on cell culture plates and tissue engineering scaffolds.[13-15] Isolated ECMs components have the advantages of well controlled composition. However, isolated ECMs components have a limitation to mimic the complex components and structures of ECMs. In contrast, decellularized ECMs have the advantage to mimic the complex components and structures of *in vivo* ECMs microenvironments. Decellularized ECMs from tissues and organs have been broadly explored and used for tissue engineering.[16-20] Except decellularized tissues and organs ECMs, decellularized ECMs biomaterials have also been prepared from cell culture.[21-24] Cell-derived ECMs is more readily customizable through the use of different types of cells,[25] thereby avoiding the problem of donor shortage of decellularized tissues and organs. Cell-derived ECMs have another advantage to dynamically mimic the remodeling ECMs components. Their composition can be adjusted thorough controlling the differentiation conditions and different differentiation stages. Cell-derived ECMs can resume the dynamic change or remodeling of ECMs during stepwise differentiation of stem cells or stepwise development of tissues and organs. They can also mimic the ECMs of different diseases at different stages. Cell-derived ECMs are good models for tissue engineering and investigation of ECM-cell interaction.[26] Human mesenchymal stem cells (hMSCs) have been cultured on two-dimensional (2D) cell-culture plates in different differentiation medium to prepare dynamically remodeling ECMs that mimic the adipose and bone tissue development.[27-29] 2D substrates are good for cell expansion culture.[30] However, for tissue engineering applications and investigation of three-dimensional (3D) ECMs-cell interactions, 3D scaffolds are required. Therefore, it is highly desirable to develop 3D ECMs scaffolds from cultured cells to mimic *in vivo* ECMs microenvironment for investigation of ECMs-cell interactions and tissue engineering applications.

3D ECMs scaffolds need reinforcement by other biomaterials because their mechanical strength is too low. When cell-derived ECMs scaffolds are used for cell culture, they are curled and shrunk by cells to form pellets due to their very low mechanical properties.[31] Tissues and organs of our body have a broad range of elasticity and fat tissue has an elasticity of 3 kPa.[32] Scaffolds should have an elasticity to match that of the native tissues and organs. To enhance the mechanical strength of ECMs components such as collagen and gelatin, hybrid scaffolds of PLGA, PLLA and collagen, gelatin have been reported by using the hybridization method.[35-37] In particular, PLGA-collagen hybrid mesh has shown high mechanical property and good biocompatibility.[38, 39] It is anticipated that PLGA-collagen hybrid mesh can be used as a good mechanical supporting skeleton for deposition of cell-derived ECMs components to prepare tissue development-mimicking 3D ECMs scaffolds.

PLGA and collagen porous scaffolds have been used for adipose tissue engineering.[40-41] They have shown supportive effects on adipogenesis. Furthermore, ECMs from decellularized adipose tissues have been reported to have conducive effect on adipogenesis.[42] Therefore, in this study, the three components (PLGA, collagen and adipose tissue-derived ECMs) were hybridized for preparation of adipose tissue engineering scaffolds and the hybrid scaffolds were used for investigation of their effects on adipogenic differentiation of hMSCs. Furthermore, the ECMs components were prepared from hMSCs controlled at different stages of adipogenesis to mimic the dynamic ECMs remodeling (Figure 2.1). PLGA-collagen hybrid mesh was used as a support for the deposition of ECMs components during cell culture. hMSCs were cultured in the PLGA-collagen hybrid mesh and their adipogenic differentiation were controlled at early (EA), late (LA) and undifferentiated (SC) stages. Three types of 3D ECMs-deposited PLGA-collagen hybrid meshes including stem cell-mimicking ECMs scaffold (SC-ECMs scaffold), early stage adipogenesis-mimicking ECMs scaffold (EA-ECMs scaffold) and late stage adipogenesis-mimicking ECMs scaffold (LA-ECMs scaffold) were prepared from the cells of different stages. The compositions of the ECMs scaffolds were examined and their influence on hMSCs functions was investigated.

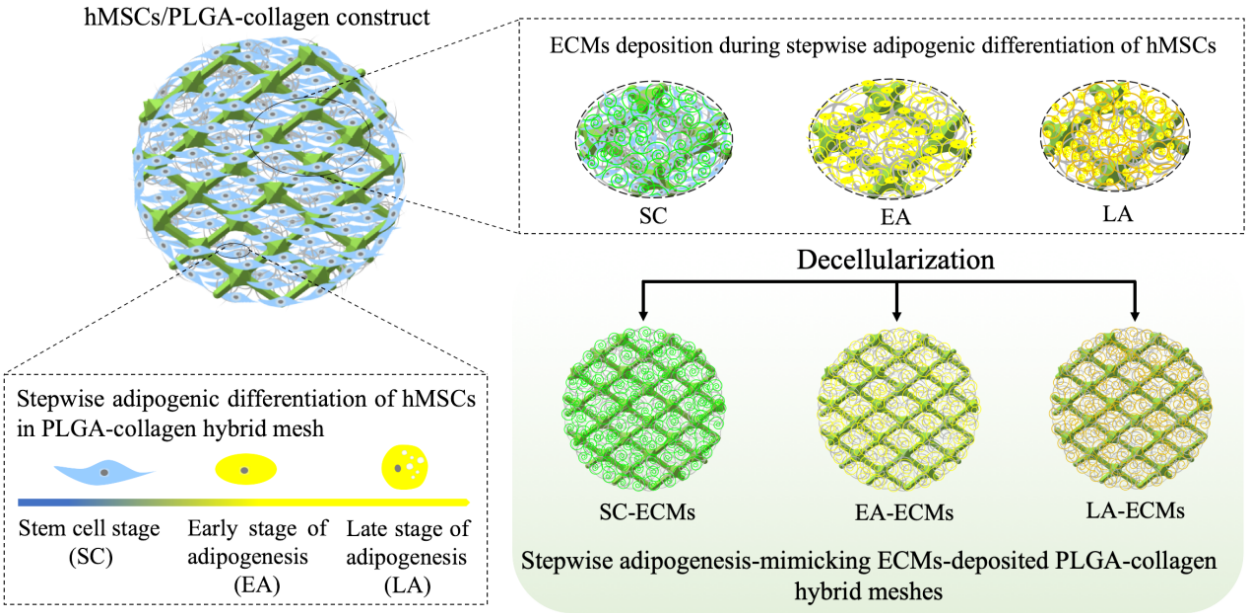


Figure 2.1. Schematic illustration of deposition of stepwise adipogenesis-mimicking ECMs in PLGA-collagen hybrid meshes.

## 2.3 Materials and methods

### 2.3.1 Preparation of PLGA−Collagen Hybrid Meshes and Culture of Cells in the Hybrid Meshes for Stepwise Differentiation

PLGA−collagen hybrid meshes were prepared by forming microsponges of collagen in the open spaces of a PLGA-knitted mesh. [40] Aqueous solution of bovine collagen I (0.5 (w/v)%) was eluted to fill the open spaces of PLGA mesh and the PLGA mesh/collagen solution constructs were frozen at -80 °C. After lyophilization and cross-linking, the hybrid meshes were obtained. The gross appearance and cross-section of PLGA mesh and PLGA−collagen hybrid mesh were recorded with a microscope. Their microporous structures were observed with a scanning electron microscope (SEM, S-4800, Hitachi, Japan).

Human mesenchymal stem cells (hMSCs, passage 4, Lonza Walkersville, MD) were used for cell culture. During hMSC seeding, a glass ring with a diameter of 12 mm (outer Ø) was used to prevent cell leakage. Briefly, 200 μL of cell suspension in MSCGM at a density of $2.5 \times 10^6$ cells/mL was dropped in each glass ring to allow hMSCs adhering in each mesh disk. Then, they were cultured for 6 h. After that, the same number of hMSCs was seeded on another side of the PLGA−collagen hybrid mesh. The cells in the medium not attached in the scaffolds were collected and counted by a cytometer for the calculation of cell seeding efficiency (n = 3). After another 12 h of culture, the culture medium was changed to an adipogenic induction medium for stepwise adipogenic differentiation. The cell/PLGA− collagen composites were cultured for 3 or 14 days to control the stepwise adipogenic differentiation of hMSCs. The composites were cultured in the basal medium for 1 week, which was between 3 and 14 days, to maintain the undifferentiated hMSCs. All of the media were changed every 2 days. The adipogenic medium and basal medium were prepared according to our previous reports. [27]

To confirm adipogenic differentiation, lipoprotein lipase (LPL) was used as a marker for early stage adipogenesis and lipid vacuoles were used as a marker of late stage adipogenesis. The cell/PLGA−collagen mesh composites were fixed with 4% paraformaldehyde and stained with Oil Red O solution. The qualitative and quantitative analyzes of lipid vacuoles in the cells were performed according to our previous study.[41] Expression of *LPL* was analyzed with real-time PCR. Total RNA of hMSCs cultured in hybrid meshes was extracted by using sepasol solution (Nacalai Tesque, Kyoto, Japan) according to our previous work.[42] 1 μg of total RNA was converted to the template cDNA by MuLV Reverse Transcriptase (Applied Biosystems, Foster City, CA). Afterwards, real-time PCR was analyzed and followed by 40 cycles of amplification. The expression levels were calculated by using a $2^{-\Delta\Delta Ct}$ method. Results were relative to the control groups after normalization to GAPDH. Information of primers and probes are shown in Table 1.

Table 1.
Primers and probes for real-time PCR analysis.

| mRNA | Description | Oligonucleotide |
|---|---|---|
| 18 S rRNA | | Hs99999901_s1 |
| *GAPDH* | glyceraldehyde-3-phosphate dehydrogenase | Hs99999905_m1 |
| *PPARG* | Peroxisome proliferator-activated receptor gamma | Hs01115510_m1 |
| *LPL* | Lipoprotein lipase | Hs00173425_m1 |
| *FABP4* | Fatty acid binding protein 4 | Hs00609791_m1 |
| *FASN* | Fatty acid synthase | Hs00188012_m1 |
| *CEBPA* | CCAAT/enhancer binding protein | Hs00269972_s1 |

### 2.3.2 Decellularization

After stepwise culture, samples were decellularized according our previous method.[17] Briefly, cells/PLGA-collagen hybrid mesh composites were frozen and thawed for 6 cycles and then immersed in 20 mM ammonia hydroxide aqueous solution for 20 minutes. After decellularization, the composites were frozen and freeze-dried for next experiments.

The cellular components were examined before and after decellularization. Cell nucleus was visualized by staining with DAPI for 10 min at 25 $^{o}$C. Actin filaments were stained by phalloidin-Alexa 488 (Invitrogen, Carlsbad, CA) for 20 minutes at 25 $^{o}$C.

### 2.3.3 Characterization of ECMs-deposited PLGA-collagen hybrid meshes

SEM observation and immunocytochemical staining were used to confirm the microstructure and ECMs deposition. The hMSCs/ECMs-PLGA-collagen composites and ECMs-deposited PLGA-collagen hybrid meshes were observed by SEM under an operating voltage of 3 kV. ECMs components in the ECMs-deposited PLGA-collagen hybrid meshes were examined by immunocytochemical staining. All the anti-human antibodies were purchased from Santa Cruz, including anti-collagen I antibody (SC-293182), anti-biglycan antibody (SC-100857), anti-decorin antibody (SC-73896), anti-versican antibody (SC-47769), anti-laminin α4 antibody (SC-130541) and anti-fibronectin antibody (SC-8422). Every three samples were used for the staining. The immunocytochemical staining intensity was analyzed by an Image J software (National Institutes of Health, Bethesda, MD). For each sample, four views were randomly selected to measure the positively stained intensity

(20 × magnification for every view). The staining intensity was calculated by the formula: Intensity = integrated density/area. (Integrated density and area were calculated by this Image J software).

DNA content of hMSCs/PLGA-collagen composites before or after decellularization was measured according to the instruction of DNA quantification kit (Sigma). Every four samples were used for the measurement (n = 4). The decellularization efficiency was calculated by the formula: (DNA content before decellularization - DNA content after decellularization)/DNA contents before decellularization × 100. Data represent means ± S.D. (n = 4).

### 2.3.4 Evaluation of adhesion and proliferation of hMSCs in ECMs-deposited PLGA-collagen hybrid meshes

hMSCs were seeded in ECMs-deposited PLGA-collagen hybrid mesh. After culture for 24 hours, some samples were taken out for SEM observation. The samples were fixed by 2.5% glutaraldehyde for 1 hour at 25 $^{o}$C. After washing, they were dehydrated in a graded ethanol-water series (v/v%) from 50% to 100% ethanol, followed by immersion in t-butylalcohol-ethanol solutions (from 50 to 100 (v/v%)). The samples were freeze-dried, coated with platinum and observed with an SEM. Cell number in the scaffolds after 6 hours culture (adhesion cell number) was measured and divided with the total number of seeded cells to calculate adhesion cell percentage. After being cultured for 6 hours after cell seeding, the cells in the medium and not attached in the scaffolds were collected and counted by a cytometer for calculation of adhesion cell number (n = 3). Some samples were cultured for 3 days and cell viability was examined by using calcein-AM and propidium iodide (PI) staining reagents (Cellstain Double Staining Kit, Dojindo, Japan). For proliferation assay, hMSCs were cultured in the scaffolds for 1, 3 and 7 days with basal medium. Proliferation of hMSCs in the scaffolds was determined by using a WST-1 assay kit (Roche Diagnostics, IN, USA).

### 2.3.5 Evaluation of Adipogenic differentiation of hMSCs in ECMs-deposited PLGA-collagen hybrid meshes

hMSCs were cultured in the PLGA-collagen and ECMs-deposited PLGA-collagen hybrid scaffolds with or without adipogenic induction factors in culture medium. Adipogenic differentiation of hMSCs was investigated by evaluation of lipid vacuoles accumulation and adipogenesis-related gene expression. The adipogenesis-related genes including *LPL*, fatty acid binding protein 4 (*FABP4*), fatty acid synthase (*FASN*), peroxisome proliferator activated receptor gamma (*PPAGR*) and CCAAT/enhancer binding protein (*CEBPA*) were analyzed by real-time PCR (n = 4).

### 2.3.6 Statistical analysis

Triple or quadruple samples were used for the snalyses. Date are presented as means ± standard deviations (S.D.). Two-tailed t-tests were used to determine the significance between two groups. One-way ANOVA with a Tukey post hoc test was used to analyze multiple groups. *P* values less than 0.05 were considered significant differences.

## 2.4 Results

### 2.4.1 PLGA-collagen hybrid mesh characterization

The hybrid mesh was prepared by forming web-like collagen microsponges in the void spaces of a PLGA knitted mesh (Figure 2.2a, b). Gross appearance of PLGA-collagen hybrid mesh showed that collagen microsponges were homogeneously formed in the openings of PLGA knitted mesh and the vertical cross-section photographs showed the hybrid mesh had same thickness of around 200 μm as that of PLGA meshes (Figure 2.2c). SEM image at a high magnification indicated that the fibers of collagen microsponges and the fiber bundles of PLGA mesh were physically locked (Figure 2.2e). The unique structure could provide sufficient surface area for cell adhesion and ECMs deposition and provide high mechanical property to support the whole scaffold.

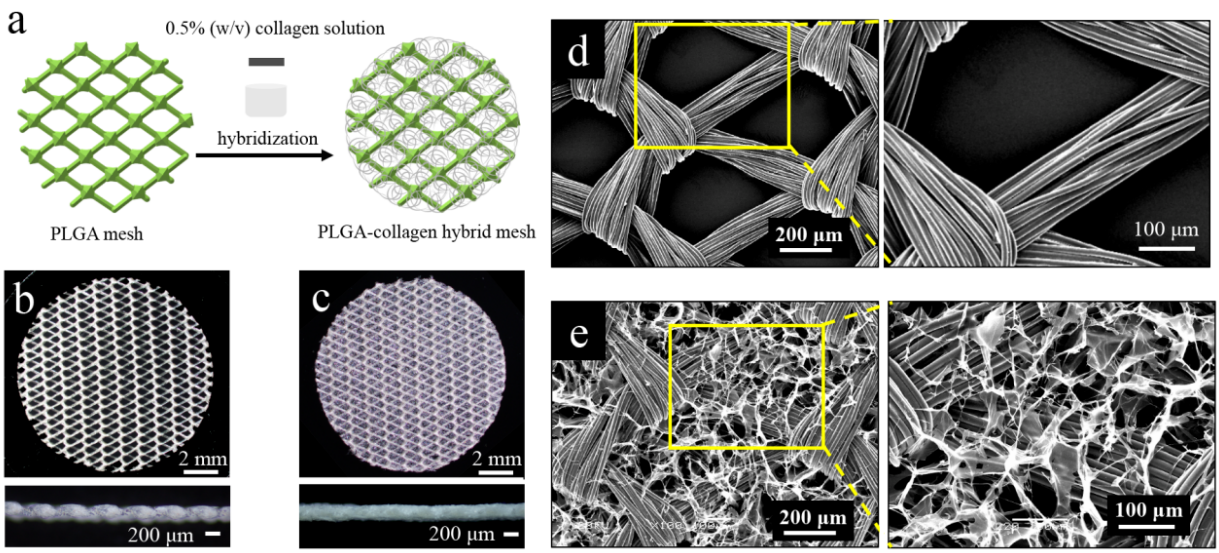


Figure 2.2. Preparation and characterization of PLGA-collagen hybrid mesh. Hybridization of PLGA and collagen (a). Gross appearance of PLGA knitted mesh (b) and PLGA-collagen hybrid mesh (c). SEM image of PLGA knitted mesh (d) and PLGA-collagen mesh (e).

### 2.4.2 Stepwise adipogenic differentiation

hMSCs were seeded in the PLGA-collagen hybrid mesh (Figure 2.3a) and their adipogenic differentiation was induced by culture in adipogenic induction medium. The cell seeding efficiency was 89.4 ± 1.1%. The cells attached in the hybrid meshed and began to spread after culture for 6 hours (Figure 2.3b). Staining of cell nucleus showed that the cells were homogeneously distributed in the hybrid mesh (Figure 2.3d). With increase of culture time, the cells proliferated and produced extracellular matrices to fill the void spaces in the hybrid mesh (Figure 2.3c). After culture for 3 days, cell distribution was still homogeneous in the hybrid mesh (Figure 2.3e). The homogeneous distribution of hMSCs in the PLGA-collagen hybrid meshes ensured the homogenous deposition of ECMs secreted from the cultured cells.

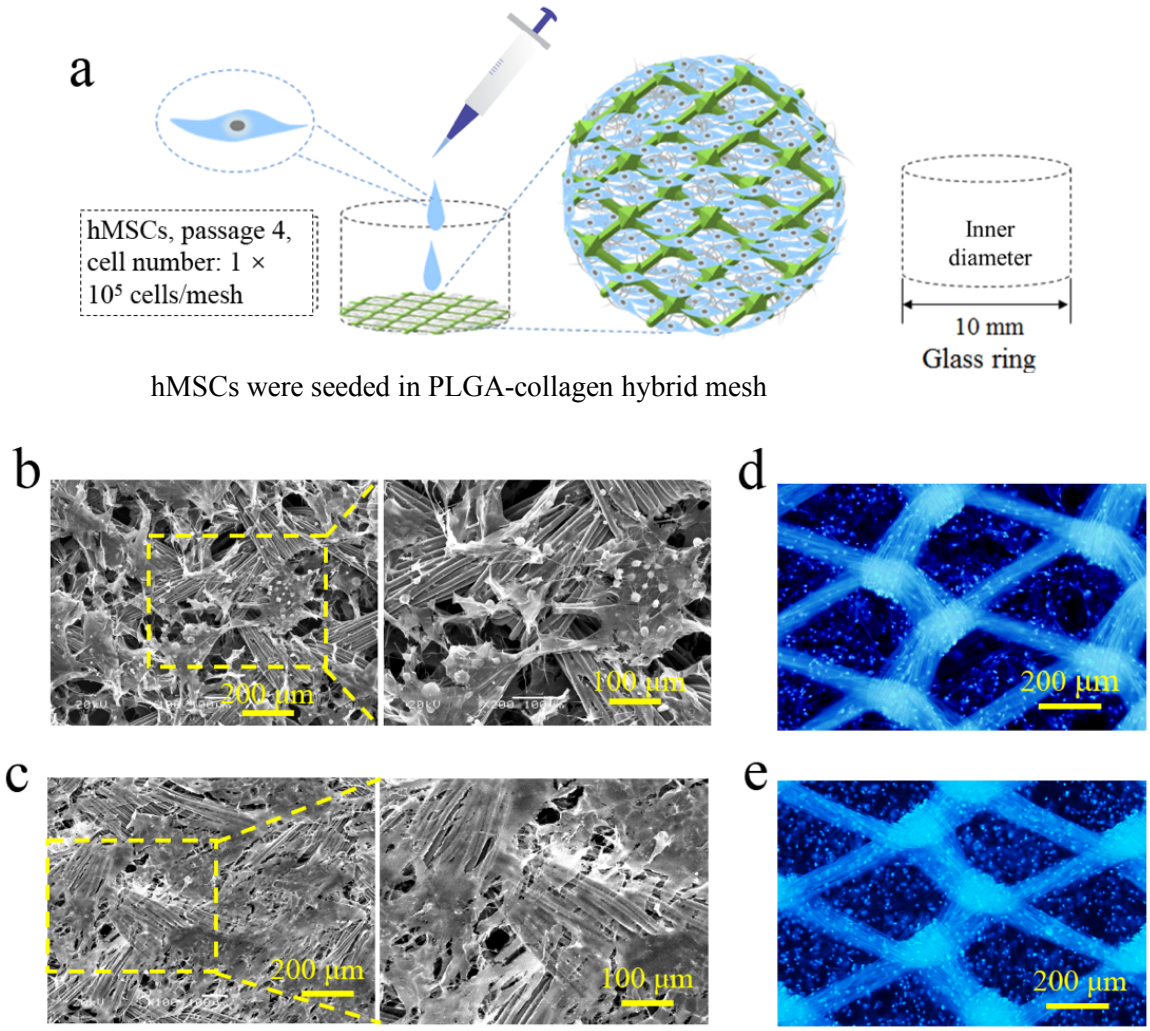


Figure 2.3. Cell seeding and distribution of hMSCS in the PLGA-collagen hybrid mesh. Cell seeding scheme in the PLGA-collagen hybrid mesh (a). SEM images of hMSCs cultured in the PLGA-collagen hybrid mesh for 6 hours (b) and 3 days (c). Nucleus staining of hMSCs after being cultured in the PLGA-collagen hybrid mesh for 6 hours (d) and 3 days in DMEM basal medium.

Through controlling the cell culture time, adipogenic differentiation of hMSCs in the hybrid mesh was controlled at early stage and late stage (Figure 2.4a). The early stage and late stage of adipogenic differentiation of hMSCs were confirmed by Oil Red O staining (Figure 2.4b) and real time PCR analysis (Figure 2.4c). *LPL* is an early stage marker of adipogenesis and lipid vacuoles a late stage marker of adipogenesis.[43, 44] As shown in Figure 2.4b and c, strong staining of lipid vacuoles was only observed after being cultured for 14 days. On the other hand, *LPL* was highly expressed after 3 days of culture in adipogenic medium. Based on these results, adipogenic differentiation of hMSCs in the PLGA-collagen hybrid mesh after 3 and 14 days of culture in adipogenic medium were defined as early stage (EA) and late stage (LA) of adipogenesis, respectively. When hMSCs were cultured in the hybrid mesh in basal medium for 7 days, neither *LPL* gene expression nor lipid vacuoles were detected. Therefore, after 7 days of culture in basal medium, cells were defined as stem cell stage (SC).r

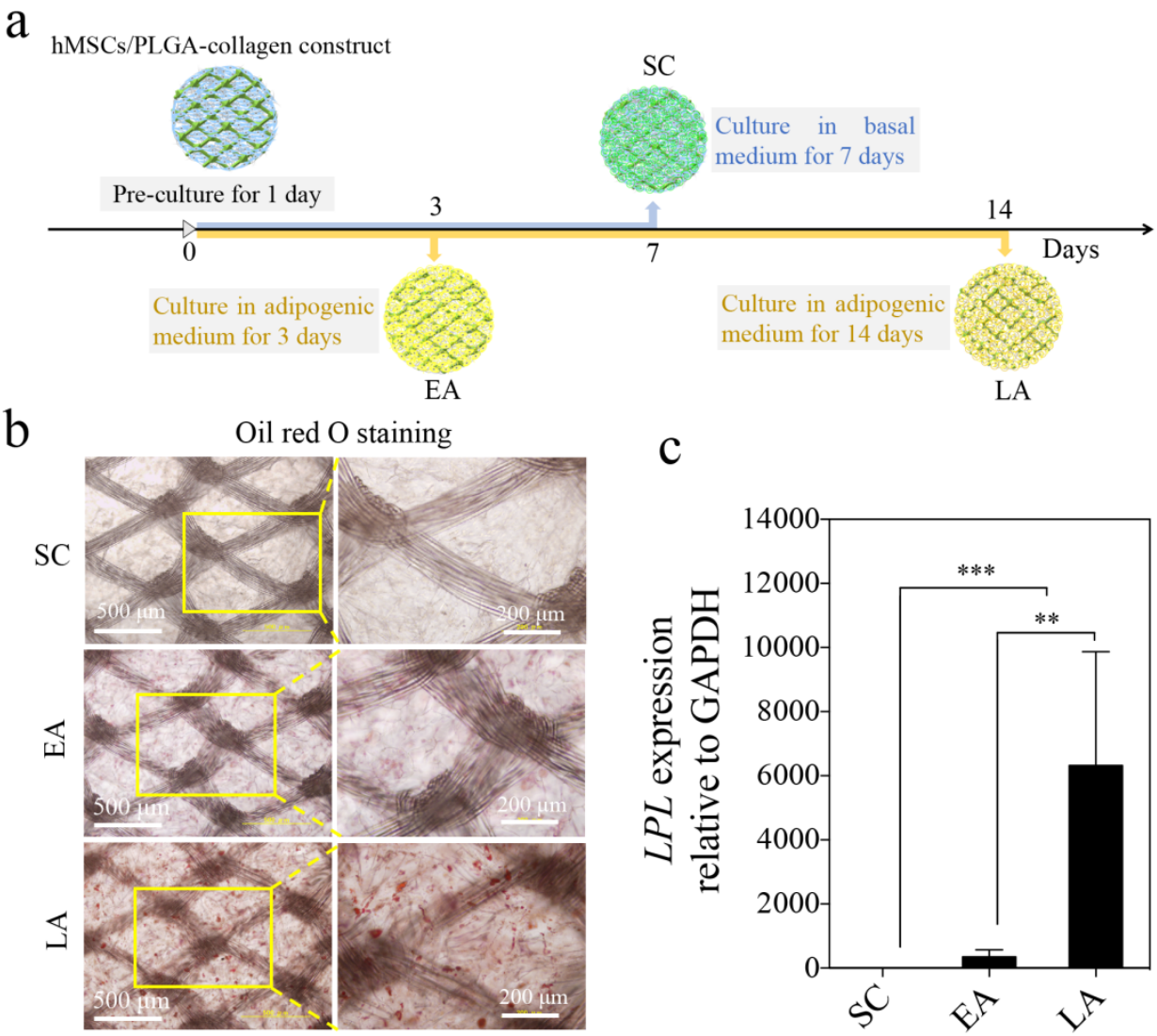


Figure 2.4. Stepwise adipogenic differentiation of hMSCs in the PLGA-collagen hybrid mesh. Cell culture scheme to obtain stem cell stage (SC), early stage (EA) and late stage (LA) of adipogenesis of hMSCs in the hybrid mesh (a). Oil Red O staining of hMSCs after being cultured in the hybrid mesh at different conditions (b). Gene expression of *LPL* in hMSCs after being cultured in the hybrid mesh at different conditions (c).

### 2.4.3 Stepwise adipogenesis-mimicking ECMs-deposited PLGA-collagen hybrid meshes and their compositions

The hMSCs/hybrid mesh constructs where adipogenic differentiation of hMSCs was controlled at early stage of adipogenesis, late stage of adipogenesis and stem cell stage were decellularized to fabricate stepwise adipogenesis-mimicking ECMs-deposited PLGA-collagen hybrid meshes (Figure 2.5a). They were defined as SC-ECMs, EA-ECMs and LA-ECMs, respectively. Fluorescence staining of cell nucleus and F-actin was performed to confirm decellularization (Figure 2.5b). Positive staining of them was observed before decellularization, while they were not observed after decellularization. Furthermore, DNA quantification showed that most of DNA in the hMSCs/hybrid mesh constructs were removed after decellularization (Figure 2.5c). The decellularization efficiency of SC, EA and LA was 99.1 ± 0.8, 98.6 ± 0.3 and 99.6 ± 0.2%,

respectively. The results indicated that most of the cellular components were removed after decellularization. SEM observation showed the cells proliferated and secreted ECMs filling the void spaces in the hMSCs/hybrid mesh constructs before decellularization. After decellularization, cellular components were removed, leaving cell-derived ECMs in the scaffolds and the scaffolds became more porous (Figure 2.5d).

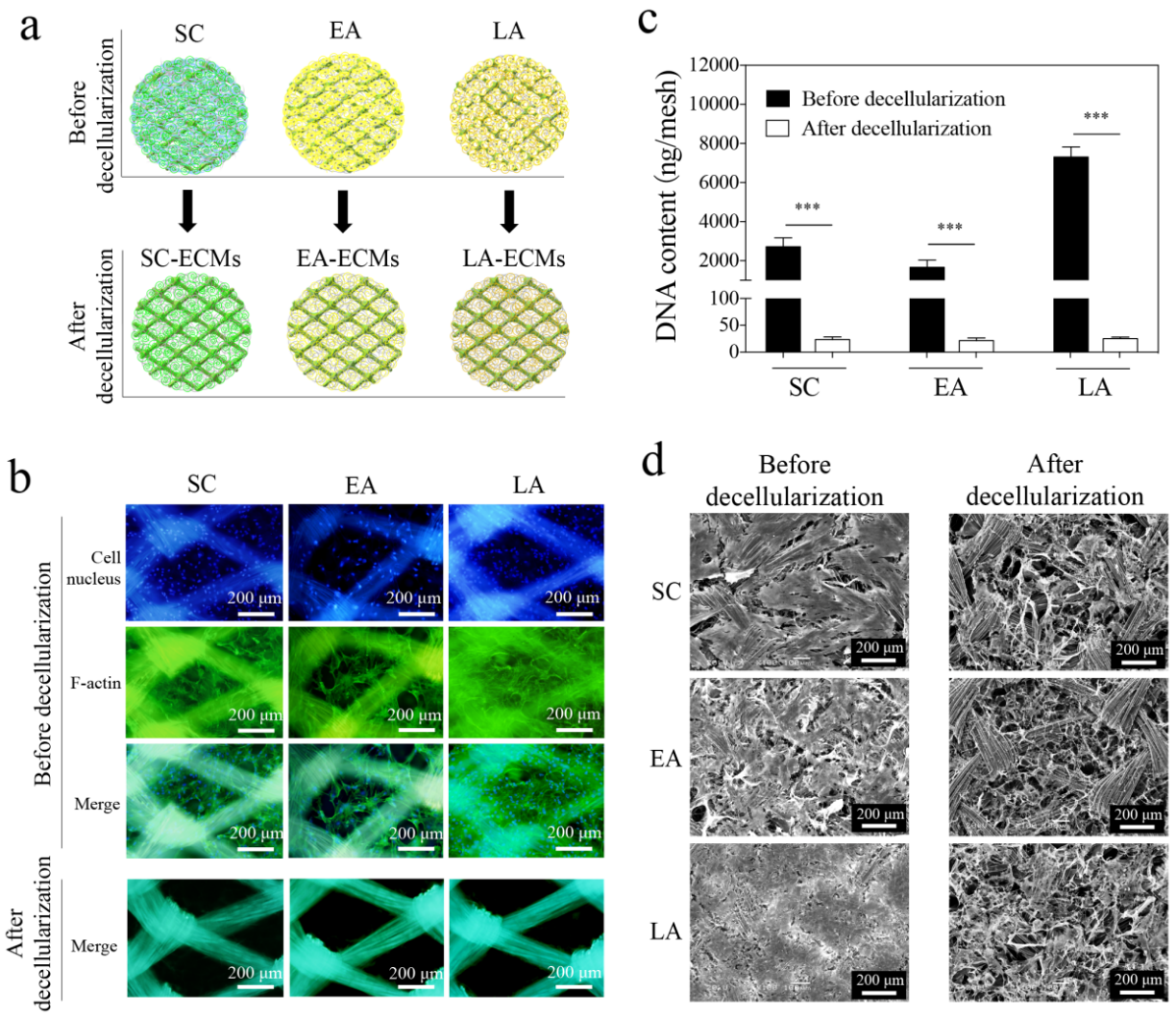


Figure 2.5. Decellularization of cell/hybrid mesh constructs. Decellularization scheme of cell/hybrid mesh constructs (a). Cell nucleus (blue fluorescence) and F-actin cytoskeleton (green fluorescence) staining before and after decellularization to confirm removal of cellular components (b). DNA quantification before and after decellularization (c). SEM images of the cell/hybrid mesh constructs before and after decellularization (d). SC, EA and LA represent the cells at stem cell stage, early stage and late stage of adipogenesis, respectively.

Components of the ECMs-deposited PLGA-collagen hybrid meshes were investigated by immunocytochemical staining of collagen I, fibronectin, laminin α4, versican and decorin (Figure 2.6a). The immunocytochemical staining intensity was quantified by an Image J software (Figure 2.6b). Collagen I, fibronectin, versican and biglycan were strongly detected in SC-scaffolds, but weekly stained in the EA- and LA-ECMs scaffolds. Decorin was weakly detected in SC-ECMs scaffolds, while hardly detected in EA-EMC and LA-ECMs scaffolds. All these five types of ECMs components decreased during the progress of adipogenesis. On the other hand, laminin α4 increased during the adipogenesis progress and was strongly

stained in LA-ECMs scaffolds. The results indicated that ECMs components in the hybrid meshes were remodeled during stepwise adipogenesis of hMSCs.

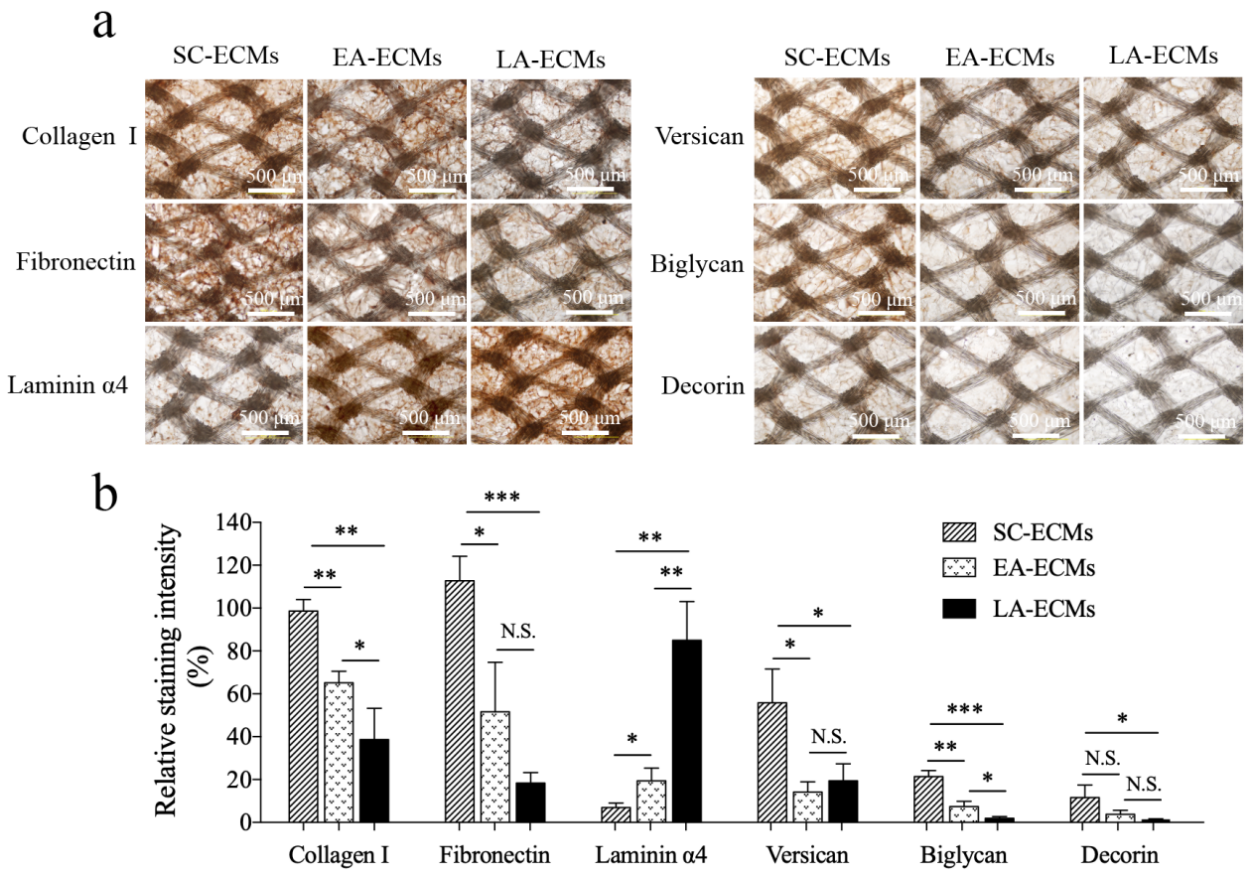


Figure 2.6. Compositional characterization of the stepwise adipogenesis-mimicking ECMs-deposited PLGA-collagen hybrid meshes. Immunocytochemical staining of collagen I, fibronectin, laminin α4, versican, biglycan and decorin in the ECMs scaffolds (a). Quantitative analysis of the immunocytochemical staining intensity (b). The staining density was normalized to that of collagen I in SC-ECMs scaffold.

### 2.4.4 Influence of stepwise adipogenesis-mimicking ECMs-deposited PLGA-collagen hybrid meshes on adhesion and proliferation of hMSCs

SEM observation showed that cells attached and spread well in all the scaffolds after 1 day of culture (Figure 2.7a). The percentage of adhesion cells to the total number of seeded cells was 92.7 ± 2.5, 90.6 ± 1.8 and 95.3 ± 2.1% for SC-ECMs, EA-ECMs and LA-ECMs, respectively. The ECM-deposited hybrid meshes showed slightly higher levels of cell adhesion that the PLGA-collagen hybrid meshes (89.4 ± 1.1 %). The results indicated that the ECMs promoted cell adhesion.

The cells showed high viability in all the scaffolds. During the 7 days culture, the cells proliferated in the scaffolds (Figure 2.7b). The hMSCs cultured in EA-ECMs scaffold for 7 days showed a little slower proliferation than those in PLGA-collagen, SC-ECMs and LA-ECMs scaffolds. The results indicated that the stepwise adipogenesis-mimicking ECMs-deposited PLGA-collagen hybrid meshes supported cell adhesion and proliferation.

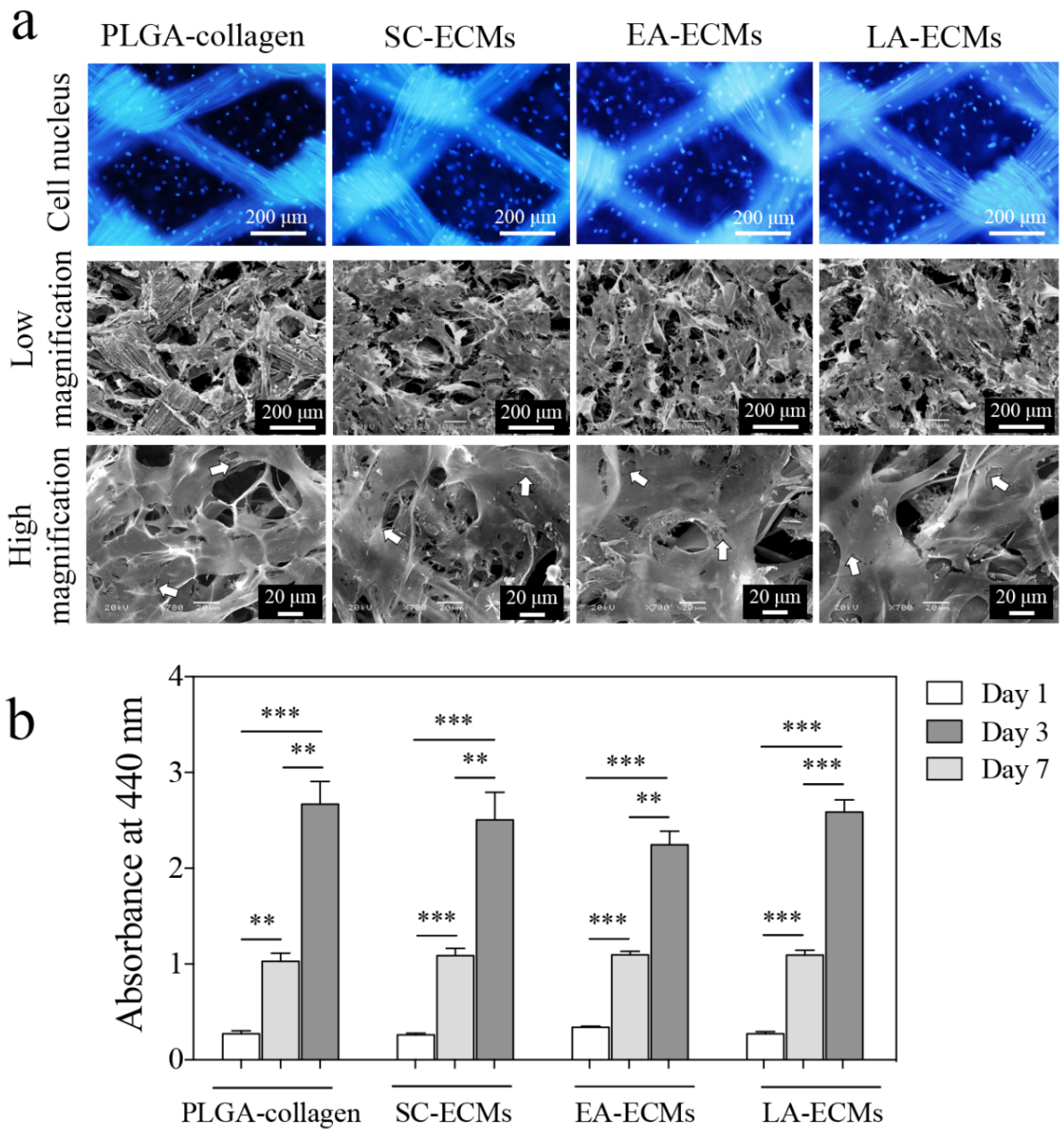


Figure 2.7. Adhesion and proliferation of hMSCs in the stepwise adipogenesis-mimicking ECMs-deposited PLGA-collagen hybrid meshes. DAPI staining and SEM images of hMSCs after being cultured in the PLGA-collagen hybrid meshes and SC-ECMs, EA-ECMs and LA-ECMs scaffolds for 1 day (a). White arrows indicate the stretched cells. Proliferation of hMSCs after being cultured in the scaffolds for 1, 3 and 7 days (b).

### 2.4.5 Influence of stepwise adipogenesis-mimicking ECMs-deposited PLGA-collagen hybrid meshes on adipogenic differentiation of hMSCs.

After hMSCs were cultured in basal medium (without adipogenic induction factor) for 14 days, no obvious lipid vacuoles were observed in any of the constructs (Figure 2.8a). Quantitative analysis of extracted Oil Red O dye showed that the absorbance was low and there was no significant difference between each group (Figure 2.8b). Furthermore, no significant differences of PPARG and LPL expression were observed among

the scaffolds (Figure 2.8c, e). Expression level of CEBPA and FASN in the cells cultured in EA-ECMs scaffolds was significantly higher than that in LA-ECMs scaffolds (Figure 2.8d, g). Expression level of FABP4 in the cells cultured in EA-ECMs scaffolds was significantly higher than that in other groups (Figure 2.8f). The results indicated that EA-ECMs scaffolds showed a little higher effect on adipogenic gene expression of hMSCs than did other scaffolds when basal medium was used for culture.

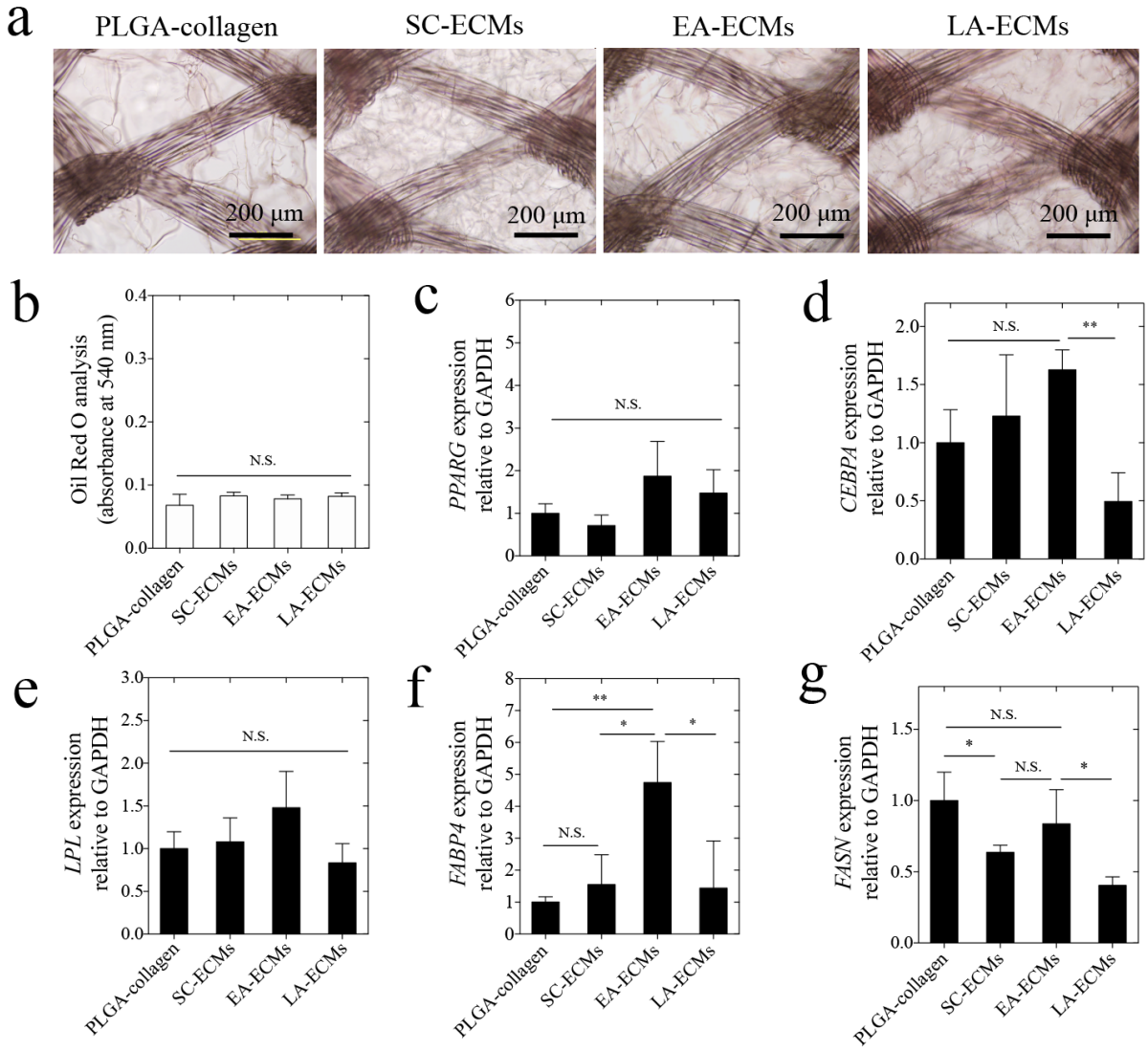


Figure 2.8. Adipogenic differentiation of hMSCs in the stepwise adipogenesis-mimicking ECMs-deposited PLGA-collagen hybrid meshes in basal medium without adipogenic induction factors. Representative images of Oil Red O staining of hMSCs in the scaffolds (a). Quantification of stained lipid vacuoles (b). Real time PCR analysis of PPARG (c), CEBPA (d), LPL (e), FABP4 (f) and FASN (g) genes.

After 14 days culture in adipogenic induction medium, the lipid vacuoles were detected in the hMSCs cultured in all the scaffolds (Figure 2.9a). Quantification of the stained lipid vacuoles showed that hMSCs cultured in the EA-ECMs scaffolds showed the most amount of lipid droplets (Figure 2.9b). The cells cultured in the SC-ECMs and LA-ECMs scaffolds had lower lipid droplets than did the cells cultured in PLGA-collagen hybrid mesh. Gene expression results showed that the hMSCs cultured in EA-ECMs scaffolds showed the highest expression level of PPARG, CEBPA, LPL, FABP4 and FASN, while the expression of these genes in hMSCs cultured in the SC-ECMs and LA-ECMs scaffolds was significantly lower than that in cells cultured in PLGA-collagen scaffolds (Figure 2.9c-g). The results indicated that EA-ECMs scaffolds promoted

adipogenic differentiation of hMSCs. On the other hand, the SC-ECMs and LA-ECMs scaffolds had an inhibitory effect on adipogenesis of hMSCs. In comparison with the expression of these genes by hMSCs cultured in PLGA-collagen hybrid meshes (before decellularization), hMSCs cultured in LA-ECMs scaffolds showed the highest gene expression, followed with late stage (LA) of adipogenesis in PLGA-collagen hybrid mesh (Figure 2.10). Expression of these genes by SC cells was the lowest, followed with early stage (EA) and late stage (LA) of adipogenesis in PLGA-collagen hybrid mesh.

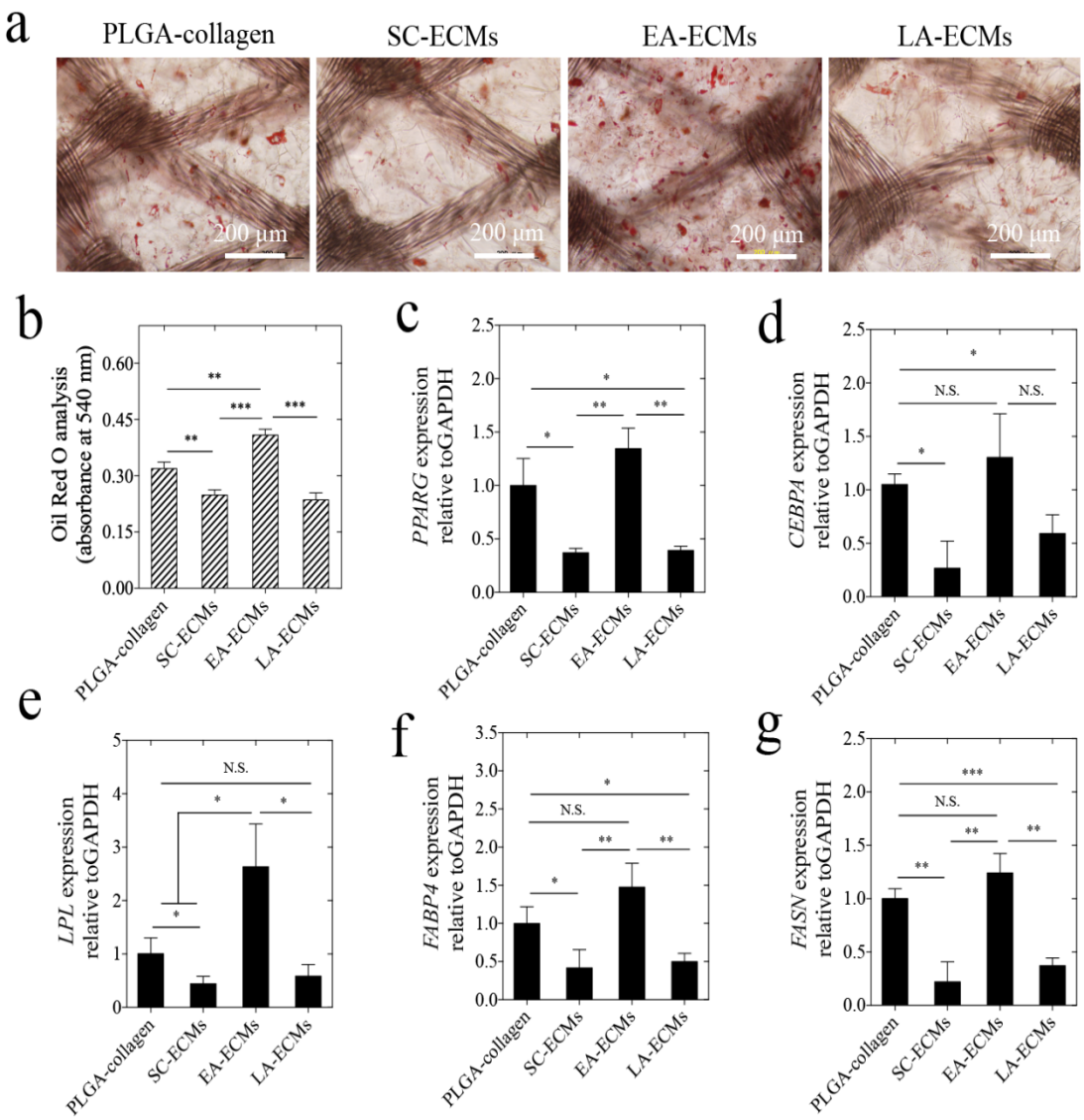


Figure 2.9. Adipogenic differentiation of hMSCs in the stepwise adipogenesis-mimicking ECMs-deposited PLGA-collagen hybrid meshes in adipogenic induction medium. Representative images of Oil Red O staining of hMSCs in the scaffolds (a). Quantification of stained lipid vacuoles (b). Real time PCR analysis of PPARG (c), CEBPA (d), LPL (e), FABP4 (f) and FASN (g) genes.

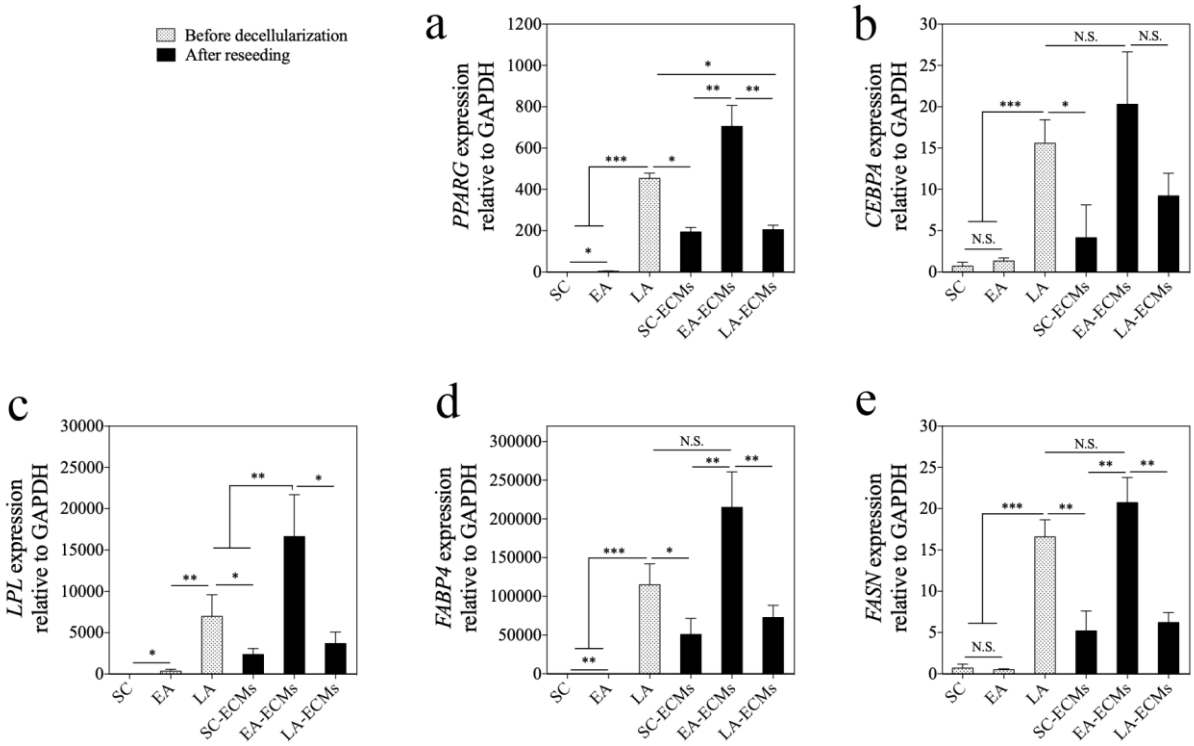


Figure 2.10. Comparison of adipogenic differentiation markers of hMSCs before decellularization and after reseeding of hMSCs in decellularized PLGA-collagen-ECMs scaffolds. Real time PCR analysis of *PPARG* (c), *CEBPA* (d), *LPL* (e), *FABP4* (f) and *FASN* (g) genes.

### 2.4.6 Discussion

ECMs surrounding cells in vivo are extremely important to control cell functions through direct interactions with cells.[45] Some of the tissue-derived ECMs products have been approved by FDA and been widely applied in tissue engineering.[46] However, tissue-derived ECMs cannot mimic the dynamical remodeling of ECMs during tissue development and stem cell differentiation. Preparation of ECMs that mimic such dynamic ECMs remodeling is desirable for investigation of ECMs-cell interactions and tissue engineering applications. On the other hand, in recent years, cell-derived ECMs have been extensively studied because of their easy availability and tunability.[47, 48] The composition of cell-derived ECMs can be tuned by changing cell culture conditions.[28, 29]

In this study, ECMs mimicking the ECMs remodeling during adipogenesis of hMSCs were prepared by controlling the adipogenic differentiation stage of hMSCs. A PLGA-collagen hybrid mesh was used to serve as a template to prepare the 3D cell-derived ECMs scaffolds. The PLGA-collagen hybrid mesh has been reported useful for tissue engineering applications.[38, 49, 50] hMSCs cultured in the PLGA-collagen hybrid mesh attached, proliferated and produced ECMs in the hybrid meshes. By adjusting culture time in adipogenic induction medium, the adipogenic differentiation of hMSCs in the PLGA-collagen hybrid mesh was controlled at early stage (3 days) and late stage (14 days) of adipogenesis. hMSCs cultured in the hybrid mesh with basal medium was maintained at stem cell stage. The stepwise adipogenic differentiation of hMSCs in the PLGA-collagen hybrid meshes was confirmed by gene expression of early stage adipogenesis marker, LPL, and staining of late stage adipogenesis marker, lipid vacuoles. After decellularization of the cells/scaffold constructs, three types of stepwise adipogenesis-mimicking ECMs-deposited PLGA-collagen hybrid meshes (SC-ECMs, EA-ECMs and LA-ECMs scaffolds) were obtained.

Immunological staining of collagen I, fibronectin, laminin α4, versican, biglycan and decorin showed different expression levels of these proteins in the 3D ECMs scaffolds. Composition of the 3D ECMs scaffolds was dependent on the adipogenesis stages. It has been reported that laminin α4 is the predominant component in native adipose tissue and a shift from fibronectin-rich stromal matrices to laminin α4-rich basement membrane is an indicative of onset of adipogenesis.[51, 52] Weakening of collagen I surrounding adipose tissue can improve the survival rate of adipocytes.[53] The change of fibronectin, laminin α4 and collagen I in the ECMs scaffolds was in a good agreement with the previous studies. The stepwise adipogenesis-mimicking ECMs-deposited PLGA-collagen hybrid meshes could reflect the ECMs composition remodeling of adipogenesis.

The stepwise adipogenesis-mimicking ECMs-deposited PLGA-collagen hybrid meshes supported adhesion and proliferation of hMSCs. The influence of the SC-ECMs, EA-ECMs and LA-ECMs scaffolds on adipogenic differentiation of hMSCs was compared with that of PLGA-collagen hybrid meshes. The EA-ECMs scaffolds promoted adipogenesis of hMSCs, while the SC-ECMs and LA-ECMs showed inhibitory effect on adipogenesis of hMSCs. The influence of the ECMs scaffolds required the synergistic effect of adipogenic induction factors in the medium. The ECMs scaffolds themselves had limited influence on adipogenic differentiation when basal medium was used.

The different effect of the ECMs scaffolds on adipogenesis of hMSCs should be due to the different ECMs composition in the ECMs scaffolds. Previous studies have demonstrated that fibronectin can interact with integrin α5β1, which is highly expressed on cell surface in preadipocytes, and inhibit adipogenesis by activating signaling pathway.[54, 55] Fibronectin was strongly detected in the SC-ECMs scaffolds but weakly detected in the EA-ECMs scaffolds and LA-ECMs scaffolds. High content of fibronectin in SC-ECMs scaffold should have inhibitory effect on adipogenesis of hMSCs. High concentration of laminin α4 can suppress adipogenesis through bounding to integrin families or blocking the interaction of fibroblast growth factor (FGF) with cells.[56] High expression of laminin α4 in the LA-ECMs scaffold should also have inhibitory effect on adipogenesis of hMSCs. The components in the ECMs scaffolds should have combination effect on cell functions. The composition of EA-ECMs scaffolds, where the expression level of collagen I, fibronectin, laminin α4, versican, biglycan and decorin was between that in SC-ECMs and LA-ECMs scaffolds, seemed to be most favorable for adipogenesis of hMSCs. The stepwise adipogenesis-mimicking ECMs-deposited PLGA-collagen hybrid meshes should be useful for investigation of ECMs-cell interactions and tissue engineering applications.

## 2.5 Conclusions

In summary, the ECMs-deposited PLGA-collagen hybrid meshes were prepared by culturing hMSCs in PLGA-collagen hybrid mesh and by controlling their adipogenic differentiation degree at stem cell stage, early and late stages. The ECMs were deposited in the PLGA-collagen hybrid mesh and their components were dependent on the differentiation stage of hMSCs. They also had different influence on adipogenic differentiation of hMSCs. The ECMs scaffold mimicking the early stage of adipogenesis enhanced the adipogenic differentiation of MSCs, while the ECMs scaffold mimicking the stem cell stage of MSCs or late stage of adipogenesis showed an inhibitory effect.

## 2.6 References

[1] G.S. Hussey, J.L. Dziki, S.F. Badylak, Extracellular matrix-based materials for regenerative medicine,

Nature Reviews Materials 3(7) (2018) 159-173.
[2] M. An, K. Kwon, J. Park, D.R. Ryu, J.A. Shin, J. Lee Kang, J.H. Choi, E.M. Park, K.E. Lee, M. Woo, M. Kim, Extracellular matrix-derived extracellular vesicles promote cardiomyocyte growth and electrical activity in engineered cardiac atria, Biomaterials 146 (2017) 49-59.
[3] J. Lou, R. Stowers, S. Nam, Y. Xia, O. Chaudhuri, Stress relaxing hyaluronic acid-collagen hydrogels promote cell spreading, fiber remodeling, and focal adhesion formation in 3D cell culture, Biomaterials 154 (2018) 213-222.
[4] X. Wang, Z. Chen, B. Zhou, X. Duan, W. Weng, Cell-Sheet-Derived ECM Coatings and Their Effects on BMSCs Responses, (2018).
[5] C. Bonnans, J. Chou, Z. Werb, Remodelling the extracellular matrix in development and disease, Nat Rev Mol Cell Biol 15(12) (2014) 786-801.
[6] H. Ragelle, A. Naba, B.L. Larson, F. Zhou, M. Prijić, C.A. Whittaker, A. Del Rosario, R. Langer, R.O. Hynes, D.G. Anderson, Comprehensive proteomic characterization of stem cell-derived extracellular matrices, Biomaterials 128 (2017) 147-159.
[7] K. Jiang, D. Chaimov, S.N. Patel, J.P. Liang, S.C. Wiggins, M.M. Samojlik, A. Rubiano, C.S. Simmons, C.L. Stabler, 3-D physiomimetic extracellular matrix hydrogels provide a supportive microenvironment for rodent and human islet culture, Biomaterials 198 (2019) 37-48.
[8] W. Yang, Q. Chen, R. Xia, Y. Zhang, L. Shuai, J. Lai, X. You, Y. Jiang, P. Bie, L. Zhang, H. Zhang, L. Bai, A novel bioscaffold with naturally-occurring extracellular matrix promotes hepatocyte survival and vessel patency in mouse models of heterologous transplantation, Biomaterials 177 (2018) 52-66.
[9] X. Wang, Z. Chen, B. Zhou, X. Duan, W. Weng, K. Cheng, H. Wang, J. Lin, Cell-Sheet-Derived ECM Coatings and Their Effects on BMSCs Responses, ACS applied materials & interfaces 10(14) (2018) 11508-11518.
[10] W.C. Chen, Z. Wang, M.A. Missinato, D.W. Park, D.W. Long, H.J. Liu, X. Zeng, N.A. Yates, K. Kim, Y. Wang, Decellularized zebrafish cardiac extracellular matrix induces mammalian heart regeneration, Science advances 2(11) (2016) e1600844.
[11] F. Pati, J. Jang, D.H. Ha, S. Won Kim, J.W. Rhie, J.H. Shim, D.H. Kim, D.W. Cho, Printing three-dimensional tissue analogues with decellularized extracellular matrix bioink, Nature communications 5 (2014) 3935.
[12] I.G. Kim, J. Ko, H.R. Lee, S.H. Do, K. Park, Mesenchymal cells condensation-inducible mesh scaffolds for cartilage tissue engineering, Biomaterials 85 (2016) 18-29.
[13] B.M. Gaub, D.J. Muller, Mechanical Stimulation of Piezo1 Receptors Depends on Extracellular Matrix Proteins and Directionality of Force, Nano letters 17(3) (2017) 2064-2072.
[14] M. Jiang, J. Qiu, L. Zhang, D. Lu, M. Long, L. Chen, X. Luo, Changes in tension regulates proliferation and migration of fibroblasts by remodeling expression of ECM proteins, Experimental and therapeutic medicine 12(3) (2016) 1542-1550.
[15] E. Lih, K.W. Park, S.Y. Chun, H. Kim, T.G. Kwon, Y.K. Joung, D.K. Han, Biomimetic Porous PLGA Scaffolds Incorporating Decellularized Extracellular Matrix for Kidney Tissue Regeneration, ACS applied materials & interfaces 8(33) (2016) 21145-21154.
[16] J.W. Lee, S. Chae, S. Oh, S.H. Kim, K.H. Choi, M. Meeseepong, J. Chang, N. Kim, K. Yong Ho, N.E. Lee, J.H. Lee, J.Y. Choi, Single-Chain Atomic Crystals as Extracellular Matrix-Mimicking Material with Exceptional Biocompatibility and Bioactivity, Nano letters 18(12) (2018) 7619-7627.
[17] H. Lu, T. Hoshiba, N. Kawazoe, G. Chen, Autologous extracellular matrix scaffolds for tissue engineering, Biomaterials 32(10) (2011) 2489-99.
[18] A.E. Jakus, M.M. Laronda, A.S. Rashedi, C.M. Robinson, C. Lee, S.W. Jordan, K.E. Orwig, T.K.

Woodruff, R.N. Shah, "Tissue Papers" from Organ-Specific Decellularized Extracellular Matrices, Adv Funct Mater 27(3) (2017).
[19] T. Rezaei Topraggaleh, M. Rezazadeh Valojerdi, L. Montazeri, H. Baharvand, A testis-derived macroporous 3D scaffold as a platform for the generation of mouse testicular organoids, Biomaterials science 7(4) (2019) 1422-1436.
[20] S.R. Cerqueira, Y.S. Lee, R.C. Cornelison, M.W. Mertz, R.A. Wachs, C.E. Schmidt, M.B. Bunge, Decellularized peripheral nerve supports Schwann cell transplants and axon growth following spinal cord injury, Biomaterials 177 (2018) 176-185.
[21] T. Hoshiba, Cultured cell-derived decellularized matrices: a review towards the next decade, Journal of Materials Chemistry B 5(23) (2017) 4322-4331.
[22] H. Ragelle, A. Naba, B.L. Larson, F. Zhou, M. Prijic, C.A. Whittaker, A. Del Rosario, R. Langer, R.O. Hynes, D.G. Anderson, Comprehensive proteomic characterization of stem cell-derived extracellular matrices, Biomaterials 128 (2017) 147-159.
[23] Y. Teng, X. Li, Y. Chen, H. Cai, W. Cao, X. Chen, Y. Sun, J. Liang, Y. Fan, X. Zhang, Extracellular matrix powder from cultured cartilage-like tissue as cell carrier for cartilage repair, Journal of Materials Chemistry B 5(18) (2017) 3283-3292.
[24] B. Nyambat, C.-H. Chen, P.-C. Wong, C.-W. Chiang, M.K. Satapathy, E.-Y. Chuang, Genipin-crosslinked adipose stem cell derived extracellular matrix-nano graphene oxide composite sponge for skin tissue engineering, Journal of Materials Chemistry B 6(6) (2018) 979-990.
[25] C.-Y. Gao, Z.-H. Huang, W. Jing, P.-F. Wei, L. Jin, X.-H. Zhang, Q. Cai, X.-L. Deng, X.-P. Yang, Directing osteogenic differentiation of BMSCs by cell-secreted decellularized extracellular matrixes from different cell types, Journal of Materials Chemistry B 6(45) (2018) 7471-7485.
[26] W. Wei, J. Li, S. Chen, M. Chen, Q. Xie, H. Sun, J. Ruan, H. Zhou, X. Bi, A. Zhuang, Z. You, P. Gu, X. Fan, In vitro osteogenic induction of bone marrow mesenchymal stem cells with a decellularized matrix derived from human adipose stem cells and in vivo implantation for bone regeneration, Journal of Materials Chemistry B 5(13) (2017) 2468-2482.
[27] R. Cai, T. Nakamoto, T. Hoshiba, N. Kawazoe, G. Chen, Matrices secreted during simultaneous osteogenesis and adipogenesis of mesenchymal stem cells affect stem cells differentiation, Acta biomaterialia 35 (2016) 185-93.
[28] T. Hoshiba, N. Kawazoe, T. Tateishi, G. Chen, Development of stepwise osteogenesis-mimicking matrices for the regulation of mesenchymal stem cell functions, The Journal of biological chemistry 284(45) (2009) 31164-73.
[29] T. Hoshiba, N. Kawazoe, T. Tateishi, G. Chen, Development of extracellular matrices mimicking stepwise adipogenesis of mesenchymal stem cells, Advanced materials (Deerfield Beach, Fla.) 22(28) (2010) 3042-7.
[30] I. Hilmi, A. Lotnyk, J.W. Gerlach, P. Schumacher, B. Rauschenbach, Influence of substrate dimensionality on the growth mode of epitaxial 3D-bonded GeTe thin films: From 3D to 2D growth, Materials & Design 168 (2019) 107657.
[31] H. Lu, T. Hoshiba, N. Kawazoe, I. Koda, M. Song, G. Chen, Cultured cell-derived extracellular matrix scaffolds for tissue engineering, Biomaterials 32(36) (2011) 9658-66.
[32] D.E. Discher, D.J. Mooney, P.W. Zandstra, Growth factors, matrices, and forces combine and control stem cells, Science 324(5935) (2009) 1673-7.
[33] F. Pu, N.P. Rhodes, Y. Bayon, J.A. Hunt, In vitro cellular response to oxidized collagen-PLLA hybrid scaffolds designed for the repair of muscular tissue defects and complex incisional hernias, J Tissue Eng Regen Med 10(10) (2016) E454-e466.
[34] G. Chen, T. Ushida, T. Tateishi, Hybrid Biomaterials for Tissue Engineering: A Preparative Method for

PLA or PLGA–Collagen Hybrid Sponges, Advanced Materials 12(6) (2000) 455-457.
[35] X. He, H. Lu, N. Kawazoe, T. Tateishi, G. Chen, A novel cylinder-type poly(L-lactic acid)-collagen hybrid sponge for cartilage tissue engineering, Tissue engineering. Part C, Methods 16(3) (2010) 329-38.
[36] H. Lu, H.H. Oh, N. Kawazoe, K. Yamagishi, G. Chen, PLLA–collagen and PLLA–gelatin hybrid scaffolds with funnel-like porous structure for skin tissue engineering, Science and technology of advanced materials 13(6) (2012) 064210.
[37] G. Chen, T. Ushida, T. Tateishi, Poly(DL-lactic-co-glycolic acid) sponge hybridized with collagen microsponges and deposited apatite particulates, Journal of Biomedical Materials Research 57(1) (2001) 8-14.
[38] G. Chen, T. Sato, T. Ushida, R. Hirochika, Y. Shirasaki, N. Ochiai, T. Tateishi, The use of a novel PLGA fiber/collagen composite web as a scaffold for engineering of articular cartilage tissue with adjustable thickness, Journal of biomedical materials research. Part A 67(4) (2003) 1170-80.
[39] G. Chen, T. Sato, H. Ohgushi, T. Ushida, T. Tateishi, J. Tanaka, Culturing of skin fibroblasts in a thin PLGA–collagen hybrid mesh, Biomaterials 26(15) (2005) 2559-2566.
[40] G. Chen, T. Ushida, T. Tateishi, A hybrid network of synthetic polymer mesh and collagen sponge, Chemical Communications (16) (2000) 1505-1506.
[41] J. Li, J. Zhang, Y. Chen, N. Kawazoe, G. Chen, TEMPO-Conjugated Gold Nanoparticles for Reactive Oxygen Species Scavenging and Regulation of Stem Cell Differentiation, ACS applied materials & interfaces 9(41) (2017) 35683-35692.
[42] N. Kawazoe, C. Inoue, T. Tateishi, G. Chen, A cell leakproof PLGA-collagen hybrid scaffold for cartilage tissue engineering, Biotechnology progress 26(3) (2010) 819-26.
[43] J. Frith, P. Genever, Transcriptional Control of Mesenchymal Stem Cell Differentiation, Transfusion Medicine and Hemotherapy 35(3) (2008) 216-227.
[44] K.F. Moseley, M.E. Doyle, S.M. Jan De Beur, Diabetic serum from older women increases adipogenic differentiation in mesenchymal stem cells, Endocrine research (2018) 1-11.
[45] F.A. Monibi, J.L. Cook, Tissue-Derived Extracellular Matrix Bioscaffolds: Emerging Applications in Cartilage and Meniscus Repair, Tissue engineering. Part B, Reviews 23(4) (2017) 386-398.
[46] C.W. Cheng, L.D. Solorio, E. Alsberg, Decellularized tissue and cell-derived extracellular matrices as scaffolds for orthopaedic tissue engineering, Biotechnology advances 32(2) (2014) 462-84.
[47] W. Zhang, Y. Zhu, J. Li, Q. Guo, J. Peng, S. Liu, J. Yang, Y. Wang, Cell-Derived Extracellular Matrix: Basic Characteristics and Current Applications in Orthopedic Tissue Engineering, Tissue engineering. Part B, Reviews 22(3) (2016) 193-207.
[48] S. Liu, S. Mou, C. Zhou, L. Guo, A. Zhong, J. Yang, Q. Yuan, J. Wang, J. Sun, Z. Wang, Off-the-Shelf Biomimetic Graphene Oxide–Collagen Hybrid Scaffolds Wrapped with Osteoinductive Extracellular Matrix for the Repair of Cranial Defects in Rats, ACS applied materials & interfaces 10(49) (2018) 42948-42958.
[49] G. Chen, T. Sato, H. Ohgushi, T. Ushida, T. Tateishi, J. Tanaka, Culturing of skin fibroblasts in a thin PLGA-collagen hybrid mesh, Biomaterials 26(15) (2005) 2559-66.
[50] W. Dai, N. Kawazoe, X. Lin, J. Dong, G. Chen, The influence of structural design of PLGA/collagen hybrid scaffolds in cartilage tissue engineering, Biomaterials 31(8) (2010) 2141-52.
[51] E. Jeffery, C.D. Church, B. Holtrup, L. Colman, M.S. Rodeheffer, Rapid depot-specific activation of adipocyte precursor cells at the onset of obesity, Nature cell biology 17(4) (2015) 376-85.
[52] J. Liu, S.M. DeYoung, M. Zhang, M. Zhang, A. Cheng, A.R. Saltiel, Changes in integrin expression during adipocyte differentiation, Cell metabolism 2(3) (2005) 165-77.
[53] T. Khan, E.S. Muise, P. Iyengar, Z.V. Wang, M. Chandalia, N. Abate, B.B. Zhang, P. Bonaldo, S. Chua, P.E. Scherer, Metabolic dysregulation and adipose tissue fibrosis: role of collagen VI, Molecular and cellular biology 29(6) (2009) 1575-91.

[54] B.M. Spiegelman, C.A. Ginty, Fibronectin modulation of cell shape and lipogenic gene expression in 3t3-adipocytes, Cell 35(3, Part 2) (1983) 657-666.
[55] D.B. Bosco, M.D. Roycik, Y. Jin, M.A. Schwartz, T.J. Lively, D.A. Zorio, Q.A. Sang, A new synthetic matrix metalloproteinase inhibitor reduces human mesenchymal stem cell adipogenesis, 12(2) (2017) e0172925.
[56] H. Yamashita, C. Goto, R. Tajima, A.T. Koparal, M. Kobori, Y. Ohki, K. Shitara, R. Narita, K. Toriyama, S. Torii, Cryptic fragment α4 LG4‐5 derived from laminin α4 chain inhibits de novo adipogenesis by modulating the effect of fibroblast growth factor‐2, Development Growth & Differentiation 50(2) (2008) 97-107.

# Chapter 3

# PLGA-collagen-ECM hybrid meshes mimicking stepwise osteogenesis and their influence on the osteogenic differentiation of hMSCs

## 3.1 Abstract

Extracellular matrixes (ECMs) are dynamically altered and remodeled during tissue development. How the dynamic remodeling of ECM affects stem cell functions remains poorly understood due to the difficulty of obtaining biomimetic ECMs. In this study, stepwise osteogenesis-mimicking ECM-deposited hybrid meshes were prepared by culturing hMSCs in PLGA-collagen hybrid meshes and controlling the stages of the osteogenesis of hMSCs. Three types of hybrid mesh mimicking the ECMs from stem cell stage of hMSCs (SC-ECM), early stage (EO-ECM) and late stage (LO-ECM) osteogenesis of hMSCs were prepared. The stepwise osteogenesis-mimicking ECM deposited PLGA-collagen hybrid meshes showed different ECM compositions associated with the stage of osteogenesis, their effects on the osteogenic differentiation of hMSCs differed. EO-ECM scaffold increased and LO-ECM scaffold moderately promoted the osteogenic differentiation of hMSCs. However, SC-ECM scaffold inhibited the osteogenic differentiation of hMSCs. The novel PLGA-collagen-ECM hybrid meshes will provide useful tools for stem cell culture and tissue engineering.

## 3.2 Introduction

Bone marrow cell-derived extracellular matrixes (ECMs) can provide a comfortable microenvironment for the maintaining human mesenchymal stem cell (hMSC) activity [1], controlling the cell adhesion [2], migration [3, 4] and regulating lineage diversity of hMSCs [5]. Furthermore, cells can mediate remodeling of ECMs through the secretion of bioactive molecules such as matrix metalloproteinases (MMPs) [6] and large amounts of ECMs [7]. The regulation of hMSC behavior mainly relies on ECM-cell interactions [8-11]. Recently, investigations of human bone marrow cell-derived ECMs and how ECM elements interact with hMSCs to modulate their functions have attracted broad attention. The most used materials for investing of ECM-cell interactions is from various tissue-derived ECMs [12-14]. However, this strategy is associated with several bottlenecks, such as limited availability of donor tissues and organs [15-17]. The motivation

to tackle these problems has led to the development of cultured cell-derived ECM for stem cell culture [18-20]. The use of cultured cell-derived ECM presents a promising way for mimicking native tissue microenvironment. Moreover, decellularized ECMs from *in vitro* cultured cells have been prepared as supporting scaffolds [5, 21-25]. The cultured cell-derived ECMs not only serve as materials supporting cell adhesion but also provide various bioactive molecules and factors that interact with cell surface receptors, thus possessing a unique signaling capacity.

Recently, some ECM scaffolds derived from cultured cell have been reported [26-28]. For instance, different types of cells derived from different tissues have been used to produce ECM scaffolds that mimic the microenvironment of their natural tissue matrixes [29, 30]. ECMs can be prepared by co-cultureing of hMSCs and human umbilical vein endothelial cells (HUVECs), they promotive ability on osteogenic differentiation of hMSCs has been demonstrated [31, 32]. Until now, most studies have focused on static parameters; however, these parameters are dynamically altered in vivo. Differentiation of stem cells to mature cells has been reported that it passes through stepwise stages of maturation [33-36]. ECMs are dynamically changed and remodeled during the stepwise development process [37]. It has been reported that the amounts of collagen type II [38] and glycosaminoglycan (GAG) [39] increase during chondrogenesis and that laminin proteins are highly secreted if the cells begin to undergo adipogenesis [40, 41]. However, the effect of the dynamic changes in ECMs on cell functions remains poorly understood.

It is highly desirable to generate biomimetic ECMs mimicking the dynamic remodeling of ECMs. Such two-dimensional (2D) ECMs have been prepared by culturing hMSCs in tissue-treated culture plates with different differentiation media [42-44]. However, these 2D microenvironments cannot mimic the *in vivo* three-dimensional (3D) microenvironments. To prepare 3D ECM scaffolds, a mechanical template is required to support the deposited ECMs during cell culture and to provide ECM scaffolds with appropriate mechanical properties. Among the previously reported scaffolds, hybrid scaffolds of poly (lactic-coglycolic acid) (PLGA)-knitted mesh and collagen sponges (PLGA-collagen hybrid mesh) present many advantages [45, 46]. They have exhibited a high mechanical strength and good biocompatibility [47]. Therefore, the PLGA-collagen hybrid mesh was used in this work. Cells were cultured on the PLGA-collagen hybrid meshes and ECMs were in situ deposited on the meshes. A novel type of osteogenesis mimicking 3D ECM scaffold with dynamically changed ECMs was developed. As shown in Scheme 1a, the hMSCs were seeded in the PLGA-collagen hybrid meshes and controlled at the stem cell stage and the early and late stages of osteogenesis. After the deposition of ECMs and further decellularization, the ECM deposited PLGA-collagen hybrid meshes were prepared. The biomimetic hybrid meshes were used for hMSCs culturing and investigating their effects on the functions of hMSCs (Scheme 1b).

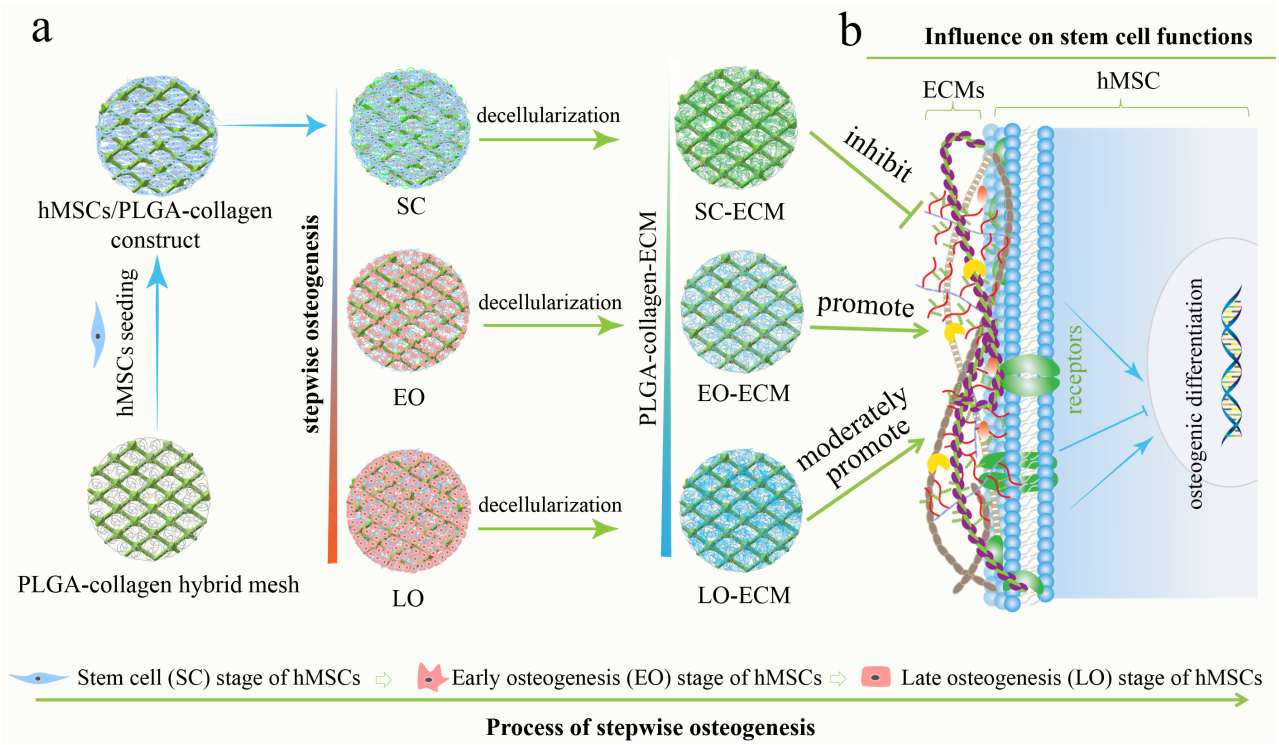


Scheme 1. Schematic illustration of the preparation of PLGA-collagen-ECM hybrid meshes mimicking stepwise osteogenesis (a) and their influence on the proliferation and osteogenic differentiation of hMSCs (b).

## 3.3 Materials and methods

### 3.3.1 PLGA-collagen hybrid mesh preparation

A PLGA-collagen mesh was obtained according to a previously reported method [48, 49]. In brief, PLGA mesh (a 90:10 copolymer of glycolic acid and lactic acid) was first immersed in an acidic bovine collagen solution (collagen type I, 0.5 wt%, Koken, Tokyo, Japan). Then, the mesh was removed from the aqueous collagen solution, with removal of the excess aqueous collagen solution, allowing a thin layer of aqueous collagen solution to fill the spaces of the PLGA mesh. Samples were frozen at -80 °C and freeze dried for 1 day. Thereafter, the harvested constructs were cross-linked with EDC/NHS (concentrations: 50 mM EDC and 20 mM NHS). After cross-linking, the glycine solution (concentration: 1 M in aqueous solution) was used to block the residual activated functional groups. Finally, the excess glycine within the PLGA-collagen mesh was rinsed out using MilliQ water. After being freeze dried, the harvested PLGA-collagen mesh was stored at 4 °C.

### 3.3.2 Culture and osteogenic differentiation of hMSCs

Human mesenchymal stem cells (hMSCs, derived from human bone marrow, passage 2) were obtained from Lonza (Walkersville, MD, LOT NO: 2F3478). The harvested hMSCs were cultured in 75 $cm^2$ tissue culture-treated flasks with MSCBM™ (Lonza, Walkersville, MD) and were further subcultured after confluence. Finally, the hMSCs (at passage 4) were collected by using 0.25% trypsin/EDTA (Sigma, USA). The osteogenic property of the subcultured hMSCs was confirmed before the hMSCs were used for following experiments.

The PLGA-collagen hybrid mesh was cut into round discs with a diameter of 11 mm. The sterilized PLGA-collagen hybrid mesh discs were covered with glass rings (an inner diameter of 10 mm and an out diameter of 12 mm) which were used to protect cell leakage during cell seeding. The expanded cells were seeded in the PLGA-collagen hybrid mesh discs by adding 200 μL of hMSCs suspension solution ($2.5 \times 10^6$ cells/mL) each glass rings and cultured at 37 °C under 5% $CO_2$. After culture for 6 hours, the PLGA-collagen hybrid mesh discs were turned over and another 200 μL of hMSCs suspension solution was seeded on another side of each scaffold. The glass rings were removed after 6 hours and the cells were culture in MSCBM™ for another 1 day. And then the medium was changed to osteogenic medium. The hMSC/scaffold constructs were further cultured with osteogenic medium for 7 days and 21 days to control the osteogenic differentiation of hMSCs at early and late stages, respectively. The media were refreshed every 2 days. The osteogenic medium was prepared according to a previous report [44, 50]. Briefly, low-glucose DMEM with 10% FBS (Gibco, NY) was mixed with 100 nM dexamethasone and 100 mM β-glycerophosphate. To generate hMSCs in an undifferentiated stage, the hMSC/scaffold constructs were cultured in basal medium without osteogenic growth factors for 7 days. The medium was prepared according to our previous report [51].

### 3.3.3 ALP, alizarin red S staining and calcium deposition assays

After the completion of culture, the hybrid samples were washed and then fixed in 4% paraformaldehyde solution for 10 minutes at 4 °C. For ALP staining, the fixed samples were immersed in ALP working solution, which was prepared according to a previous report [52]. Incubation was performed at 25 °C for 10 minutes, followed by washing. To measure calcium deposition in the hybrid meshes, the fixed samples were immersed in a 0.1% alizarin red S solution at 25 °C for 10 minutes and washed with calcium-free PBS solution. For quantitative analysis, the stained samples were air dried and immersed in 5% perchloric acid for 20 minutes to elute the stain. The absorbance of the elution solution was measured at 405 nm using a microplate reader.

### 3.3.4 Decellularization

The decellularization procedure was performed on the hMSC/scaffold constructs after cell culturing [53]. The samples were subjected to 6 freeze and thaw cycles, followed by being immersed in a 20 nM ammonia hydroxide aqueous solution by gentle agitation. Thereafter, the harvest hybrid meshes were collected and stored for further experimental use. To confirm the decellularization efficiency, actin filaments were visualized with phalloidin-Alexa 488 (Invitrogen, Carlsbad, CA). Cell nuclei were stained by DAPI (Dojindo, Kumamoto, Japan).

### 3.3.5 Immunohistochemistry

The immunohistochemical staining was performed on PLGA-collagen-ECM hybrid meshes according the manufacturer's instructions. The rabbit anti-human antibodies were used, including collagen type I, fibronectin, biglycan, decorin, versican and laminin α4 antibody (Santa Cruz, CA). The constructs were observed under an optical microscope. The representative photomicrographs of the stained ECM deposited hybrid mesh were taken at the central regions of hybrid meshes with an

optical microscope.

### 3.3.6 Cell attachment and proliferation assays

After hMSCs were cultured in basal medium for 1 day, the hMSC/PLGA-collagen-ECM hybrid meshes were treated according to our previous methods [24]. After that, the cell/scaffold constructs were sprayed with gold and observed by SEM (JSM-6400Fs; Tokyo, Japan) under an operating voltage of 3 kV.

The proliferation of the hMSCs in the stepwise cell derived ECM-deposited hybrid meshes was determined by using a tetrazolium salt (WST-1) assay kit (Roche). Briefly, $1.0 \times 10^5$ hMSCs were seeded in the ECM deposited hybrid meshes and cultured in basal medium. The medium was refreshed every 2 days. After 1, 3 and 7 days of culture, the WST-1 assay was performed according to the product instructions. After 2 hours of incubation at 37 °C in the dark, 200 μL of the supernatant was transferred to a 96-well culture plate and analyzed at 440 nm with a plate reader. Each sample was evaluated in triplicate in parallel wells.

### 3.3.7 Real-time polymerase chain reaction (RT-PCR):

The Sepasol solution (Nacalai Tesque, Japan) was used to extract the total RNA from hMSCs according to a previously reported method [54]. the SuperScript™ IV VILOTM Mater Mix kit (Invitrogen) was used to reverse the total RNA to cDNA. The cDNA was used as a template for RT-PCR analysis. Afterwards, RT-PCR analysis was conducted in 25 μL of a solution system. The expression levels were calculated according to the comparative Ct method. The results are normalized to GAPDH and reported relative to the control groups. Each target gene was measured 3 times. Information of all the primers and probes was showed in Supplementary Table 1.

Table 1.
Primers and probes for real-time PCR analysis.

| mRNA | Description | Oligonucleotide |
|---|---|---|
| *GAPDH* | glyceraldehyde-3-phosphate dehydrogenase | Hs99999905_m1 |
| | | Forward 5'-GACCCTTGACCCCCACAAT-3' |
| *ALP* | Alkaline phosphatase | Reverse 5'-GCTCGTACTGCATGTCCCCT-3' |
| | | Probe 5'-TGGACTACCTATTGGGTCTCTTCGAGCCA-3' |
| | | Forward 5'-TGCCTTGAGCCTGCTTCC-3' |
| *IBSP* | Bone sialoprotein 2 | Reverse 5'-GCAAAATTAAAGCAGTCTTCATTTTG-3' |
| | | Probe 5'-CTCCAGGACTGCCAGAGGAAGCAATCA-3' |
| | | Forward 5'-CTCAGGCCAGTTGCAGCC-3' |
| *SPP1* | Secreted phosphoprotein 1 | Reverse 5'-CAAAAGCAAATCACTGCAATTCTC -3' |
| | | Probe 5'-AAACGCCGACCAAGGAAAACTCACTACC-3' |

| | | |
|---|---|---|
| *SP7* | Osterix | Hs00541729_m1 |
| *RUNX2* | Runt-related transcription factor-2 | Hs00231692_m1 |

### 3.3.8 Statistical analysis

Significant differences between two experiment groups were determined by a two-tailed t-test. For multiple groups analysis, a one-way analysis of variance was used. For all the statistical tests, *P* values less than 0.05 were considered to indicate significant differences.

## 3.4 Results

### 3.4.1 Stepwise osteogenesis of hMSCs in the PLGA-collagen hybrid mesh

The PLGA-collagen hybrid mesh was harvested via the well-established hybridization method (Figure 3.1a). The web-like collagen microsponges were formed in the openings of the PLGA knitted mesh (Figure 3.1b). Observations under high magnification of SEM showed that collagen fibers extended over the fiber bundles of the PLGA mesh holding the collagen microsponges in the openings (Figure 3.1b).

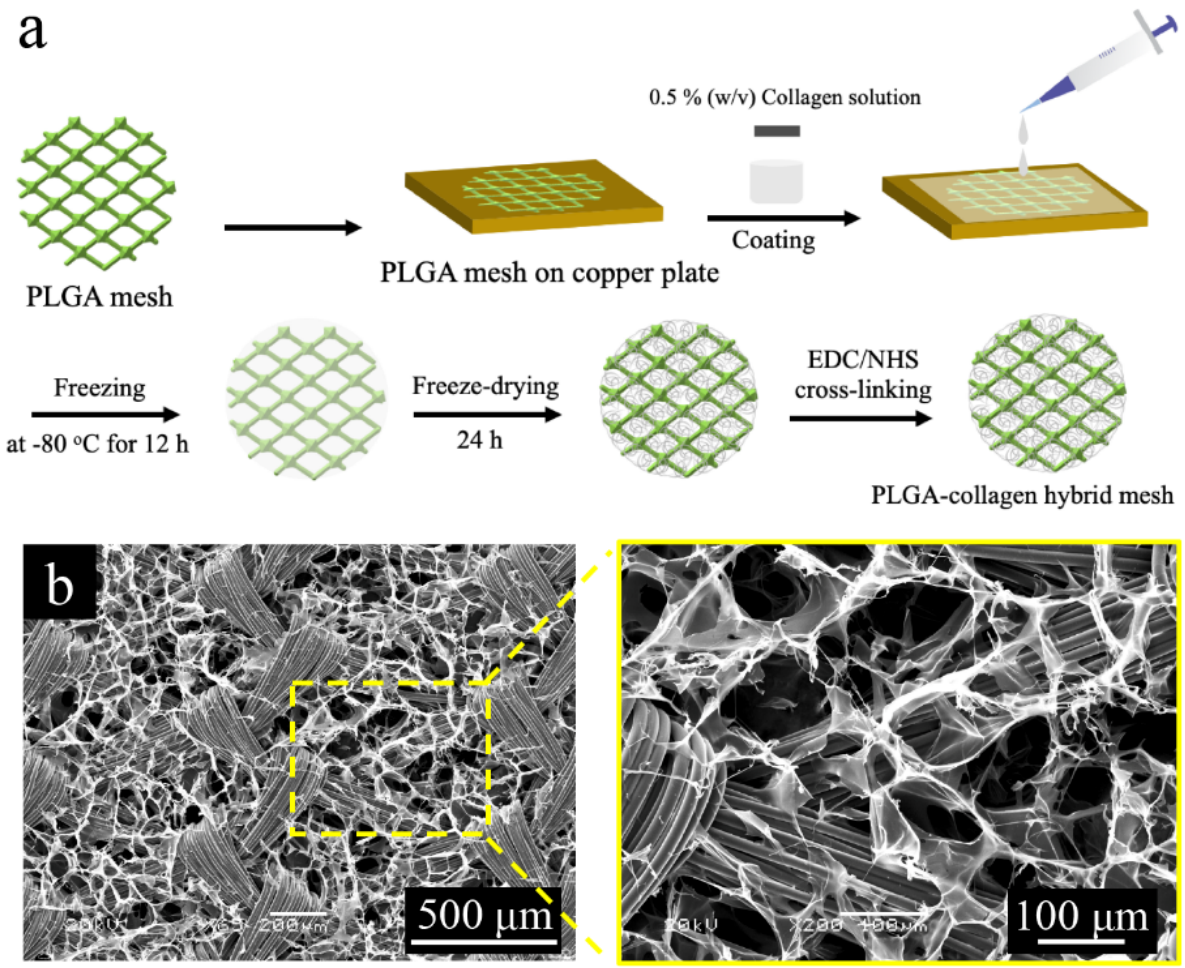


Figure 3.1. Preparation of PLGA-collagen hybrid mesh. Schematic illustration of the hybridization of collagen and PLGA mesh (a). SEM images of the PLGA-collagen hybrid mesh at low and high magnifications (b).

After cell seeding, the hMSCs/PLGA-collagen hybrid mesh was further cultured for 7 days. The results of cell nucleus staining indicated a homogeneous cell distribution (Figure 3.2).

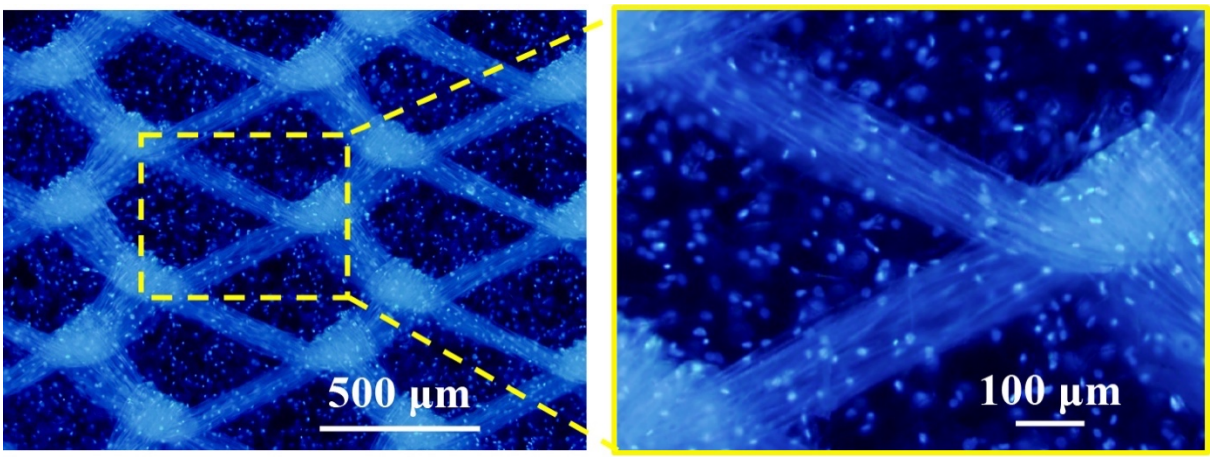


Figure 3.2. Fluorescence microscopy images of hMSCs cultured in the PLGA-collagen hybrid mesh for 7 days after DAPI staining. The blue dots were the stained nuclei of hMSCs.

The stepwise osteogenic differentiation of the hMSCs was performed according to the procedures as shown in Figure 3.3a. The results of staining analysis showed that the cell/PLGA-collagen hybrid mesh constructs showed obvious positive staining for ALP but no obvious calcium deposition after 7 days of culture in osteogenic medium (Figure 3.3b EO). After 21 days, obvious alizarin red S staining was observed in the constructs (Figure 3.3b LO). Both ALP staining and calcium deposition were negative in the hMSCs/PLGA-collagen constructs when being cultured in basal medium for 7 days (Figure 3.3b SC). The expression of *ALP* was high in the cell/hybrid mesh constructs after being cultured in osteogenic medium for 7 days (Figure 3.3c). While, *IBSP* was not highly expressed until the constructs were cultured in osteogenic medium for 21 days. Therefore, the early stage (EO) and late stage (LO) of osteogenesis were defined as 7 days and 21 days, respectively, of hMSC culture in the PLGA-collagen hybrid meshes with osteogenic medium. The stem cell stage (SC) was defined as 7 days of culture of the constructs with basal medium.

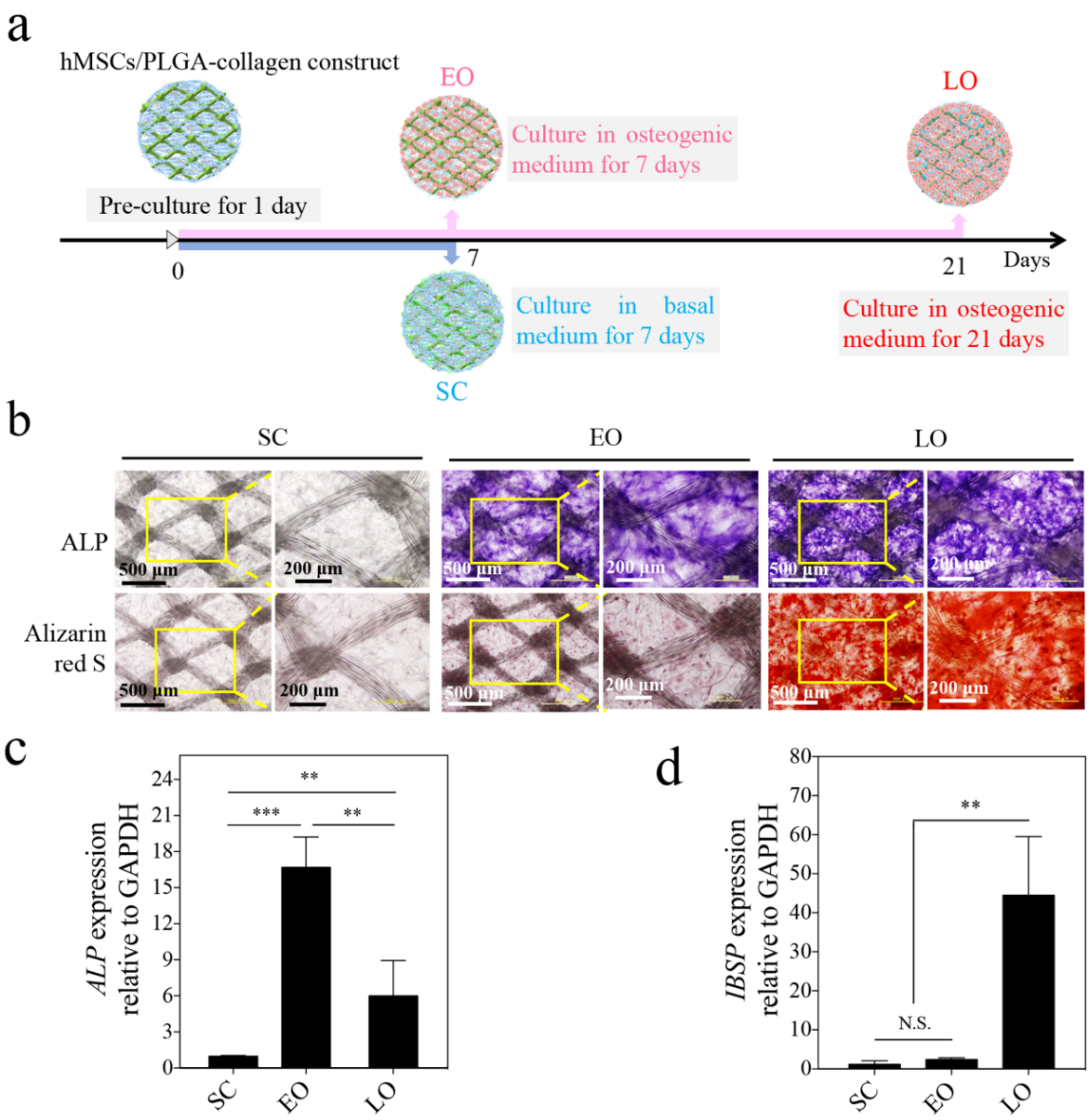


Figure 3.3. Stepwise osteogenic differentiation of hMSCs in the PLGA-collagen hybrid mesh. Cell culture scheme for obtaining hMSCs in the SC, EO, and LO stages of osteogenesis in the hybrid mesh (a). ALP and

alizarin red S staining of hMSCs after being cultured in the hybrid mesh under different conditions (b). Gene expression of *ALP* (c) and *IBSP* (d).

### 3.4.2 Preparation of stepwise osteogenesis mimicking ECM deposited PLGA-collagen hybrid meshes

Decellularization of the cell/hybrid mesh constructs were accorded to a previously reported decellularization method [53]. As shown in Figure 3.4a, stepwise ECM scaffolds were prepared from the constructs in which hMSCs were controlled at SC, EO and LO. The ECM scaffolds were referred to as the SC-ECM scaffold (stem cell stage-mimicking ECM), EO-ECM scaffold (early osteogenesis stage mimicking ECM) and LO-ECM (late osteogenesis stage mimicking ECM) scaffold. To evaluate the efficiency of decellularization, the cell/hybrid mesh constructs were analyzed by actin cytoskeleton staining, cell nucleus staining and DNA quantification. The staining analysis showed that actin proteins and cell nuclei could be fond before decellularization but that positive staining was not observed after decellularization (Figure 3.4b). Quantification of DNA contents before and after decellularization confirmed that 99.1% of the DNA (2638.2 ± 645.1 ng/mesh vs. 23.4 ± 8.9 ng/mesh) in SC, 99% of the DNA (2947.3 ± 635.4 ng/mesh vs. 27.1 ± 5.3 ng/mesh) in EO and 99.5% of the DNA (10472.1 ± 902.9 ng/mesh vs. 42.6 ± 4.3 ng/mesh) in LO was removed by decellularization (Figure 3.4c). The staining and DNA contents analysis showed that the cell components were effective removed after decellularization.

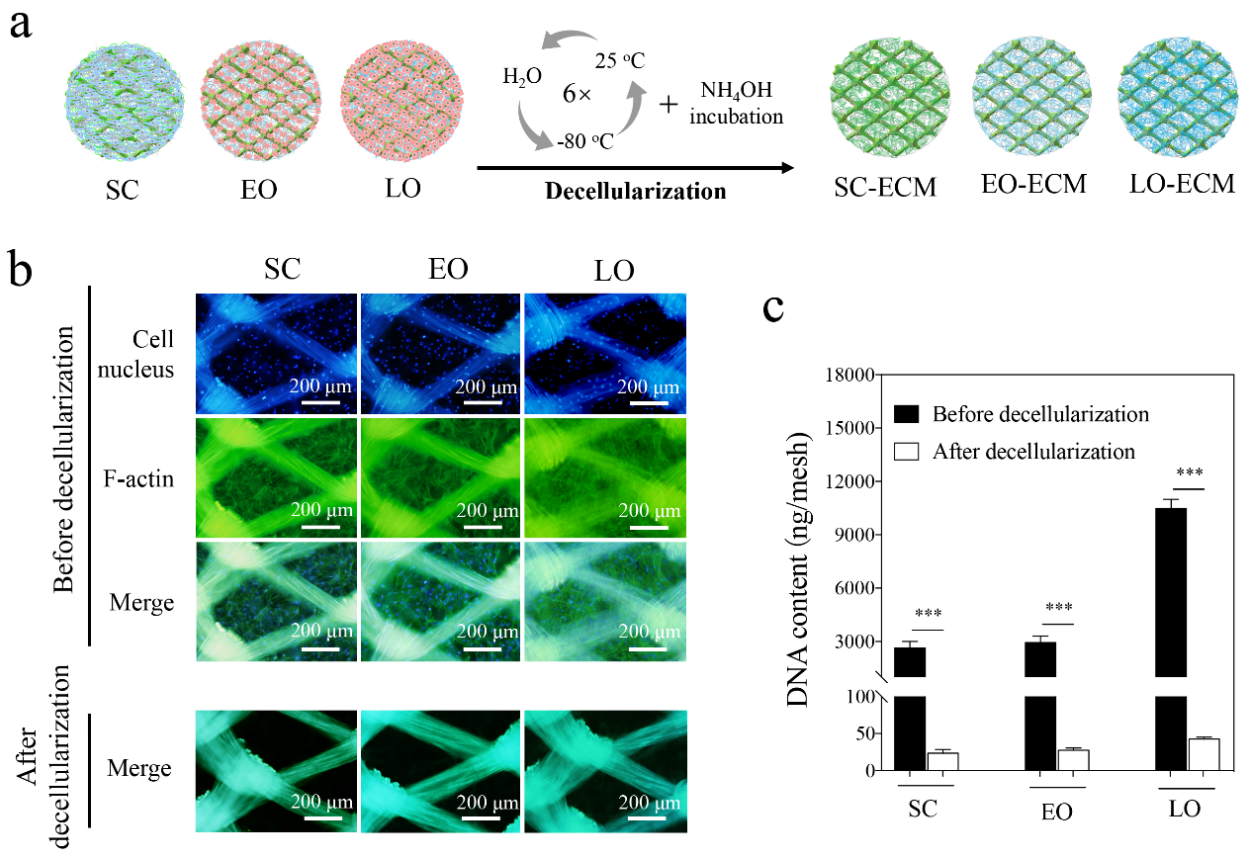


Figure 3.4. Decellularization of the cell/scaffold constructs. Decellularization scheme of cell/hybrid mesh constructs (a). Actin cytoskeleton (green fluorescence) and cell nucleus (blue fluorescence) staining before

and after decellularization to confirm the removal of cellular components (b). DNA quantification before and after decellularization (c).

### 3.4.3 Morphology and composition of PLGA-collagen-ECM hybrid meshes

SEM observations of cell/hybrid mesh constructs showed obvious differences in the constructs before and after decellularization (Figure 3.5). Before decellularization, the cells and deposited ECMs occupied the spaces of the PLGA-collagen hybrid meshes. After decellularization, the hybrid meshes showed porous structures. The porous structure of the PLGA-collagen-ECM hybrid meshes was different from that of the PLGA-collagen hybrid mesh because the deposited ECMs caused the pores to become slightly smaller.

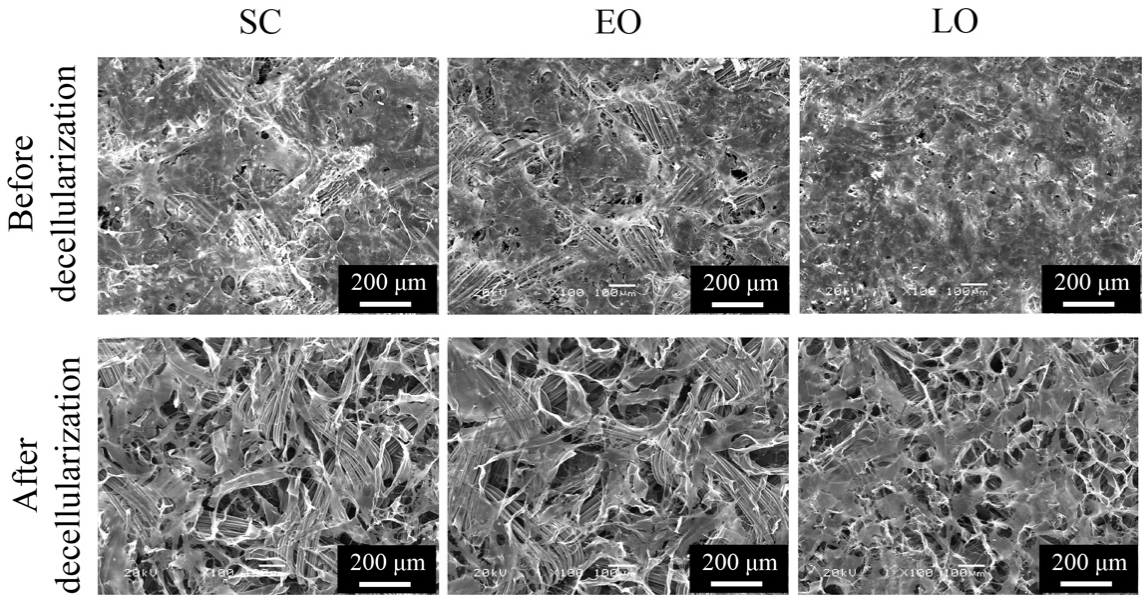


Figure 3.5. SEM images of cell/scaffold constructs before and after decellularization.

The immunohistochemical IHC staining showed that the deposited ECM components were homogeneously distributed in the PLGA-collagen hybrid meshes. The homogeneous distribution of ECM components should be due to the homogenous cell adhesion and cell distribution in the PLGA-collagen hybrid meshes during cell culture as shown in Figure 3.3. The representative photomicrographs of the IHC staining are shown in Figure 3.6. Collagen type I and fibronectin were positively stained in all the ECM scaffolds. LO-ECM scaffold showed the highest staining density. Biglycan was detected in the SC-ECM scaffold but showed only weak staining in the EO-ECM and LO-ECM scaffolds. Decorin was strongly detected in the EO-ECM scaffold but weakly detected in the SC-ECM scaffold. The staining intensity of versican was in the order of SC-ECM > EO-ECM > LO-ECM. Laminin α4 was weakly stained in the SC-ECM and EO-ECM scaffolds but not in the LO-ECM scaffold. The staining intensity showed that the laminin α4 content decreased during osteogenic differentiation. The results indicated that the components of ECM were dependent on the stepwise stage of osteogenesis of hMSCs.

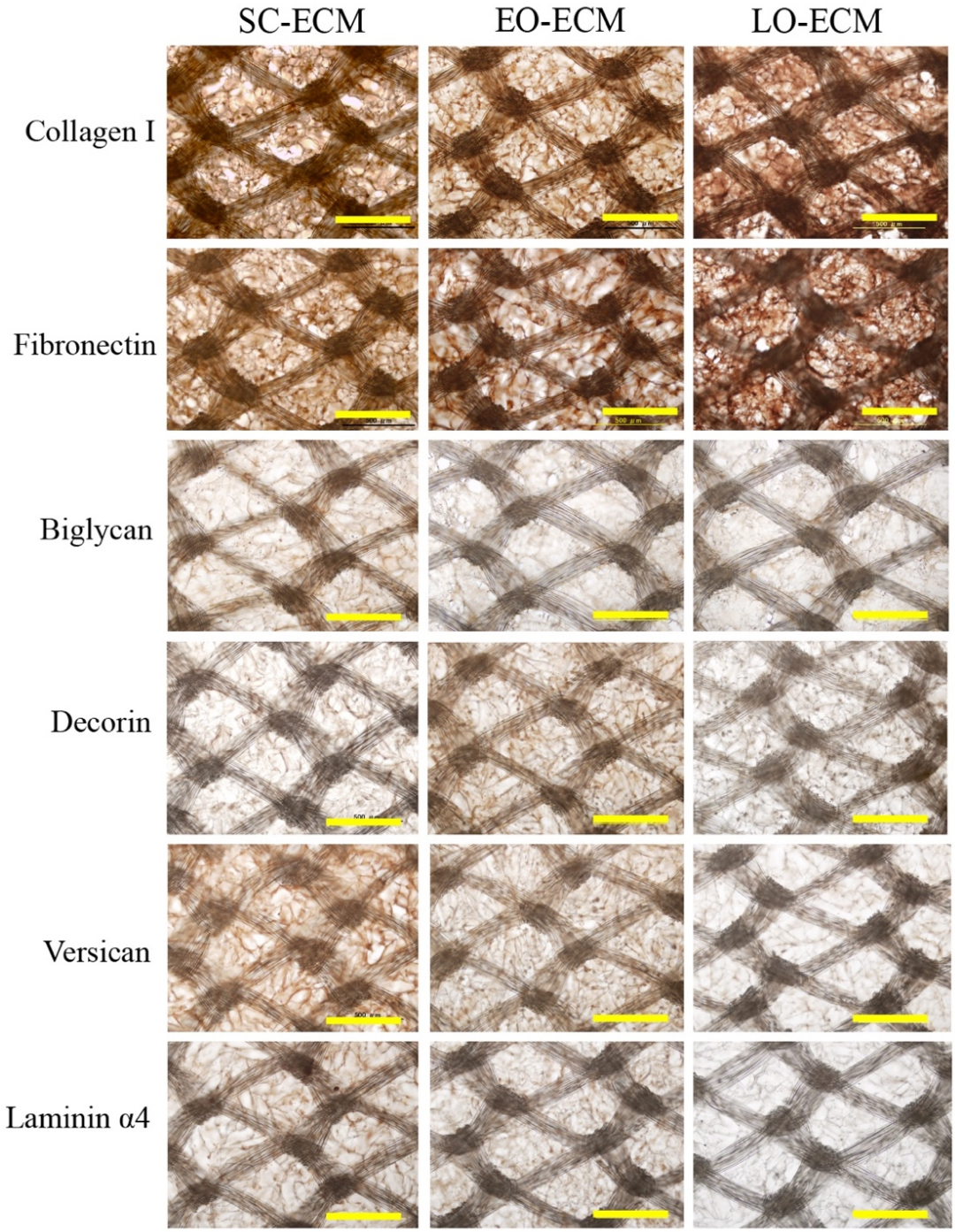


Figure 3.6. Compositional characterization of the PLGA-collagen-ECM hybrid meshes mimicking stepwise osteogenesis. Immunohistochemical staining of collagen I, fibronectin, biglycan, decorin, versican and laminin α4. Scale bar: 500 μm.

### 3.4.4 Adhesion and proliferation of hMSCs in PLGA-collagen hybrid meshes

SEM observations showed that the hMSCs adhered and spread well in all the ECM scaffolds and PLGA-collagen hybrid mesh after being cultured for 1 day (Figure 3.7a). The good cell adhesion in the ECM scaffolds is assumed to be due to the interaction between RGD sequences in the ECM

scaffolds and the integrin receptors present in hMSCs, such as the integrin αvβ3 receptor [56-58].

The proliferation of the stem cells in the PLGA-collagen-ECM hybrid meshes was evaluated via WST-1 assays (Figure 3.7b). The cells in all the hybrid meshes proliferated with culture time. Although cell proliferation in the EO-ECM scaffold was slightly lower than in the other scaffolds, the difference was not significant. The results indicated that all the ECM scaffolds supported the adhesion and proliferation of hMSCs.

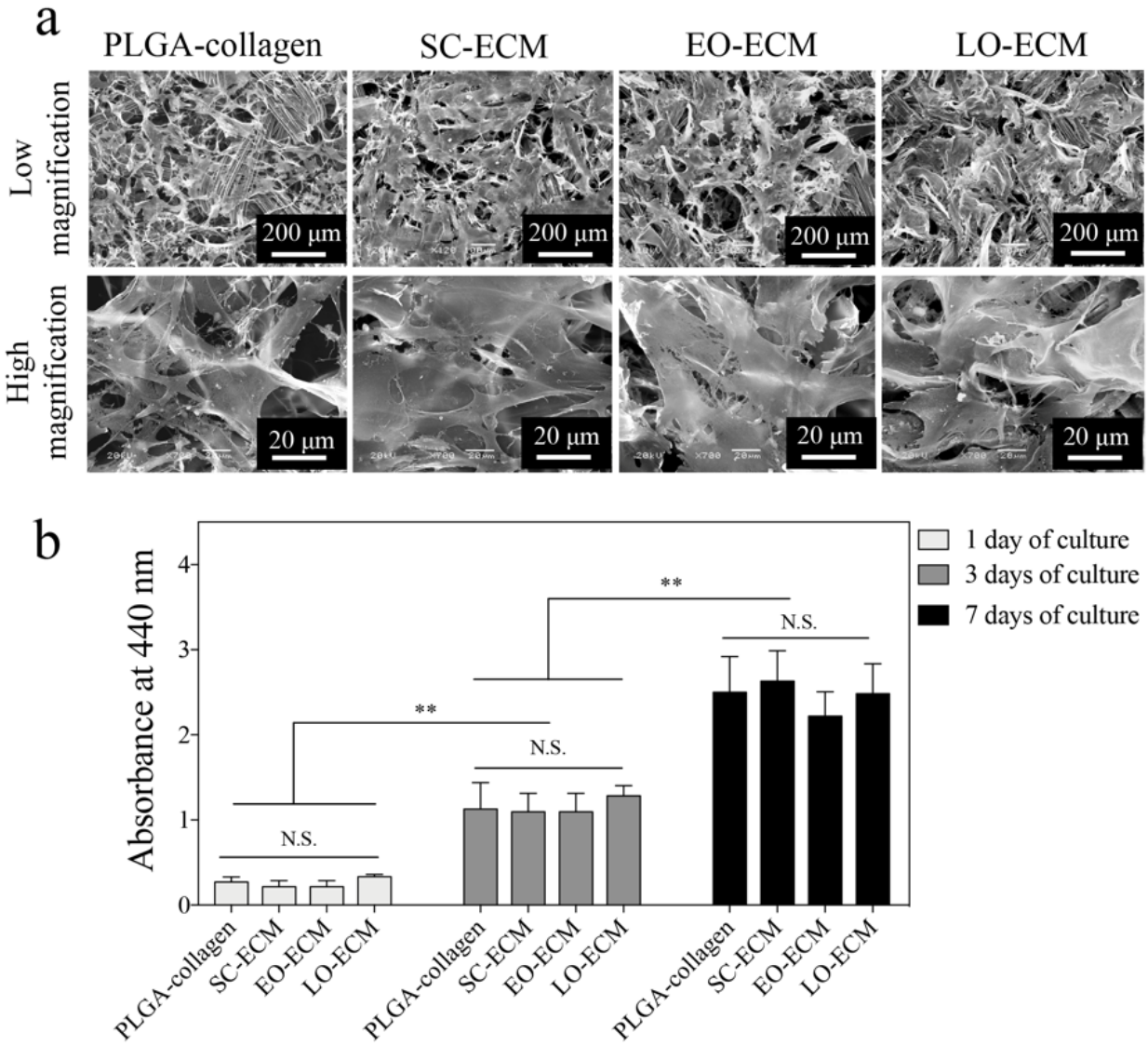


Figure 3.7. Adhesion and proliferation of hMSCs in the PLGA-collagen-ECM hybrid scaffolds mimicking stepwise osteogenesis. SEM images of hMSCs after being cultured in the PLGA-collagen hybrid meshes and SC-ECM, EO-ECM and LO-ECM scaffolds for 1 day (a). Proliferation of hMSCs after culture in the scaffolds for 1, 3 and 7 days (b).

### 3.4.5 Influence of ECM scaffolds on osteogenesis of hMSCs

After culturing the cell/ECM scaffold constructs in basal medium, a low level of staining density was observed in the EO-ECM and LO-ECM scaffolds but not in SC-ECM or the PLGA-collagen groups (Figure 3.8a). Quantitative analysis of alizarin red S staining showed no significant difference between each scaffold, although EO-ECM and LO-ECM scaffolds showed slightly higher levels than

the other two scaffolds (Figure 3.8b). The significantly higher expression of *RUNX2*, *SP7*, *IBSP* and *SPP1* was observed in the cells cultured in the EO-ECM scaffolds than the cells cultured in the SC-ECM and control scaffolds (Figure 3.8c-f). The cells in EO-ECM scaffolds also showed significantly higher expression of *SP7*, *IBSP* and *SPP1* than the cells cultured in the LO-ECM scaffold. The cells cultured in the LO-ECM scaffold showed significantly higher expression of *IBSP* but no significant difference in the expression of *RUNX2*, *SP7*, and *SPP1* compared to those cultured in the control scaffold. The expression levels of all the genes in the cells/SC-ECM constructs were not significantly different from those in the PLGA-collagen meshes. From the above results, it was indicated that the EO-ECM scaffold had a higher potential for promoting the osteogenic differentiation of hMSCs than the other scaffolds when the cells were cultured in basal medium without osteogenic induction factors.

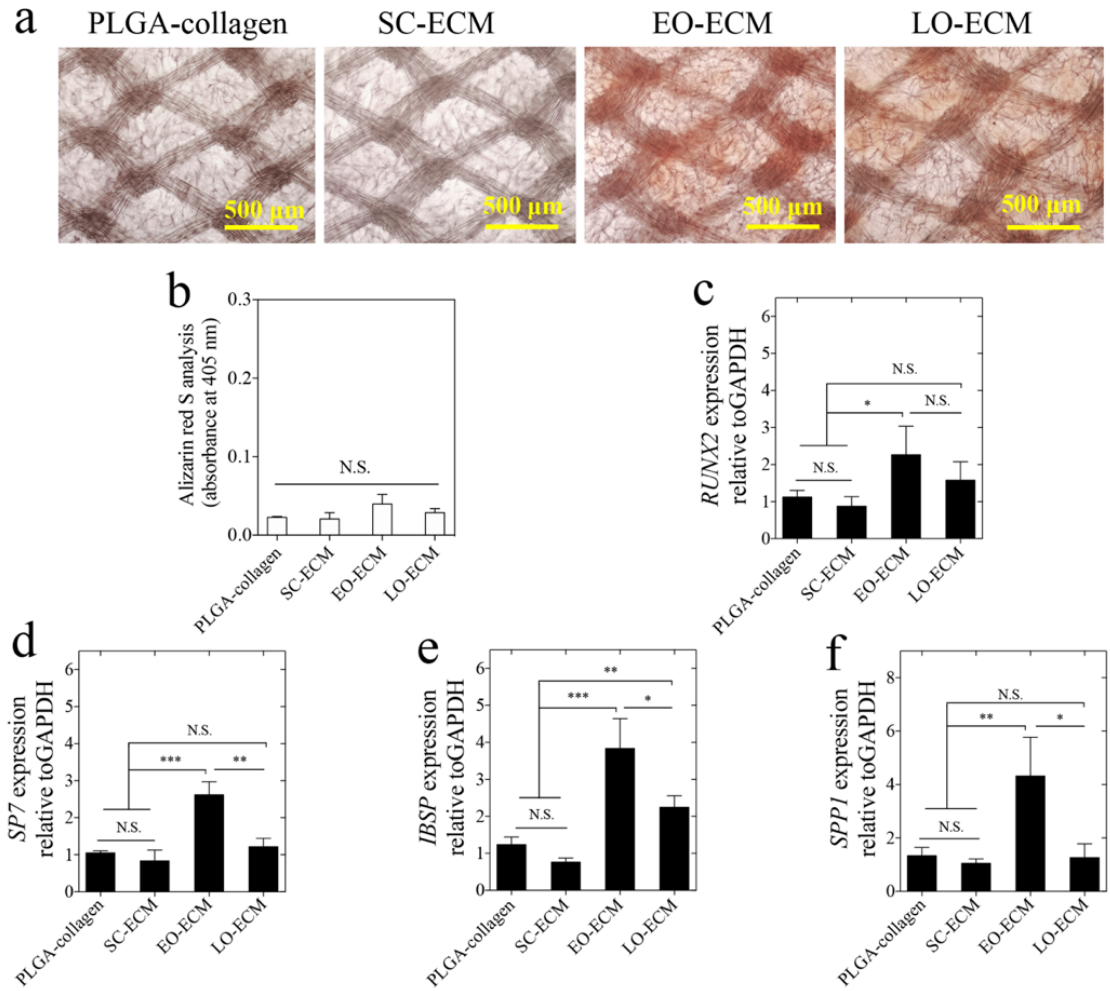


Figure 3.8. Osteogenic differentiation of hMSCs in PLGA-collagen-ECM hybrid meshes (after 21 days of culture). Alizarin red S staining of hMSCs in the scaffolds (a). Quantification of alizarin red S staining (b). Real-time PCR analysis of the *RUNX2* (c), *SP7* (d), *IBSP* (e), and *SPP1* (f) genes. Data represent means ± S.D. (n = 3).

Stem cell lineages are often guided through the use of soluble growth factors [59]. Osteogenic induction factors were used to explore the synergistic influence of the stepwise ECM and osteogenic growth factors on osteogenic differentiation of hMSCs. After hMSCs being cultured in ECM scaffolds in culture medium containing osteogenic induction factors for 21 days, alizarin red S staining showed positive staining in all the scaffolds (Figure 3.9a). The staining density was much higher than that in the cells cultured in basal medium

(Figure 3.9a and Figure 3.8a). The cells cultured in the EO-ECM scaffold were more strongly stained by alizarin red S than the cells cultured in the other scaffolds. The quantification of the alizarin red S staining indicated that the cells cultured in the EO-ECM scaffolds showed significantly higher deposition of calcium than the cells cultured in the other scaffolds (Figure 3.9b). The alizarin red S staining intensity showed a trend of EO-ECM>LO-ECM>PLGA-collagen>SC-ECM. The gene expression results showed that the hMSCs cultured in the EO-ECM scaffold showed the highest gene expression of *RUNX2*, *SP7*, *IBSP* and *SPP1* (Figure 3.9c-f). When the cells were cultured in the LO-ECM scaffolds, only *IBSP* gene expression was significantly upregulated, while the expression of *RUNX2*, *SP7* and *SPP1* was not significantly different from that in the cells cultured in the PLGA-collagen hybrid mesh. In contrast, the expression of *RUNX2* and *IBSP* in the hMSCs cultured in the SC-ECM scaffold was significantly lower than that in the cells cultured in the PLGA-collagen scaffolds (Figure 3.9c, e). The results indicated that the osteogenic differentiation of the hMSCs in the EO-ECM scaffolds was increased, while an inhibitory effect was observed when hMSCs were cultured in SC-ECM scaffolds. The LO-ECM scaffolds showed a moderate effect on the promotion of the osteogenic differentiation of hMSCs.

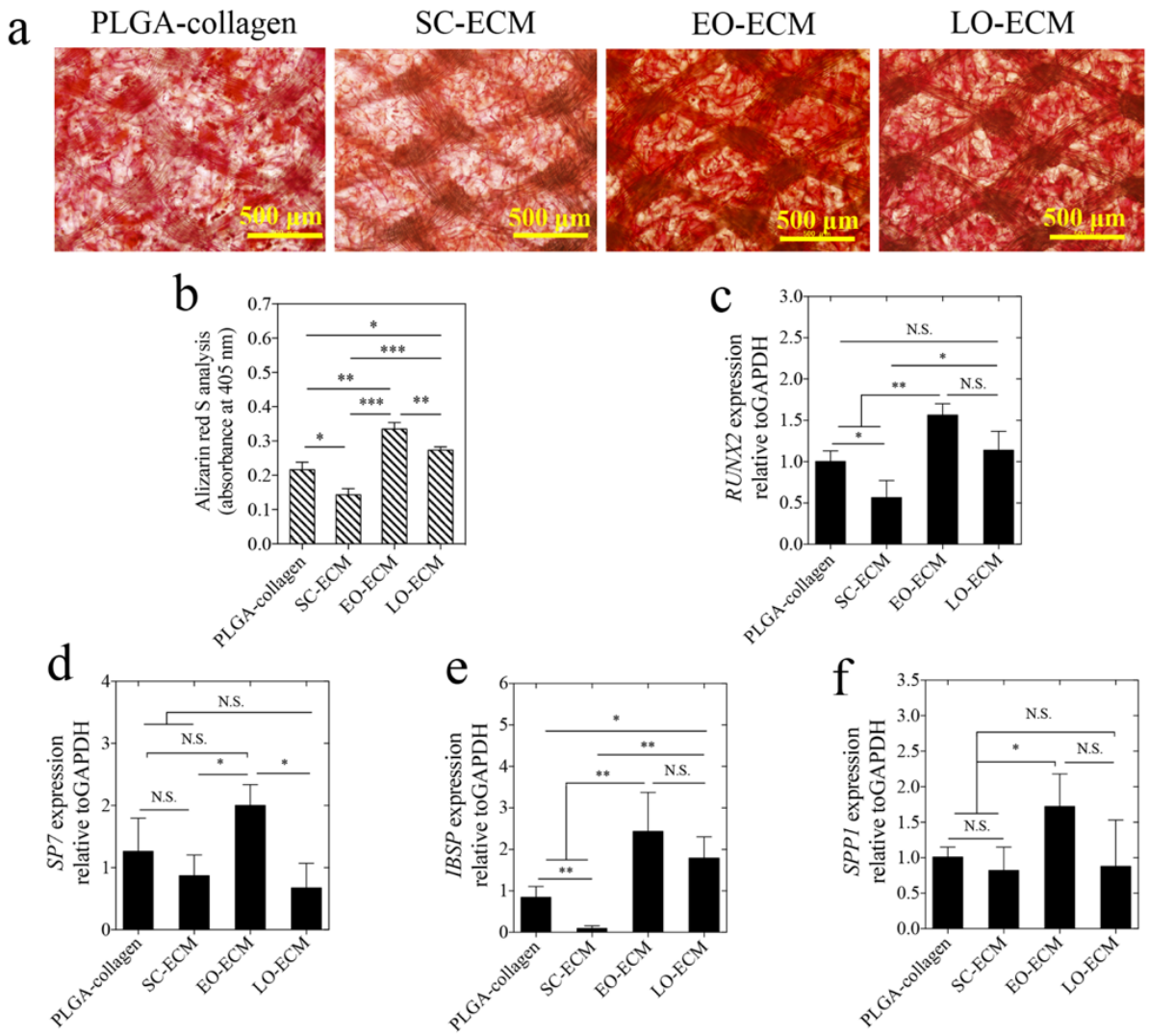


Figure 3.9. Osteogenic differentiation of hMSCs in PLGA-collagen-ECM hybrid meshes (after 21 days of culture). Alizarin red S staining of hMSCs in the scaffolds (a). Quantification of alizarin red S staining (b). Real-time PCR analysis of the *RUNX2* (c), *SP7* (d), *IBSP* (e), and *SPP1* (f) genes. Data represent the means ±

S.D. (n = 3).

### 3.4.6 Discussion

During tissue development, stepwise differentiated stem cells are known to be determining factors for the dynamical alteration and remodeling of the ECM composition [60-62]. The interaction of stem cells and the dynamically changing ECM requires an understanding of how the ECMs direct stem cells to the desired lineage. A major obstacle in defining the exact role of ECMs in the surrounding environment of cells is the lack of suitable *in vitro* methods that mimic the dynamically changed ECM microenvironment. Recently, ECMs derived from cells have been widely investigated, and it has become common knowledge that cell-derived ECMs can mimic the composition of natural tissue matrixes [18, 63-65]. Therefore, the preparation of stepwise cell-derived ECM scaffolds that are robust enough to support 3D cell culture is required. In this study, three types of PLGA-collagen-ECM hybrid meshes mimicking stepwise osteogenesis were prepared for the 3D cell culturing. The PLGA-collagen hybrid meshes were seeded by hMSCs to allow deposition of ECM during the stepwise osteogenesis of hMSCs. Although scaffold stiffness has been reported to affect osteogenic differentiation, the stepwise differentiation of hMSCs in this study was controlled by osteogenic induction culture time and culture medium [66]. The same PLGA-collagen hybrid meshes were used to prepare SC-ECM, EO-ECM and LO-ECM scaffolds.

Expression of ECM components of collagen type I, fibronectin, biglycan, decorin, versican and laminin α4 were examined by IHC staining because these six types of components have been reported to be correlated with differentiation of hMSCs [67]. Laminin has many subtypes. Laminin α4 was chosen because laminin α4 is a subdomain in laminin chain and it has an inhibitory effect on adipogenic differentiation of hMSCs [68]. The PLGA-collagen-ECM hybrid meshes showed dynamic change of these ECM components as shown by the IHC staining (Figure 5). The ECM scaffolds supported the adhesion and proliferation of hMSCs. The influence of the SC-ECM, EO-ECM and LO-ECM scaffolds on the osteogenic differentiation of hMSCs was dependent on the ECM types. The EO-ECM scaffold showed the strongest promotive effect, and the LO-ECM scaffold showed a moderate promotive effect on the osteogenic differentiation of hMSCs, while the SC-ECM scaffold showed an inhibitory effect.

The components of ECM have been reported to play an important role on the decision of stem cell fate [69]. The dynamically remodeling ECM components in the PLGA-collagen-ECM hybrid meshes should be related with their different influence on osteogenic differentiation of hMSCs. Collagen type I is one of the major structure proteins, making up microfibers that strengthen the soft tissues. It has been reported that collagen type I promotes the osteogenic differentiation through activation of ERK (Extracellular signal-Related Kinase) signaling pathway [70]. The highly deposited collagen type I proteins were observed in all of the three types of ECM scaffolds. Fibronectin has a gradient effect on osteogenesis of hMSCs where the lower fibronectin-density elicits stronger osteogenic expression [71]. Higher amount of fibronectin was deposited in LO-ECM scaffold than the other two types of ECM scaffolds, which might contribute to the inhibitory effects of LO-ECM scaffold on osteogenesis of hMSCs. Biglycan shows inhibition effects on osteogenic differentiation [72, 73]. The positive staining of biglycan was only observed in SC-ECM scaffold, while barely detected in the EO-ECM and LO-ECM scaffolds, which might result in an inhibitory effect of SC-ECM scaffold on osteogenic differentiation of hMSCs. Decorin has a promotive effect on osteogenic differentiation of hMSCs, which can be achieved through Wnt/β-catenin signaling

pathway [74]. The positive staining of decorin was only observed in the EO-ECM scaffold, which might contribute the promotive effects of EO-ECM scaffold on osteogenic differentiation of hMSCs. Versican and laminin are the ECM components that related to chondrogenesis and adipogenesis of hMSCs [68, 75]. Both of versican and laminin have no obvious influence on osteogenic differentiation of hMSCs. Their expression levels were decreased during osteogenesis of hMSC (Figure 5). Although decellularized tissue-derived ECMs and decellularized cell-derived ECMs have been reported to have some different influence on proliferation and the early late and late stage ECM scaffolds are closer to tissue-derived ECMs, the difference of ECM components should be one of the main seasons for the different influence [67].

Not only the different components of the SC-ECM, EO-ECM and LO-ECM scaffolds had some influence on osteogenic differentiation of hMSCs, but also the combination of the ECM scaffolds with osteogenic induction factors further exerted synergistic effects on the osteogenic differentiation (Figure 8). Interestingly, the similar osteogenic differentiation tendency was observed in the 3D ECM scaffolds when cells were cultured in both basal medium and osteogenic induction medium (Figure 7 and Figure 8). This phenomenon suggested that the ECM parameters might provide the initial condition to guide the lineage specification of hMSCs and that their influence is magnified synergistically with the addition of osteogenic induction factors. In this study, hMSCs were cultured in the PLGA-collagen hybrid meshes and the deposited ECM components were considered as one of the main reasons for the different influence of ECM scaffolds on osteogenic differentiation of hMSCs. Growth factors secreted by hMSCs and deposited in the ECM scaffolds might also have influence on osteogenic differentiation of hMSCs although their influence was not investigated in this study. Other cell types or a few cell types can also be cultured or co-cultured in the PLGA-collagen hybrid meshed to generate their respective ECM scaffold models. It has been reported that ECM scaffolds secreted from co-cultured hMSCs and human umbilical vein endothelial cells had significant enhancement on osteogenic differentiation of hMSCs [32, 76]. Co-culture of a few cell types can produce a mixture ECM microenvironment for investigation the complex ECM-cell interaction. The method to prepare stepwise 3D PLGA-collagen-ECM hybrid meshes should offer a novel solution for the challenging target of mimicking the dynamic remolding of the 3D ECM during cell development and for investigating its influence on stem cell functions.

## 3.5 Conclusions

In this study, we prepared deposited PLGA-collagen-ECM hybrid meshes mimicking stepwise osteogenesis by culturing hMSCs in PLGA-collagen hybrid meshes and controlling the degree of their osteogenic differentiation at the stem-cell stage, early-stage and late-stage of osteogenesis. The stepwise ECM scaffolds exhibited different compositions depending on the stage of osteogenesis. They also showed different influences on the osteogenic differentiation of hMSCs. The ECM scaffold mimicking the early stage of osteogenesis promoted the osteogenic differentiation of hMSCs, and the ECM scaffold mimicking the late stage of osteogenesis showed a moderate effect on the promotion of the osteogenic differentiation of hMSCs. However, the ECM scaffold mimicking the stem cell stage of hMSCs exhibited an inhibitory effect. The PLGA-collagen-ECMs hybrid meshes could be used as useful tools with a wide range of applications, from the investigation of the roles of ECMs in stem cell differentiation to tissue engineering.

## 3.6. References

[1] R. Kaukonen, G. Jacquemet, H. Hamidi, J. Ivaska, Cell-derived matrices for studying cell proliferation and directional migration in a complex 3D microenvironment, Nature Protocols 12 (2017) 2376.
[2] A. Haage, K. Goodwin, A. Whitewood, D. Camp, A. Bogutz, C.T. Turner, D.J. Granville, L. Lefebvre, S. Plotnikov, B.T. Goult, G. Tanentzapf, Talin Autoinhibition Regulates Cell-ECM Adhesion Dynamics and Wound Healing In Vivo, Cell reports 25(9) (2018) 2401-2416.e5.
[3] K.M. Wisdom, K. Adebowale, J. Chang, J.Y. Lee, S. Nam, R. Desai, N.S. Rossen, M. Rafat, R.B. West, L. Hodgson, O. Chaudhuri, Matrix mechanical plasticity regulates cancer cell migration through confining microenvironments, Nature communications 9(1) (2018) 4144.
[4] J.M. Silva Garcia, A. Panitch, S. Calve, Functionalization of hyaluronic acid hydrogels with ECM-derived peptides to control myoblast behavior, Acta biomaterialia 84 (2019) 169-179.
[5] P.E. Bourgine, E. Gaudiello, B. Pippenger, C. Jaquiery, T. Klein, S. Pigeot, A. Todorov Jr., S. Feliciano, A. Banfi, I. Martin, Engineered Extracellular Matrices as Biomaterials of Tunable Composition and Function, Advanced Functional Materials 27(7) (2017) 1605486.
[6] A. Duro-Castano, N.H. Lim, I. Tranchant, M. Amoura, F. Beau, H. Wieland, O. Kingler, M. Herrmann, M. Nazaré, O. Plettenburg, V. Dive, M.J. Vicent, H. Nagase, In Vivo Imaging of MMP-13 Activity Using a Specific Polymer-FRET Peptide Conjugate Detects Early Osteoarthritis and Inhibitor Efficacy, Advanced Functional Materials 28(37) (2018) 1802738.
[7] H.O. Ozguldez, J. Cha, Y. Hong, I. Koh, P. Kim, Nanoengineered, cell-derived extracellular matrix influences ECM-related gene expression of mesenchymal stem cells, Biomaterials research 22 (2018) 32.
[8] A.D. Rape, M. Zibinsky, N. Murthy, S. Kumar, A synthetic hydrogel for the high-throughput study of cell–ECM interactions, Nature communications 6 (2015) 8129.
[9] Y. Peng, Q.J. Liu, T. He, K. Ye, X. Yao, J. Ding, Degradation rate affords a dynamic cue to regulate stem cells beyond varied matrix stiffness, Biomaterials 178 (2018) 467-480.
[10] T. Ahmad, J. Lee, Y.M. Shin, H.J. Shin, S.K. Madhurakat Perikamana, S.H. Park, S.W. Kim, H. Shin, Hybrid-spheroids incorporating ECM like engineered fragmented fibers potentiate stem cell function by improved cell/cell and cell/ECM interactions, Acta biomaterialia 64 (2017) 161-175.
[11] J. Zhang, C. Cheng, J.L. Cuellar-Camacho, M. Li, Y. Xia, W. Li, R. Haag, Thermally Responsive Microfibers Mediated Stem Cell Fate via Reversibly Dynamic Mechanical Stimulation, Advanced Functional Materials 28(47) (2018) 1804773.
[12] G.S. Hussey, T.J. Keane, S.F. Badylak, The extracellular matrix of the gastrointestinal tract: a regenerative medicine platform, Nature reviews. Gastroenterology & hepatology 14(9) (2017) 540-552.
[13] G.M. Cunniffe, P.J. Díaz-Payno, E.J. Sheehy, S.E. Critchley, H.V. Almeida, P. Pitacco, S.F. Carroll, O.R. Mahon, A. Dunne, T.J. Levingstone, C.J. Moran, R.T. Brady, F.J. O'Brien, P.A.J. Brama, D.J. Kelly, Tissue-specific extracellular matrix scaffolds for the regeneration of spatially complex musculoskeletal tissues, Biomaterials 188 (2019) 63-73.
[14] X. Wang, J. Zhang, J. Li, Y. Chen, Y. Chen, N. Kawazoe, G. Chen, Bifunctional scaffolds for the photothermal therapy of breast tumor cells and adipose tissue regeneration, Journal of Materials Chemistry B 6(46) (2018) 7728-7736.
[15] N. Movilla, C. Borau, C. Valero, J.M. García-Aznar, Degradation of extracellular matrix regulates osteoblast migration: A microfluidic-based study, Bone 107 (2018) 10-17.
[16] D.A. Taylor, L.C. Sampaio, Z. Ferdous, A.S. Gobin, L.J. Taite, Decellularized matrices in regenerative medicine, Acta biomaterialia 74 (2018) 74-89.

[17] G.S. Hussey, J.L. Dziki, S.F. Badylak, Extracellular matrix-based materials for regenerative medicine, Nature Reviews Materials 3(7) (2018) 159-173.
[18] T. Hoshiba, N. Kawazoe, G. Chen, Preparation of Cell-Derived Decellularized Matrices Mimicking Native ECM During the Osteogenesis and Adipogenesis of Mesenchymal Stem Cells, Methods in molecular biology (Clifton, N.J.) 1577 (2018) 71-86.
[19] L. Hou, J. Coller, V. Natu, T.J. Hastie, N.F. Huang, Combinatorial extracellular matrix microenvironments promote survival and phenotype of human induced pluripotent stem cell-derived endothelial cells in hypoxia, Acta biomaterialia 44 (2016) 188-99.
[20] I.G. Kim, C.H. Gil, J. Seo, S.J. Park, R. Subbiah, T.H. Jung, J.S. Kim, Y.H. Jeong, H.M. Chung, J.H. Lee, M.R. Lee, S.H. Moon, K. Park, Mechanotransduction of human pluripotent stem cells cultivated on tunable cell-derived extracellular matrix, Biomaterials 150 (2018) 100-111.
[21] H. Lu, T. Hoshiba, N. Kawazoe, G. Chen, Autologous extracellular matrix scaffolds for tissue engineering, Biomaterials 32(10) (2011) 2489-99.
[22] N. Hou, Y. Yang, I.C. Scott, X. Lou, The Sec domain protein Scfd1 facilitates trafficking of ECM components during chondrogenesis, Developmental biology 421(1) (2017) 8-15.
[23] Y. Liu, D. Luo, M. Yu, Y. Wang, S. Jin, Z. Li, S. Cui, D. He, T. Zhang, T. Wang, Y. Zhou, Thermodynamically Controlled Self-Assembly of Hierarchically Staggered Architecture as an Osteoinductive Alternative to Bone Autografts, Advanced Functional Materials 29(10) (2019) 1806445.
[24] Y. Chen, K. Lee, N. Kawazoe, Y. Yang, G. Chen, PLGA-collagen-ECM hybrid scaffolds functionalized with biomimetic extracellular matrices secreted by mesenchymal stem cells during stepwise osteogenesis-co-adipogenesis, Journal of materials chemistry. B 7(45) (2019) 7195-7206.
[25] Y. Chen, K. Lee, Y. Chen, Y. Yang, N. Kawazoe, G. Chen, Preparation of Stepwise Adipogenesis-Mimicking ECM-Deposited PLGA–Collagen Hybrid Meshes and Their Influence on Adipogenic Differentiation of hMSCs, ACS Biomaterials Science & Engineering 5(11) (2019) 6099-6108.
[26] K. Lee, Y. Chen, X. Li, Y. Wang, N. Kawazoe, Y. Yang, G. Chen, Solution viscosity regulates chondrocyte proliferation and phenotype during 3D culture, Journal of materials chemistry. B 7(48) (2019) 7713-7722.
[27] A.I. Hoch, V. Mittal, D. Mitra, N. Vollmer, C.A. Zikry, J.K. Leach, Cell-secreted matrices perpetuate the bone-forming phenotype of differentiated mesenchymal stem cells, Biomaterials 74 (2016) 178-87.
[28] H. Zhan, D.W.P.M. Löwik, A Hybrid Peptide Amphiphile Fiber PEG Hydrogel Matrix for 3D Cell Culture, Advanced Functional Materials 29(16) (2019) 1808505.
[29] H. Lu, T. Hoshiba, N. Kawazoe, I. Koda, M. Song, G. Chen, Cultured cell-derived extracellular matrix scaffolds for tissue engineering, Biomaterials 32(36) (2011) 9658-66.
[30] Y. Mao, T. Block, A. Singh-Varma, A. Sheldrake, R. Leeth, S. Griffey, J. Kohn, Extracellular matrix derived from chondrocytes promotes rapid expansion of human primary chondrocytes in vitro with reduced dedifferentiation, Acta biomaterialia 85 (2019) 75-83.
[31] M.S. Carvalho, J.C. Silva, R.N. Udangawa, J.M.S. Cabral, F.C. Ferreira, C.L. da Silva, R.J. Linhardt, D. Vashishth, Co-culture cell-derived extracellular matrix loaded electrospun microfibrous scaffolds for bone tissue engineering, Materials Science and Engineering: C 99 (2019) 479-490.
[32] S.M. Nassiri, R. Rahbarghazi, Interactions of mesenchymal stem cells with endothelial cells, Stem cells and development 23(4) (2014) 319-32.
[33] J. Frith, P. Genever, Transcriptional Control of Mesenchymal Stem Cell Differentiation, Transfusion Medicine and Hemotherapy 35(3) (2008) 216-227.
[34] R.-K. Ramani-Mohan, I. Schwedhelm, A. Finne-Wistrand, M. Krug, T. Schwarz, F. Jakob, H. Walles, J. Hansmann, Deformation strain is the main physical driver for skeletal precursors to undergo osteogenesis in earlier stages of osteogenic cell maturation, Journal of Tissue Engineering and Regenerative Medicine 12(3)

(2018) e1474-e1479.
[35] K. Kanke, H. Masaki, T. Saito, Y. Komiyama, H. Hojo, H. Nakauchi, Alexander C. Lichtler, T. Takato, U.-i. Chung, S. Ohba, Stepwise Differentiation of Pluripotent Stem Cells into Osteoblasts Using Four Small Molecules under Serum-free and Feeder-free Conditions, Stem Cell Reports 2(6) (2014) 751-760.
[36] T. Hoshiba, N. Kawazoe, G. Chen, The balance of osteogenic and adipogenic differentiation in human mesenchymal stem cells by matrices that mimic stepwise tissue development, Biomaterials 33(7) (2012) 2025-2031.
[37] A.M. Rosales, K.S. Anseth, The design of reversible hydrogels to capture extracellular matrix dynamics, Nature Reviews Materials 1 (2016) 15012.
[38] M. Dai, B. Sui, Y. Xue, X. Liu, J. Sun, Cartilage repair in degenerative osteoarthritis mediated by squid type II collagen via immunomodulating activation of M2 macrophages, inhibiting apoptosis and hypertrophy of chondrocytes, Biomaterials 180 (2018) 91-103.
[39] G.C.J. Lindberg, A. Longoni, K.S. Lim, A.J. Rosenberg, G.J. Hooper, D. Gawlitta, T.B.F. Woodfield, Intact vitreous humor as a potential extracellular matrix hydrogel for cartilage tissue engineering applications, Acta biomaterialia 85 (2019) 117-130.
[40] D. Barros, P. Parreira, J. Furtado, F. Ferreira-da-Silva, E. Conde-Sousa, A.J. Garcia, M.C.L. Martins, I.F. Amaral, A.P. Pego, An affinity-based approach to engineer laminin-presenting cell instructive microenvironments, Biomaterials 192 (2019) 601-611.
[41] M. Song, Y. Liu, L. Hui, Preparation and characterization of acellular adipose tissue matrix using a combination of physical and chemical treatments, Molecular medicine reports 17(1) (2018) 138-146.
[42] T. Hoshiba, N. Kawazoe, T. Tateishi, G. Chen, Development of extracellular matrices mimicking stepwise adipogenesis of mesenchymal stem cells, Advanced materials (Deerfield Beach, Fla.) 22(28) (2010) 3042-7.
[43] R. Cai, T. Nakamoto, T. Hoshiba, N. Kawazoe, G. Chen, Matrices secreted during simultaneous osteogenesis and adipogenesis of mesenchymal stem cells affect stem cells differentiation, Acta biomaterialia 35 (2016) 185-93.
[44] T. Hoshiba, N. Kawazoe, T. Tateishi, G. Chen, Development of stepwise osteogenesis-mimicking matrices for the regulation of mesenchymal stem cell functions, The Journal of biological chemistry 284(45) (2009) 31164-73.
[45] H. Lu, H.H. Oh, N. Kawazoe, K. Yamagishi, G. Chen, PLLA-collagen and PLLA-gelatin hybrid scaffolds with funnel-like porous structure for skin tissue engineering, Science and technology of advanced materials 13(6) (2012) 064210.
[46] X. He, H. Lu, N. Kawazoe, T. Tateishi, G. Chen, A novel cylinder-type poly(L-lactic acid)-collagen hybrid sponge for cartilage tissue engineering, Tissue engineering. Part C, Methods 16(3) (2010) 329-38.
[47] W. Dai, N. Kawazoe, X. Lin, J. Dong, G. Chen, The influence of structural design of PLGA/collagen hybrid scaffolds in cartilage tissue engineering, Biomaterials 31(8) (2010) 2141-52.
[48] H. Lu, N. Kawazoe, T. Kitajima, Y. Myoken, M. Tomita, A. Umezawa, G. Chen, Y. Ito, Spatial immobilization of bone morphogenetic protein-4 in a collagen-PLGA hybrid scaffold for enhanced osteoinductivity, Biomaterials 33(26) (2012) 6140-6.
[49] G. Chen, N. Kawazoe, Porous Scaffolds for Regeneration of Cartilage, Bone and Osteochondral Tissue, Advances in experimental medicine and biology 1058 (2018) 171-191.
[50] Y. Yang, X. Wang, T.-C. Huang, X. Hu, N. Kawazoe, W.-B. Tsai, Y. Yang, G. Chen, Regulation of mesenchymal stem cell functions by micro–nano hybrid patterned surfaces, Journal of Materials Chemistry B 6(34) (2018) 5424-5434.
[51] R. Cai, N. Kawazoe, G. Chen, Influence of surfaces modified with biomimetic extracellular matrices on adhesion and proliferation of mesenchymal stem cells and osteosarcoma cells, Colloids and surfaces. B,

Biointerfaces 126 (2015) 381-6.
[52] J. Li, J.J. Li, J. Zhang, X. Wang, N. Kawazoe, G. Chen, Gold nanoparticle size and shape influence on osteogenesis of mesenchymal stem cells, Nanoscale 8(15) (2016) 7992-8007.
[53] H. Lu, T. Hoshiba, N. Kawazoe, G. Chen, Comparison of decellularization techniques for preparation of extracellular matrix scaffolds derived from three-dimensional cell culture, Journal of biomedical materials research. Part A 100(9) (2012) 2507-16.
[54] G. Chen, D. Liu, M. Tadokoro, R. Hirochika, H. Ohgushi, J. Tanaka, T. Tateishi, Chondrogenic differentiation of human mesenchymal stem cells cultured in a cobweb-like biodegradable scaffold, Biochemical and biophysical research communications 322(1) (2004) 50-5.
[55] C. Deng, R. Lin, M. Zhang, C. Qin, Q. Yao, L. Wang, J. Chang, C. Wu, Micro/Nanometer-Structured Scaffolds for Regeneration of Both Cartilage and Subchondral Bone, Advanced Functional Materials 29(4) (2019) 1806068.
[56] T.M. Danilucci, P.K. Santos, B.C. Pachane, G.F.D. Pisani, R.L.B. Lino, B.C. Casali, W.F. Altei, H.S. Selistre-de-Araujo, Recombinant RGD-disintegrin DisBa-01 blocks integrin alphavbeta3 and impairs VEGF signaling in endothelial cells, Cell communication and signaling : CCS 17(1) (2019) 27.
[57] A.E. Rodda, F. Ercole, V. Glattauer, D.R. Nisbet, K.E. Healy, A.P. Dove, L. Meagher, J.S. Forsythe, Controlling integrin-based adhesion to a degradable electrospun fibre scaffold via SI-ATRP, Journal of Materials Chemistry B 4(45) (2016) 7314-7322.
[58] J. Kim, I.K. Shim, D.G. Hwang, Y.N. Lee, M. Kim, H. Kim, S.-W. Kim, S. Lee, S.C. Kim, D.-W. Cho, J. Jang, 3D cell printing of islet-laden pancreatic tissue-derived extracellular matrix bioink constructs for enhancing pancreatic functions, Journal of Materials Chemistry B 7(10) (2019) 1773-1781.
[59] R. Chen, J. Wang, C. Liu, Biomaterials Act as Enhancers of Growth Factors in Bone Regeneration, Advanced Functional Materials 26(48) (2016) 8810-8823.
[60] K. Garg, M.D. Boppart, Influence of exercise and aging on extracellular matrix composition in the skeletal muscle stem cell niche, Journal of applied physiology (Bethesda, Md. : 1985) 121(5) (2016) 1053-1058.
[61] F. Gattazzo, A. Urciuolo, P. Bonaldo, Extracellular matrix: a dynamic microenvironment for stem cell niche, Biochimica et biophysica acta 1840(8) (2014) 2506-19.
[62] H. Ragelle, A. Naba, B.L. Larson, F. Zhou, M. Prijic, C.A. Whittaker, A. Del Rosario, R. Langer, R.O. Hynes, D.G. Anderson, Comprehensive proteomic characterization of stem cell-derived extracellular matrices, Biomaterials 128 (2017) 147-159.
[63] Y. Yang, H. Lin, H. Shen, B. Wang, G. Lei, R.S. Tuan, Mesenchymal stem cell-derived extracellular matrix enhances chondrogenic phenotype of and cartilage formation by encapsulated chondrocytes in vitro and in vivo, Acta biomaterialia 69 (2018) 71-82.
[64] J.N. Harvestine, H. Orbay, J.Y. Chen, D.E. Sahar, J.K. Leach, Cell-secreted extracellular matrix, independent of cell source, promotes the osteogenic differentiation of human stromal vascular fraction, Journal of materials chemistry. B 6(24) (2018) 4104-4115.
[65] G. Chen, N. Kawazoe, Biomimetic Extracellular Matrices and Scaffolds Prepared from Cultured Cells, Advances in experimental medicine and biology 1078 (2018) 465-474.
[66] N. Huebsch, P.R. Arany, A.S. Mao, D. Shvartsman, O.A. Ali, S.A. Bencherif, J. Rivera-Feliciano, D.J. Mooney, Harnessing traction-mediated manipulation of the cell/matrix interface to control stem-cell fate, Nat Mater 9(6) (2010) 518-26.
[67] Y. Sun, L. Yan, S. Chen, M. Pei, Functionality of decellularized matrix in cartilage regeneration: A comparison of tissue versus cell sources, Acta biomaterialia 74 (2018) 56-73.
[68] H. Yamashita, C. Goto, R. Tajima, A.T. Koparal, M. Kobori, Y. Ohki, K. Shitara, R. Narita, K. Toriyama, S. Torii, T. Niimi, Y. Kitagawa, Cryptic fragment alpha4 LG4-5 derived from laminin alpha4 chain inhibits de

novo adipogenesis by modulating the effect of fibroblast growth factor-2, Development, growth & differentiation 50(2) (2008) 97-107.
[69] L.E. Niklason, Understanding the Extracellular Matrix to Enhance Stem Cell-Based Tissue Regeneration, Cell Stem Cell 22(3) (2018) 302-305.
[70] S. Viale-Bouroncle, M. Gosau, C. Morsczeck, Collagen I induces the expression of alkaline phosphatase and osteopontin via independent activations of FAK and ERK signalling pathways, Archives of oral biology 59(12) (2014) 1249-55.
[71] A.B. Faia-Torres, T. Goren, T.O. Ihalainen, S. Guimond-Lischer, M. Charnley, M. Rottmar, K. Maniura-Weber, N.D. Spencer, R.L. Reis, M. Textor, N.M. Neves, Regulation of human mesenchymal stem cell osteogenesis by specific surface density of fibronectin: a gradient study, ACS applied materials & interfaces 7(4) (2015) 2367-75.
[72] A.M. Hocking, T. Shinomura, D.J. McQuillan, Leucine-rich repeat glycoproteins of the extracellular matrix, Matrix biology : journal of the International Society for Matrix Biology 17(1) (1998) 1-19.
[73] M. Moreno, R. Munoz, F. Aroca, M. Labarca, E. Brandan, J. Larrain, Biglycan is a new extracellular component of the Chordin-BMP4 signaling pathway, The EMBO journal 24(7) (2005) 1397-405.
[74] X.G. Han, D.K. Wang, F. Gao, R.H. Liu, Z.G. Bi, Bone morphogenetic protein 2 and decorin expression in old fracture fragments and surrounding tissues, Genetics and molecular research : GMR 14(3) (2015) 11063-72.
[75] N. Kamiya, H. Watanabe, H. Habuchi, H. Takagi, T. Shinomura, K. Shimizu, K. Kimata, Versican/PG-M regulates chondrogenesis as an extracellular matrix molecule crucial for mesenchymal condensation, The Journal of biological chemistry 281(4) (2006) 2390-400.
[76] A. Aguirre, J.A. Planell, E. Engel, Dynamics of bone marrow-derived endothelial progenitor cell/mesenchymal stem cell interaction in co-culture and its implications in angiogenesis, Biochemical and biophysical research communications 400(2) (2010) 284-91.

# Chapter 4

# PLGA–collagen–ECM hybrid scaffolds functionalized with biomimetic extracellular matrices secreted by mesenchymal stem cells during stepwise osteogenesis-co-adipogenesis

## 4.1 Abstract

A shift in osteogenesis toward adipogenesis of hMSCs is a crucial pathological factor in the progression of osteoporosis. The development of an in vitro three-dimensional (3D) model that reflects the dynamic remodeling of extracellular matrices (ECMs) during simultaneous osteogenesis and adipogenesis of hMSCs can provide a useful tool to mimic the process and to investigate how 3D ECMs balance the osteogenic and adipogenic differentiation of hMSCs. In this study, ECMs secreted by hMSCs during their stepwise osteogenesis-co-adipogenesis were deposited on hybrid meshes of poly(lactide-co-glycolide) (PLGA) and collagen to prepare biomimetic PLGA–collagen–ECM hybrid scaffolds. Four types of stepwise differentiation ECMs were pre- pared: ECMs secreted by hMSCs at early stages of osteogenesis and adipogenesis (EOEA–ECMs), hMSCs at early stages of osteogenesis and late stages of adipogenesis (EOLA–ECMs), hMSCs at late stages of osteogenesis and early stages of adipogenesis (LOEA–ECMs) and hMSCs at late stages of osteogenesis and late stages of adipogenesis (LOLA–ECMs). The deposited ECMs had different compositions that were dependent on the different stages of osteogenesis and adipogenesis. They also showed different effects on balancing the adipogenic and osteogenic differentiation of hMSCs. The EOEA–ECM scaffold had a promotive effect on adipogenesis and a suppressive effect on the osteogenesis of hMSCs. The LOEA– ECM and LOLA–ECM scaffolds showed a promotive effect on osteogenesis and a moderate effect on the adipogenic differentiation of hMSCs. The EOLA–ECM scaffold exhibited a suppressive effect on both osteogenesis and adipogenesis of hMSCs. However, the EOLA–ECM scaffold promoted hMSC prolifera- tion more strongly than the other ECM scaffolds. The results indicated that dynamically remodeling ECM scaffolds could affect the osteogenic and adipogenic differentiation of hMSCs and should provide a useful 3D cell culture model for the investigation of ECM–cell interactions.

## 4.2 Introduction

Osteoporosis is a common age-related disorder that is characterized by an imbalance between the processes of bone formation.[1-3] The pathological mechanisms of osteoporosis stem from a shift of osteogenesis towards adipogenesis of hMSCs.[4-7] hMSCs are multipotent and can differentiate into different types of cells such as osteoblasts, adipose cells, chondroblasts and myogenic cells.[8, 9] Current osteoporosis therapies are predominantly through treatments with drugs or small molecules, while these treatments are associated with several side effects, such as bone loss after drug discontinuation[10] and osteonecrosis.[11, 12] As an alternative approach to treat osteoporosis, transplantation of stem cells for tissue regeneration (stem cell transplantation) has attracted much attention.[13-15] Stem cell transplantation has the uncertainty of stem cell fate and proliferation after *in vivo* transplantation, which is one of the main problems for hMSC-based osteoporosis therapy. Especially, stem cell functions are mainly regulated by their surrounding extracellular matrices (ECMs) *in vivo*.[16-21]

To elucidate the osteoporosis-related ECMs on hMSC functions and further understand their regulatory mechanism, an *in vitro* osteoporosis-ECM mimicking model is highly desirable. Development of decellularized ECMs from tissues or cultured cells is one of the existing *in vitro* approaches for investigation of ECM-cell interactions.[22-27] Previous research has reported osteoporotic models based on animals, which are typically subjected to either ovariectomy or glucocorticoid agents that induce bone loss.[28, 29] However, the tissue-derived osteoporotic ECM model is uneconomic and difficult to popularize. Meanwhile, ECMs dynamically change and remodel their components to provide a desirable microenvironment to the surrounded cells. Tissue-decellularized ECMs cannot reflect the dynamic remodeling composition of ECM because there is difficulty in obtaining tissues from animals with different stages of osteoporosis.

Cell-derived ECMs are an alternative way to provide biomimetic matrices for biomedical applications.[30-34] Cultured stem cells can be differentiated to a specific phenotype and controlled at different stages of osteogenesis, adipogenesis and osteogenesis-co-adipogenesis to deposit biomimetic ECMs on dimensional (2D) cell culture substrates.[35] However, 2D biomimetic ECMs are different from the 3D microenvironment surrounding cells in vivo. Biomimetic 3D ECMs are desirable to reproduce the in vivo microenvironments for investigation of their interaction and influence on stem cells. Generally, cell-derived ECMs are mechanically too weak and need to be reinforced with porous scaffolds with high mechanical properties. On the other hand, synthetic polymers such as poly(lactic-co-glycolic acid) (PLGA), naturally derived polymers such as collagen and their hybrid scaffolds have been broadly used in biomedical applications.[36-39] The hybrid scaffolds of PLGA and collagen have high mechanical properties, good biocompatibility and degradability. Therefore, in this study, a PLGA-collagen hybrid mesh was used as a porous support for the deposition of biomimetic ECMs to prepare 3D biomimetic scaffolds. hMSCs were cultured in PLGA-collagen hybrid mesh, and their osteogenic differentiation and adipogenic differentiation were simultaneously controlled at early or late stages. The ECMs secreted by the cells were deposited in situ on the hybrid mesh to prepare PLGA-collagen-ECM hybrid meshes mimicking osteogenesis-co-adipogenesis of hMSCs. Biomimetic ECM scaffolds were used for 3D culture of hMSCs to investigate how they balance the osteogenic and adipogenic differentiation of hMSCs.

## 4.3 Materials and methods

### 4.3.1 PLGA–collagen hybrid meshes and culture of hMSCs

At first, PLGA–collagen hybrid mesh was prepared by hybridiz- ing a PLGA knitted mesh and collagen microsponge.[40] PLGA mesh (Vicryl knitted mesh) was wetted with aqueous solution of bovine type I collagen (0.5 (w/v)%) by immersing the mesh in the solution. The interstices of PLGA mesh were filled with collagen aqueous solution, and the mesh/solution construct was frozen at -80 °C for 12 hours. The frozen construct was freeze-dried under a vacuum of 0.2 Torr for 24 hours. Subsequently, the freeze-dried construct was cross-linked by sequential treatment with cross-linking solutions containing EDC (1-ethyl-3-(3-dimethylaminopropyl, 50 mM) and NHS (N-hydroxysuccinimide, 20 mM) in ethanol/water mixture solvent, each 8 hours at room temperature. The mixture ratio of ethanol and water was changed from 95/5, 90/10 to 85/15 (v/v). Finally, the construct was washed with Milli-Q water 3 times and immersed in 0.1 M aqueous glycine solution for 24 hours to block the unreacted NHS residues. After being washed with Mill-Q water 6 times and freeze-dried, PLGA-collagen hybrid mesh was obtained. The microporous structures of PLGA knitted mesh and PLGA-collagen hybrid mesh were observed by a scanning electron microscope (SEM) operated at 3 kV.

The PLGA-collagen hybrid mesh was punched to PLGA-collagen hybrid mesh discs with a diameter of 12 mm. The mesh discs were sterilized by immersing them into 70% ethanol for 40 minutes. After being washed with sterile PBS 3 times, the PLGA-collagen hybrid mesh discs were used for the culture of hMSCs. Human bone marrow derived mesenchymal stem cells (hMSCs, P2) were purchased from Lona (Walkersville, MD; Material No: PT-2501, Batch No: 18TL1113327). The hMSCs were subcultured twice in 75 $cm^2$ tissue culture flasks with MSCBM™ (Lonza, Walkersville, MD) and used for subsequent experiments at passage 4. Confluent hMSCs were collected by treatment with 0.25% trypsin/EDTA (Sigma, USA). The cells were suspended in MSCGMTM at a cell density of $2.5 \times 10^6$ cells/mL, which was used for cell seeding.

The sterilized PLGA-collagen mesh discs were placed in each well of 24-well plates. A glass ring (inner Ø = 10 mm, outer Ø = 12 mm) was placed on each mesh disc to prevent cell leakage during cell seeding. Two hundred microliters of the cell suspension were seeded on one side of each mesh disc and cultured for 6 hours. Then, the mesh discs were turned over, and the other side was seeded with the same number of hMSCs. After another 6 hours of culture, glass rings were removed, and the hMSCs/PLGA-collagen constructs were cultured under different conditions as shown below for controlling osteogenic-co-adipogenic differentiation and in situ deposition of ECMs. To observe cell adhesion and distribution in PLGA collagen hybrid mesh, hMSCs after culture for 30 minutes were washed, freeze-dried and observed by SEM.

### 4.3.2 Osteogenic-co-adipogenic differentiation of hMSCs

After hMSCs were seeded into PLGA-collagen hybrid mesh discs, the cells were cultured in a mixture medium of osteogenic medium (OM) and adipogenic medium (AM). The mixture medium was prepared by mixing OM and AM at different ratios (Table 1). The mixture media at OM/AM ratios of 95/5, 85/15, 70/30 and 50/50 were used for simultaneous differentiation according to our previous study.[41] The hMSCs were cultured in the mixture medium for different times to induce stepwise osteogenic-co-adipogenic differentiation

of hMSCs (Table 1).[35] Osteogenic medium was composed of Dulbecco's modified Eagle's medium (DMEM, Sigma, Louis, MO), 10% fetal bovine serum (FBS, Gibco, Grand Island, NY), 1000 mg/l glucose, 584 mg/l glutamine, 100 units/ml penicillin, 100 mg/l streptomycin, 0.1 mM nonessential amino acid, 1 mM sodium pyruvate, 0.4 mM proline, 50 mg/l ascorbic acid, 10 nM dexamethasone and 10 mM b-glycerolphosphate. Adipogenic medium was composed of DMEM, 10% FBS, 4500 mg/l glucose, 584 mg/l glutamine, 100 units/ml penicillin, 100 mg/l streptomycin, 0.1 mM nonessential amino acid, 1 mM odium pyruvate, 0.4 mM proline, 50 mg/l ascorbic acid, 1 μM dexamethasone, 0.5 mM methyl-isobutylxanthine, 10 μg/mL insulin, and 100 mM indomethacin. The stepwise osteogenic-co-adipogenic differentiation culture conditions are shown in Table 1. hMSCs cultured in basal medium were maintained at stem cell tage. Basal medium was composed of DMEM, 10% FBS, 1000 mg/l glucose, 584 mg/l glutamine, 100 units/ml penicillin, 100 mg/l streptomycin, 0.1 mM nonessential amino acid, 1 mM sodium pyruvate, 0.4 mM proline, and 50 mg/l ascorbic acid. After being cultured under each condition, the hMSCs/PLGA-collagen hybrid mesh constructs were observed by SEM.

Table 1.
The culture conditions of stepwise osteogenesis-co-adipogenesis of hMSCs.
OM: osteogenic medium; AM: adipogenic medium

| Groups | SC | EOEA | EOLA | LOEA | LOLA |
|---|---|---|---|---|---|
| Stepwise osteogenesis-co-adipogenesis | | | | | |
| Culture medium | Basal medium (BM) | OM/AM ratio of 85/15 (O85A15) | OM/AM ratio of 50/50 (O50A50) | OM/AM ratio of 95/5 (O95A5) | OM/AM ratio of 70/30 (O70A30) |
| Culture time (days) | 7 | 5 | 14 | 21 | 21 |

Stem stage (SC) of hMSC
Early osteogenesis (EO) stage cell
Late osteogenesis (LO) stage cell
Early adipogenesis (EA) stage cell
Late adipogenesis (LA) stage cell

### 4.3.3 ALP staining and ALP activity assays

The hMSCs cultured under the conditions shown in Table 1 were washed with PBS and fixed with 4% paraformaldehyde for 10 min. Afterwards, the constructs were immersed with 0.1% naphthol AS-MX phosphate (Sigma, St. Louis, MO) and 0.1% fast blue RR salt (Sigma, St. Louis, MO) in 56 mM 2-amino-2-methyl-1,3-propanediol (pH 9.9, Sigma, St. Louis, MO) working solution for 10 min at room temperature. After being washed with PBS twice, the constructs were observed under an optical microscope (Olympus, Tokyo, Japan).

For the ALP activity assay, a Sensolyte® pNPP alkaline phosphatase assay kit (Anaspec, USA) was used. The experimental procedure was performed according to the manufacturer's instructions. Briefly, the hMSCs/hybrid mesh disc constructs were crushed into powder using an electric crusher. Then, the powder was moved into 1.0 mL assay buffer in a 1.5 mL tube by spatula carefully. After incubation for 10 minutes under agitation, the cell suspensions were centrifuged at 10000 g/min for 15

minutes to collect the supernatant. All the steps described above were carried out at 4 °C. The supernatant was incubated with pNPP alkaline phosphatase substrate solution for 30 minutes at room temperature. The absorbance was measured using a microplate reader (Bio-Rad, California USA) at a wavelength of 405 nm. For normalization of the relative ALP amount, the DNA content of each sample was measured using a DNA quantitation kit (DNAQF; Sigma, St. Louis, MO, USAF). First, the samples were frozen at -80 °C and freeze-dried. Then, each sample was digested with 500 μL of papain solution at 60 °C for 6 hours under shaking. Finally, the amount of DNA in the lysate was measured. Every three samples were used for the analysis (n = 3).

### 4.3.4 Alizarin Red S staining and calcification assays

For alizarin red S staining, the hMSCs/hybrid mesh disc constructs were first fixed with 4% paraformaldehyde and then immersed in 0.1% alizarin red S solution for 10 minutes at room temperature. Afterwards, the constructs were rinsed with PBS and observed under an optical microscope. The calcium deposits were quantified using the QuantiChrom calcium assay Kit (BioAssay Systems, Hyward, CA) according to the manufacturer's recommendations. Briefly, the hMSCs/hybrid mesh disc constructs were frozen and freeze-dried. Then, the deposited calcium was extracted from the constructs by overnight (24 hours) solubilization of the deposits with 0.5 M HCl aqueous solution. The extracts were cleaned by centrifugation (10000 g/min for 5 minutes) and measured by the Kit. Every three samples were used for the analysis (n = 3).

### 4.3.5 Oil Red O staining

The hMSCs cultured under the conditions shown in Table 1 were rinsed twice with pre-warmed PBS and fixed with 4% paraformaldehyde solution. Afterwards, the samples were treated with 60% 2-propanol solution for 5 minutes at room temperature. Finally, the samples were soaked in Oil Red O working solution for 5 minutes, washed with PBS and observed under an optical microscope. For quantitative analysis, the samples were air-dried and then soaked in 2-propanol solution to extract the Oil Red O dye. The absorbance of each sample was read at 540 nm by a microplate reader. Every three samples were used for the analysis (n = 3).

### 4.3.6 Quantitative real-time PCR (RT-PCR)

The hMSCs cultured under the conditions shown in Table 1 were washed with PBS, and total RNA was extracted from cells using sepasol reagent (Nacalai Tesque, Kyoto, Japan) according to our previous work.[42] The expression of genes encoding alkaline phosphatase (*ALP*), bone sialoprotein 2 (*IBSP*) and lipoprotein lipase (*LPL*) was analyzed. The complementary cDNA was synthesized from 1 μg of purified total RNA in a 20 μL reaction volume using a SuperScriptTM IV VILOTM Mater Mix kit (Invitrogen). Real-time PCR analysis was performed using cDNA as a template. The reaction was conducted in a 25 μL solution containing 12.5 μL of power SYBR Green PCR Master Mix (Applied Bio-systems, Irvine, CA, USA), 9.25 μL nuclease-free water, 1 μL cDNA and 1.25 primers. Real-time PCR was performed on a QuantStudio 3 Real-Time PCR System (Applied Biosystems, Irvine, CA, USA) followed by 40 cycles of amplification (2 min at 50 °C, 10 min at 95 °C and 1 min at 60 °C). All reactions were performed in triplicate, and the relative gene expression was normalized to GAPDH and calculated using the comparative Ct method. All the specific primers and

probes used for real-time PCR are listed in Table S2. Every three samples were used for the analysis (n = 3).

### 4.3.7 Preparation of PLGA-collagen-ECM hybrid meshes by decellularization

PLGA-collagen-ECM hybrid meshes were prepared by decellularizing the hMSCs/hybrid mesh disc constructs. After being cultured at the conditions shown in Table 1, the hMSCs/hybrid mesh disc constructs were decellularized according to the protocols reported previously.[43] Briefly, the hMSCs/hybrid mesh disc constructs were frozen and thawed for 6 cycles and then immersed in 20 mM ammonia hydroxide aqueous solution for 20 min. After washing with PBS 6 times, PLGA-collagen-ECM hybrid meshes were obtained. They were frozen and freeze-dried for subsequent experiments. The micro-structures of the scaffolds were observed by SEM.

To check the decellularization effect, cell nuclei and actin filaments were examined before and after the decellularization treatment. Cell nuclei were visualized by staining with DAPI for 10 min at room temperature. Actin filaments were stained with phalloidin-Alexa 488 (Invitrogen, Carlsbad, CA) for 20 min at room temperature. The DNA content of each sample before and after decellularization was measured using a DNA quantitation kit. The method was the same as above-described. Every four samples were used for the analysis (n = 4).

### 4.3.8 Analysis of composition in PLGA–collagen–ECMs hybrid meshes

The PLGA-collagen-ECM hybrid meshes were first blocked by incubation with 1% BSA/PBS at room temperature for 1 hour. Then, they were incubated with primary antibodies for 2 additional hours at room temperature. The primary antibodies of rabbit anti-human type I collagen antibody (Santa Cruz, CA, SC-293182), mouse anti-human fibronectin antibody (Santa Cruz, CA, SC-8422), rabbit anti-human biglycan antibody (Santa Cruz, CA, SC-100857), rabbit anti-human decorin antibody (Santa Cruz, CA, SC-73896), rabbit anti-human versican antibody (Santa Cruz, CA, SC-47769) and rabbit anti-human laminin α4 antibody (Santa Cruz, CA, SC-130541) were used. Then, the samples were rinsed in PBS and incubated with peroxidase-conjugated secondary antibody (Dako, Carpinteria, CA) at room temperature for 1 hour. Finally, the color was developed with 3,3'-diaminobenzidine (DAB) substrate-chromogen (Dako, Carpinteria, CA) to visualize peroxidase-labeled antibodies. The constructs were observed under an optical microscope. The immunocytochemical staining intensity was quantified using ImageJ software (NIH, Bethesda, MD) as previously reported.[44] For each sample, four views were randomly selected to count the positively stained intensity (20 × magnification for each view), and triplicates were performed. The staining intensity was defined by the equation: Intensity = integrated intensity/area, where the integrated intensity and area were calculated by ImageJ software.

### 4.3.9 Water uptake measurement and mechanical strength test of hybrid meshes

The water uptake of PLGA-collagen and PLGA-collagen-ECM scaffolds was analysed by measuring the water held by each mesh. First, the dry weight of each mesh disc was measured. Subsequently, each mesh was immersed in PBS (pH = 7.4) solution at room temperature for 1 h. Finally, the wet mesh was removed from PBS solution, blotted with filter paper to remove any excess PBS solution and weighed. The tensile properties of the PLGA mesh, PLGA-collagen and PLGA-collagen-ECM hybrid meshes were measured by a static tensile mechanical test (TA-XT2i, Stable Micro Systems, Godalming, UK). Every three samples were used for the

analysis (n = 3).

### 4.3.10 Cell adhesion, proliferation and adioegenic and osteogenic differentiation in PLGA-collagen-ECM hybrid meshes

To investigate the influence of deposited ECMs in the PLGA-collagen-ECM hybrid meshes on hMSC adhesion and proliferation, hMSCs were seeded in the PLGA-collagen-ECM hybrid meshes. Glass rings were used during cell seeding as described above. Every scaffold was seeded once with 200 μL of $5.0 \times 10^5$ cells/mL suspension solution of hMSCs. After culture in basal medium for one day, the cell/scaffold constructs were washed thrice with pre-warm PBS and fixed with 2.5% glutaraldehyde at room temperature for 1 hour. Subsequently, the samples were washed with PBS and dehydrated in a graded ethanol-water series (v/v%) from 50% to 100% ethanol. Finally, the samples were immersed in t-butylalcohol-ethanol solutions (v/v%) (from 50% to 100%), followed by being frozen and freeze-dried. The cell/scaffold constructs were observed by SEM under an operating voltage of 3 kV.

To analyze cell proliferation, a tetrazolium salt (WST-1) assay kit (Roche Diagnostics, Indianapolis, IN, USA) was used. After hMSCs were cultured in the PLGA-collagen-ECM hybrid meshes for 1, 3 and 7 days, the cell/scaffold constructs were washed thrice with pre-warm PBS. WST-1 reagent was added to each well. After incubation at 37 $^{o}$C in the dark for 2 hours, the absorbance of the supernatant from each well was measured at 440 nm with a plate reader (Benchmark Plus, Bio-Rad, Hercules, CA, USA). Every three samples were used for the analysis (n = 3).

Adipogenic differentiation of hMSCs in the ECM caffolds was evaluated by culturing hMSCs in the ECM scaffolds with basal medium or adipogenic medium for 14 days. After culture for 14 days, Oil Red O staining and quantification were conducted. The expression of genes encoding peroxisome proliferator-activated receptor gamma (PPARG), CCAAT/enhancer binding protein (CEBPA), fatty acid binding protein 4 (FABP4), LPL and fatty acid synthase (FASN) was analyzed by RT-PCR. Every three samples were used for the analysis (n = 3).

Osteogenic differentiation of hMSCs was examined by culturing hMSCs in the ECM scaffolds with basal medium or osteogenioc medium for 21 days. After culture in basal medium or osteogenioc medium for 21 days, alizarin red S staining and quantification were conducted. The expression of osteogenesis-related genes of osterix (SP7), secreted phosphoprotein 1 (SPP1), IBSP and runt-related transcription factor 2 (RUNX2) was measured by RT-PCR. All the specific primers and probes used for real-time PCR are listed in Table S2. Every three samples were used for the analysis (n = 3).

### 4.3.11 Statistical analysis

All the data are presented as the mean ± standard deviation (S.D.) ($n \geq 3$). A two-tailed t-test was used to determine the significance between the two groups. The multiple groups were analyzed by one-way ANOVA with a Tukey post hoc test. For all the statistical tests, P values less than 0.05 were considered significant differences.

## 4.4 Results

### 4.4.1 Preparation of PLGA-collagen hybrid mesh and stepwise osteogenesis-co-adipogenesis of hMSCs in PLGA-collagen hybrid mesh

PLGA-collagen hybrid mesh was prepared by hybridizing a PLGA knitted mesh with collagen microsponges. The openings of the PLGA mesh were filled with collagen microsponges (Figure 4.1a,b). When hMSCs were cultured in the PLGA-collagen hybrid mesh, the cells adhered to the pore surfaces of collagen microsponges (Figure 4.1c).

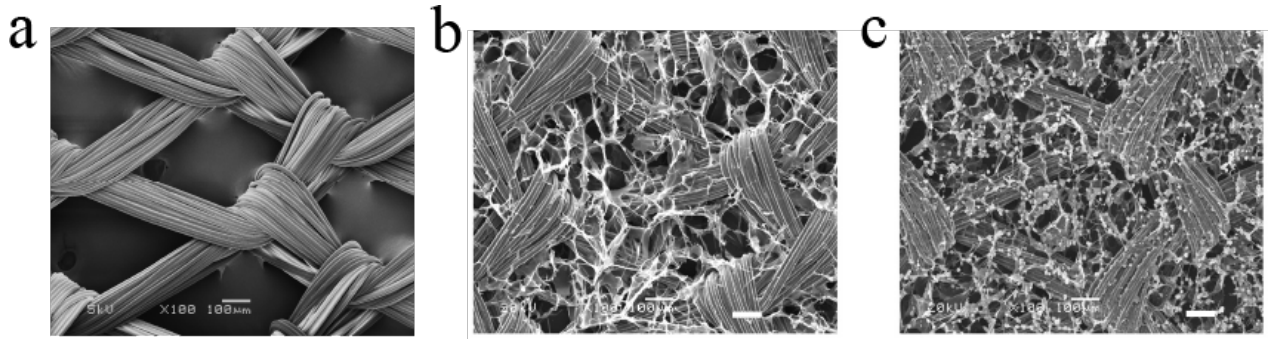


Figure 4.1. SEM images of PLGA mesh (a), PLGA-collagen hybrid mesh (b) and hMSCs cultured in the hybrid mesh in basal medium for 30 min (c). Scale bar: 100 μm.

ALP staining was positive in the EOEA, EOLA, LOEA and LOLA groups, while only the LOEA and LOLA groups showed positive staining for calcium deposition (alizarin red S staining) (Figure 4.2). Quantitative analysis of ALP staining showed that ALP activity was increased in all groups after induction culture and that ALP activity in EOEA and EOLA was higher than that in the LOEA and LOLA groups (Figure 4.3a). Quantitative analysis of calcium deposition showed that calcium deposition in LOEA and LOLA was significantly higher than that in EOEA and EOLA (Figure 4.3b). ALP was expressed by all the groups of EOEA, EOLA, LOEA and LOLA and was most highly expressed by the EOEA group (Figure 4.2b). Gene expression of IBSP in the LOEA and LOLA groups was significantly higher than that in the EOEA and EOLA groups (Figure 4.2c).

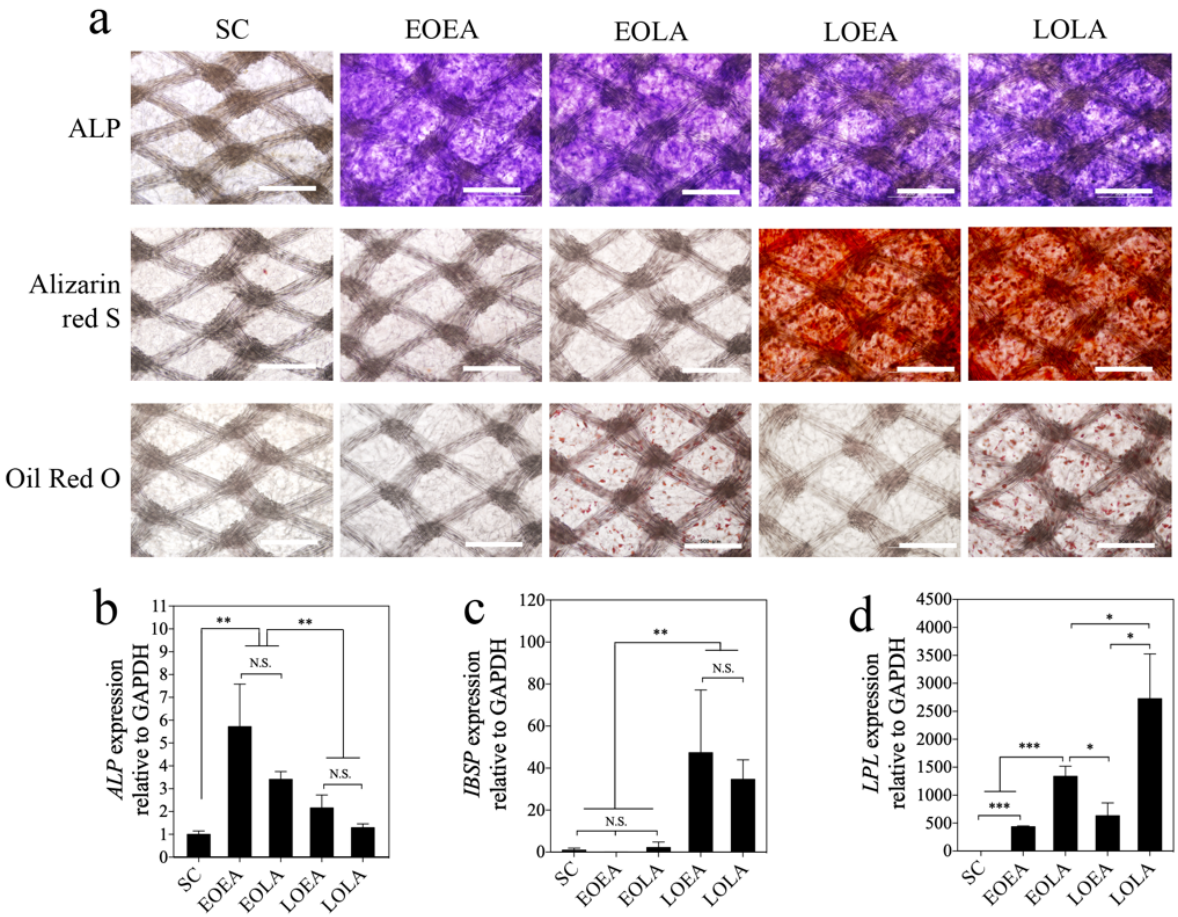


Figure 4.2. qualitative and real-time PCR analysis of hMSCs/PLGA-collagen constructs after stepwise differentiation. ALP, alizarin red S and Oil red O staining of the constructs after stepwise differentiation (a). RT-PCR analysis for the expression of osteogenesis-related marker gene ALP (b), IBSP (c) and adipogenesis-related marker gene LPL (d). Scale bar: 500 μm.

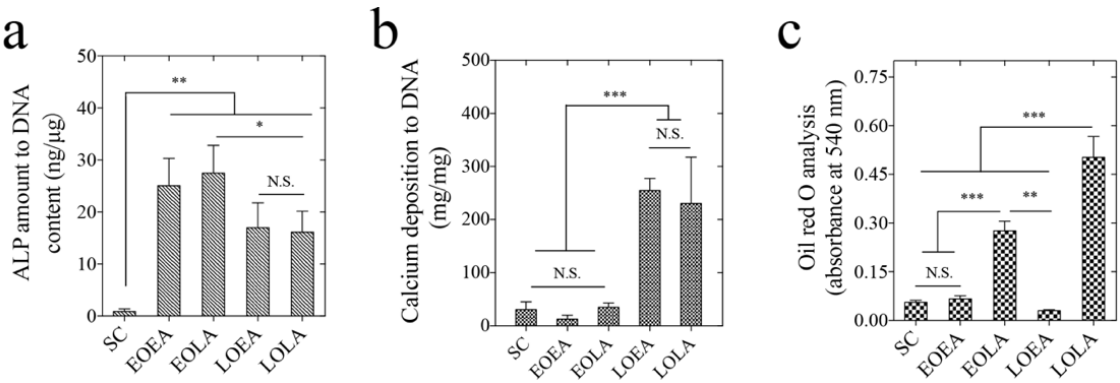


Figure 4.3. Quantitative analysis of ALP activity (a), calcium deposition (b) and Oil red O staining (c). Date represent means ± S.D. (n = 3).

Oil Red O staining showed that lipid vacuoles were only observed in the EOLA and LOLA groups. Extraction of lipid vacuole staining showed that EOLA and LOLA had significantly higher absorbance than other groups (Figure 4.3c). The LPL gene was expressed in all the EOEA, EOLA, LOEA and LOLA groups, and its expression in the EOLA and LOLA groups was significantly higher than that in

the EOEA and LOEA groups (Figure 4.2d). These results indicated that hMSCs cultured in the mixture media were simultaneously differentiated into stepwise stages of osteogenesis and adipogenesis. Four different stages of osteogenic-co-adipogenic differentiation of hMSCs were achieved. When hMSCs were cultured in PLGA–collagen hybrid mesh with basal medium, no positive staining of ALP, Alizarin S or Oil Red O was observed (Figure 4.2). The expression of ALP, IBSP and LPL was very low, indicating that hMSCs cultured in basal medium retained the SC stage.

### 4.4.2 Preparation and characterization of PLGA–collagen–ECM scaffolds deposited with ECMs mimicking stepwise osteogenesis-co-adipogenesis of hMSCs.

PLGA–collagen–ECM hybrid meshes were prepared by decellularizing the hMSCs/PLGA–collagen hybrid mesh constructs exhibiting SC, EOEA, EOLA, LOEA and LOLA stages of stepwise osteogenic-co-adipogenic differentiation. During osteogenic-co-adipogenic differentiation of hMSCs, hMSCs proliferated and secreted ECMs filling the void spaces in the PLGA–collagen hybrid mesh (Figure 4.4). Before decellularization, cell nuclei and actin filaments were visualized by fluorescence staining (Figure 4.5a). No cell nuclei or actin filaments were stained after decellularization. Measurement of DNA content in the constructs before and after decellularization showed that more than 98.9% of DNA was removed after decellularization (Figure 4.5b and Table 2). These results demonstrated that decellularization was effective.

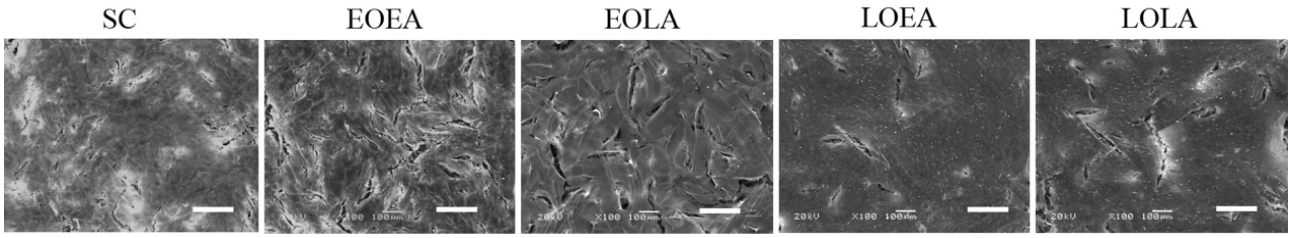


Figure 4.4 SEM images of the hMSCs/PLGA-collagen hybrid mesh constructs after stepwise osteogenic-co-adipogenic differentiation. Scale bar: 200 μm.

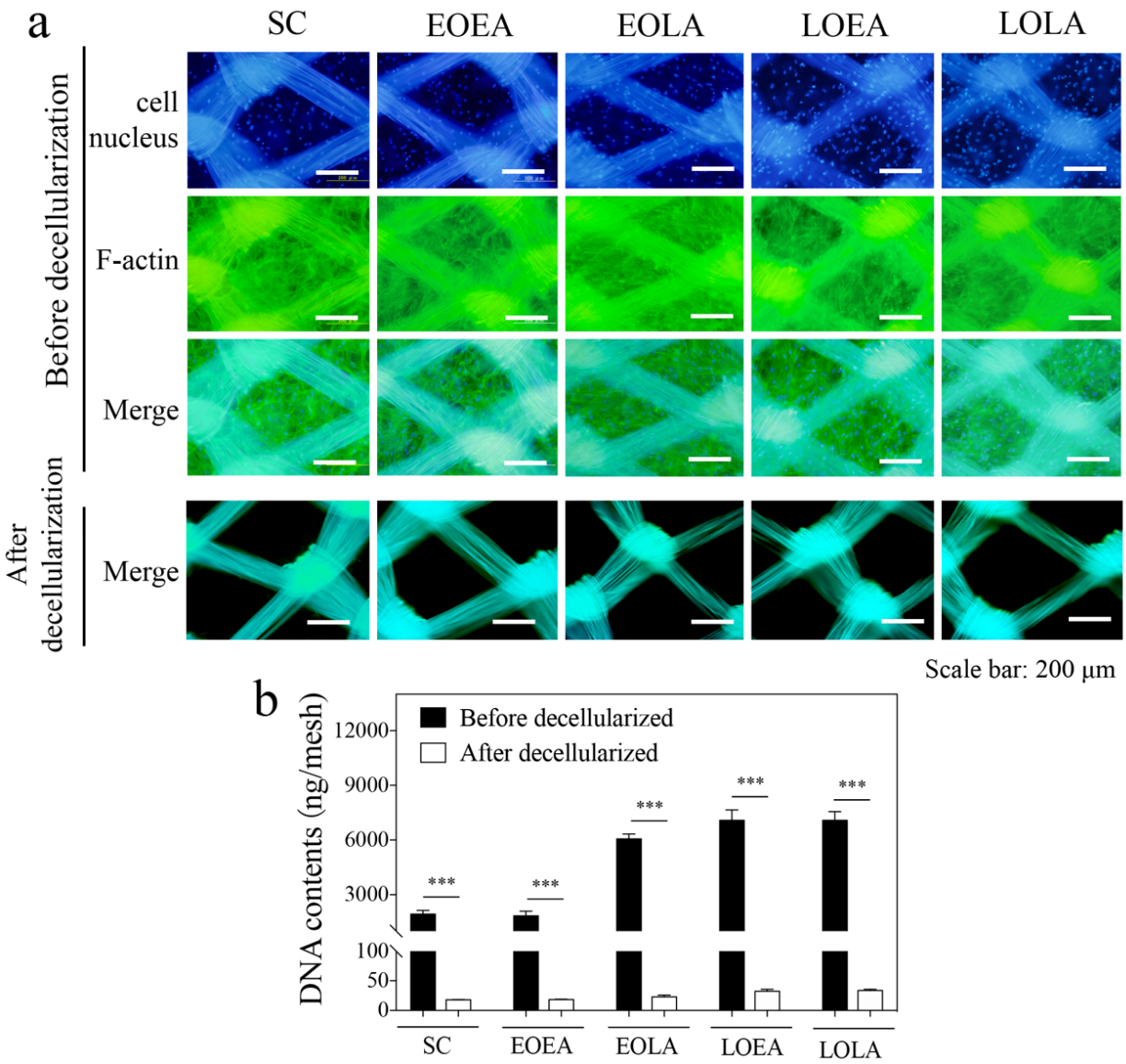


Figure 4.5. Decellularization of the hMSCs/PLGA-collagen hybrid mesh constructs. Cell nucleus and f-actin staining of the hMSCs/PLGA-collagen constructs before and after decellularization (a). DNA quantification of the hMSCs/PLGA-collagen hybrid mesh constructs before and after decellularization (b).

Table 2.
Decellularization efficiency based on DNA quantification.

| SC | EOEA | EOLA | LOEA | LOLA |
|---|---|---|---|---|
| 99.1 ± 0.1% | 98.9 ± 0.3% | 99.6 ± 0.8% | 99.4 ± 0.1% | 99.3 ± 0.4% |

The decellularized scaffolds were defined as SC–ECMs, EOEA–ECMs, EOLA–ECMs, LOEA–ECM and LOLA–ECM scaffolds. SEM observation showed that all the PLGA–collagen–ECM scaffolds were highly porous (Figure 4.6). ECM components in the PLGA–collagen–ECM scaffolds were examined through immunocyotchemical staining of collagen I, fibronectin, biglycan, deconrin, versican and laminin (Figure 4.7a). The immunocytochemical staining intensity was quantified and is shown in Figure 4.7b. Collagen I was positively stained in all five ECM scaffolds, while the staining

was weak in the EOLA–ECM scaffolds. Fibronectin was strongly stained in all the ECM scaffolds except for the EOEA–ECM scaffold. Biglycan was highly detected in SC- and LOEA-ECM scaffolds, weekly detected in EOEA–ECM scaffolds while scarcely stained in EOLA- and LOLA-ECMs scaffolds. Decorin was only stained in EOLA- and LOLA- ECM scaffolds. Versican was weakly stained in EOEA-ECMs scaffold and strongly stained in the other four ECMs scaffolds. Laminin was present in EOEA-, EOLA-, LOEA- and LOLA-ECMs scaffolds, but was not in SC-ECMs scaffold. The results indicated the dynamic change of ECMs composition during stepwise osteogenic-co-adipogenic differentiation of hMSCs. The composition was dependent on the stage of simultaneous osteogenic and adipogenic differentiation.

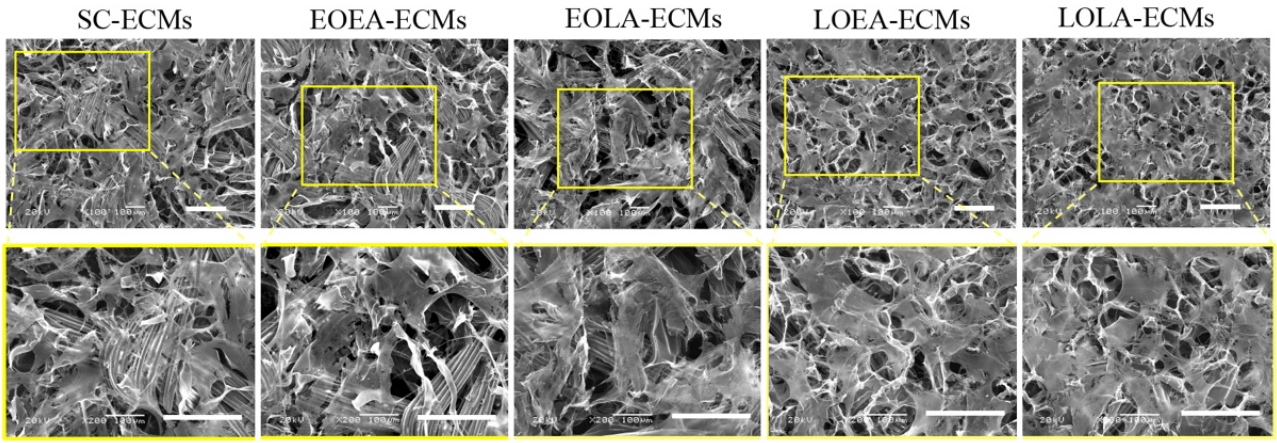


Figure 4.6. SEM images of PLGA-collagen-ECMs scaffolds at low and high magnification. Scale bar: 200 μm.

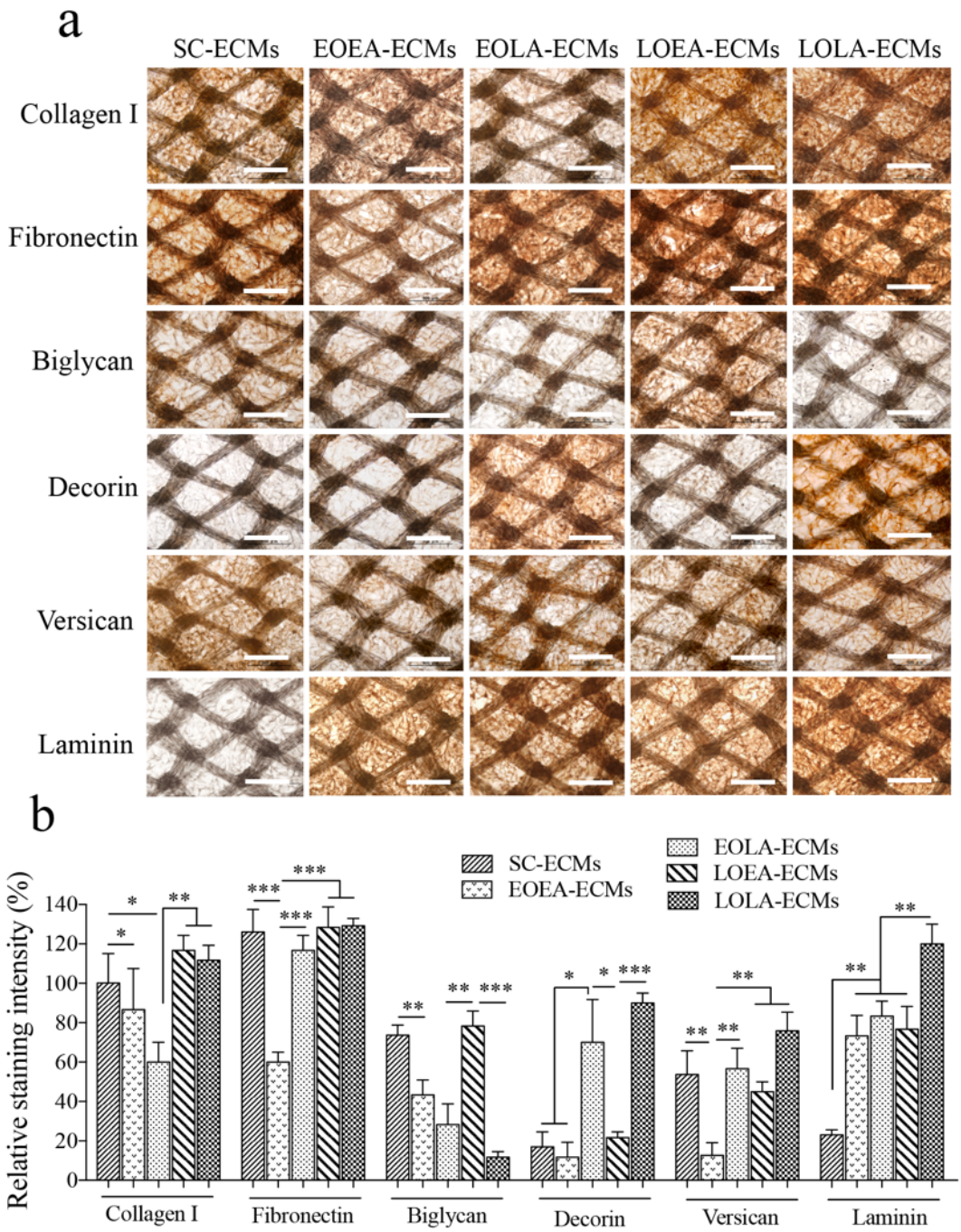


Figure 4.7. Characterization of ECMs components in PLGA-collagen-ECMs scaffolds. The ECMs components were detected by immunohistological staining, including collagen I, fibronectin, biglycan, deconrin, versican and laminin (a). Quantitative analysis of the immunocytochemical staining intensity normalized to the level of collagen I in SC-ECM scaffold (b). Date represent means ± S.D. (n = 3). Scale bar: 500 μm.

Tensile strength of the PLGA mesh, PLGA–collagen and PLGA–collagen–ECM hybrid scaffolds was measured by a static tensile test (Figure 4.8a). The Young's modulus of PLGA mesh, PLGA–collagen hybrid scaffold, SC–ECM–ECM, EOEA–ECM and EOLA–ECM hybdrid scaffolds was not significantly different, although a slight decrease in the Young's modulus of SC–ECM, EOEA–ECM and EOLA–ECM hybrid scaffolds was observed. The Young's modulus of the LOEA–ECM and LOLA–ECM hybrid scaffolds was significantly lower than that of the previous five scaffolds. This

should be due to the partial degradation of PLGA mesh after culture for 21 days. ECM water uptake of the hybrid meshes was measured (Figure 4.8b). The PLGA mesh had much lower water uptake than did the hybrid scaffolds. The PLGA–collagen and PLGA–collagen–ECM hybrid scaffolds showed the same level of water uptake.

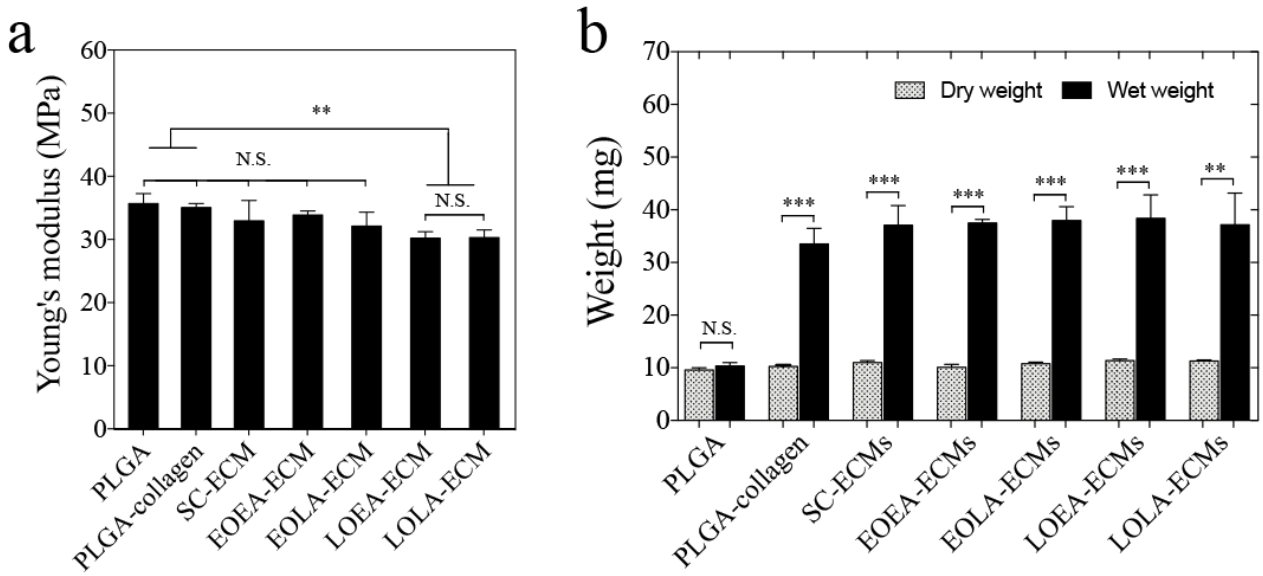


Figure 4.8. The mechanical properties (a) and water uptake (b) of PLGA-collagen and ECM-scaffolds groups

The results indicated that the hydrophilicity of the PLGA mesh was improved after hybridization with collagen. The PLGA–collagen–ECM hybrid scaffolds had the same hydrophilicity as that of the PLGA–collagen hybrid scaffold. Hydrophilicity is good for seeding the cell suspension solution into the hybrid meshes.

### 4.4.3 Adhesion, proliferation and differentiation of hMSCs in PLGA–collagen–ECM hybrid meshes

The adhesion and morphology of hMSCs in the ECM scaffolds were observed by SEM. hMSCs adhered and spread well in all scaffolds after 1 day of culture (Figure 4.9a). They proliferated with increasing culture time (Figure. 4.9b). After culture for 7 days, hMSCs showed the highest proliferation in PLGA–collagen and SC–ECM scaffolds. EOEA–ECM, LOEA–ECM and LOLA–ECM scaffolds had significantly lower effects on cell proliferation than SC–ECM and EOLA–ECM scaffolds.

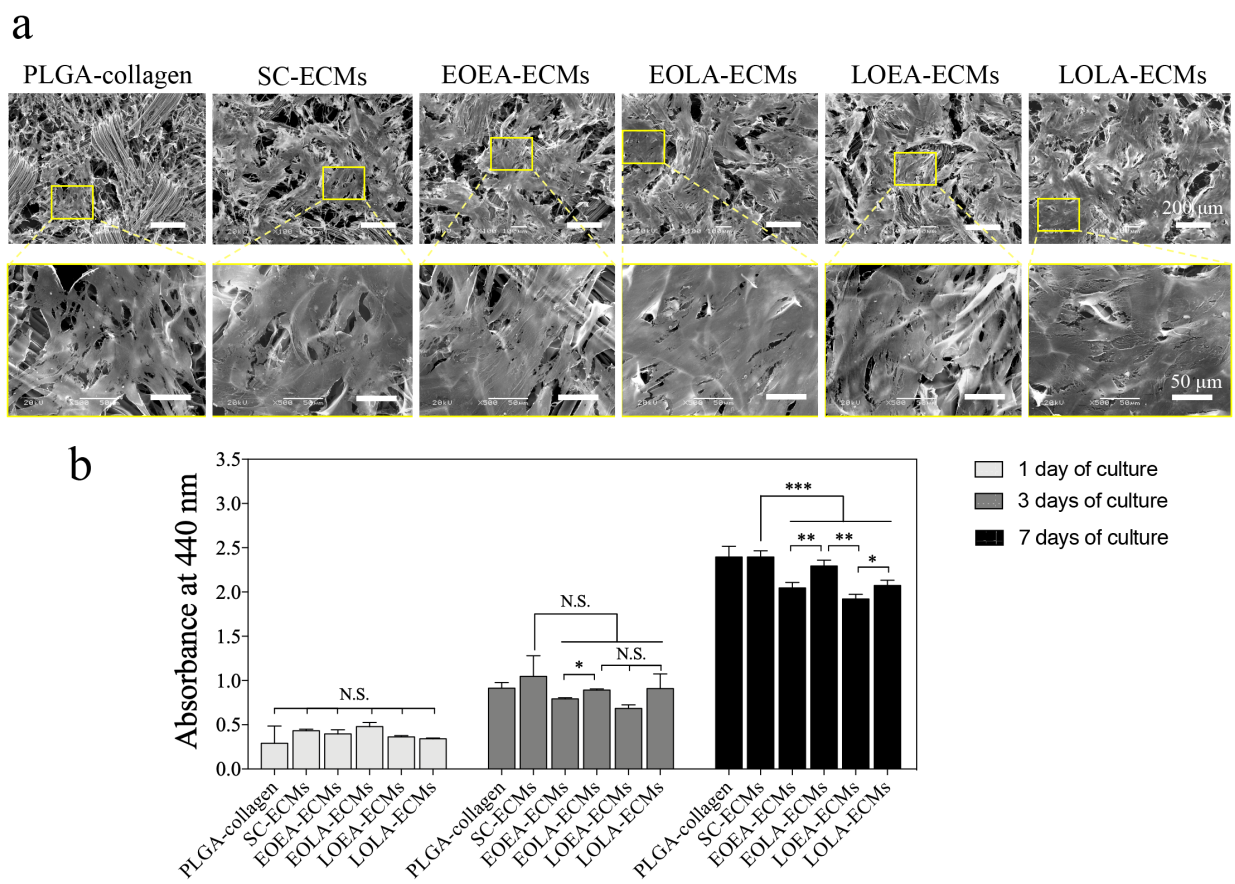


Figure 4.9. Adhesion and proliferation of hMSCs in the PLGA-collagen-ECMs scaffolds and PLGA-collagen hybrid mesh. SEM images of cell/PLGA-collagen-ECM constructs and cell/PLGA-collagen constructs at low magnification (scale bar: 200 μm) and high magnification (scale bar: 50 μm) (a). Cell proliferation in PLGA-collagen-ECMs scaffolds and PLGA-collagen hybrid mesh after being cultured for 1, 3 and 7 days (b). n = 3.

After being cultured in basal medium, there were no lipid vacuoles observed in either ECM scaffolds or PLGA–collagen hybrid mesh (Figure 4.10a). Quantification of the Oil Red O staining showed that the absorbance was low in all groups, and no significant difference was observed (Figure 4.10b). Gene expression results showed that hMSCs cultured in PLGA–collagen and EOEA–ECM scaffolds showed significantly higher expression of CEBPA and PPARG than other groups (Figure 4.10). The expression levels of genes encoding LPL and FASN showed no significant difference among all the groups. The expression of FABP4 was at the highest level in the cells cultured in EOEA–ECM scaffolds.

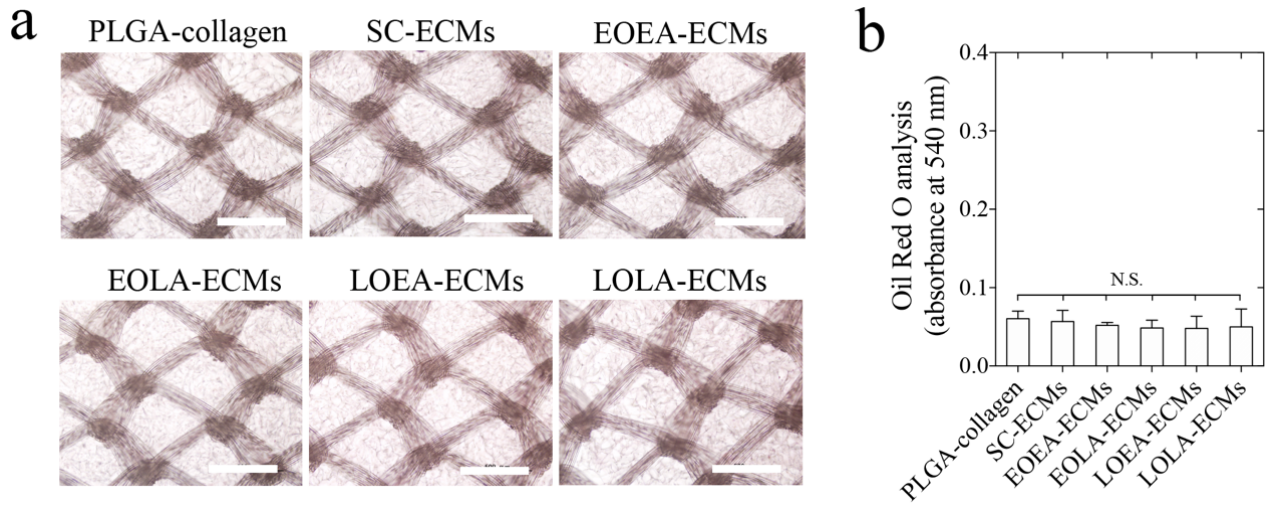


Figure 4.10. Measurement of the lipid vacuoles in the cells/ECMs-scaffold and cells/PLGA-collagen constructs when being cultured in basal medium. Qualitative analysis of the constructs by Oil red O staining after culture in basal medium (a), and quantitative analysis of the lipid vacuoles dye after culture in basal medium (b). n = 3. Scale bar: 500 μm.

When hMSCs were cultured in the scaffolds with adipogenic inductive medium, hMSCs in all the scaffolds were positively stained by Oil Red O (Figure 4.11a). Cells cultured in EOEA–ECM scaffolds and PLGA–collagen hybrid mesh showed significantly higher staining intensity than did cells cultured in the other groups (Figure 11b). Furthermore, cells cultured in SC–ECMs and EOLA–ECMs scaffolds showed the lowest staining intensity. Culture in adipogenic induction medium also showed a very significant increase in adipogenesis-related genes (Figure 4.12). When each scaffold was compared, PLGA–collagen and EOEA–ECM scaffolds exhibited the highest expression levels of CEBPA, PPARG, LPL, FASN and FABP4, while EOLA–ECM scaffolds showed the lowest expression levels of these genes. A similar expression tendency of CEBPA and PPARG was observed for hMSCs cultured with either basal medium or adipogenic induction medium, suggesting that the adipogenic differentiation of hMSCs was guided by the osteogenesis-co-adipogenesis mimicking ECM scaffolds and that their influence could be synergistically magnified with the addition of adipogenic induction factors. These results revealed that the matrices mimicking early stage osteogenesis-co-early stage adipogenesis (EOEA) were more favorable to adipogenesis of hMSCs than the other biomimetic ECM scaffolds.

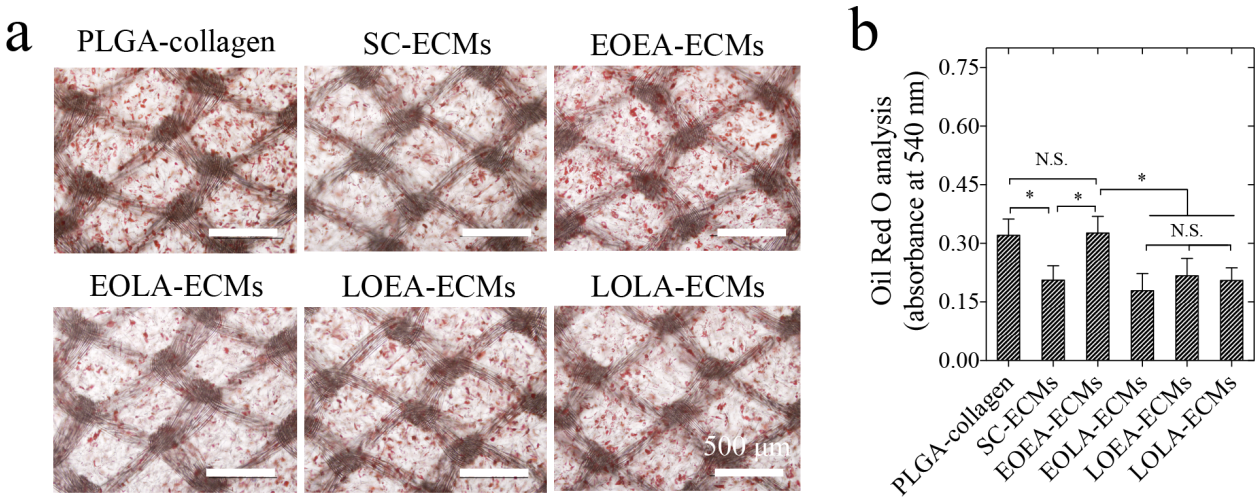


Figure 4.11. Measurement of the lipid vacuoles in the cells/ECMs-scaffold and cells/PLGA-collagen constructs after culture in adipogenic medium. Qualitative analysis of the constructs by Oil Red O staining after 14 days of culture (a), and quantitative analysis of the lipid vacuoles dye after 14 days of culture (b). n = 3. Scale bar: 500 μm.

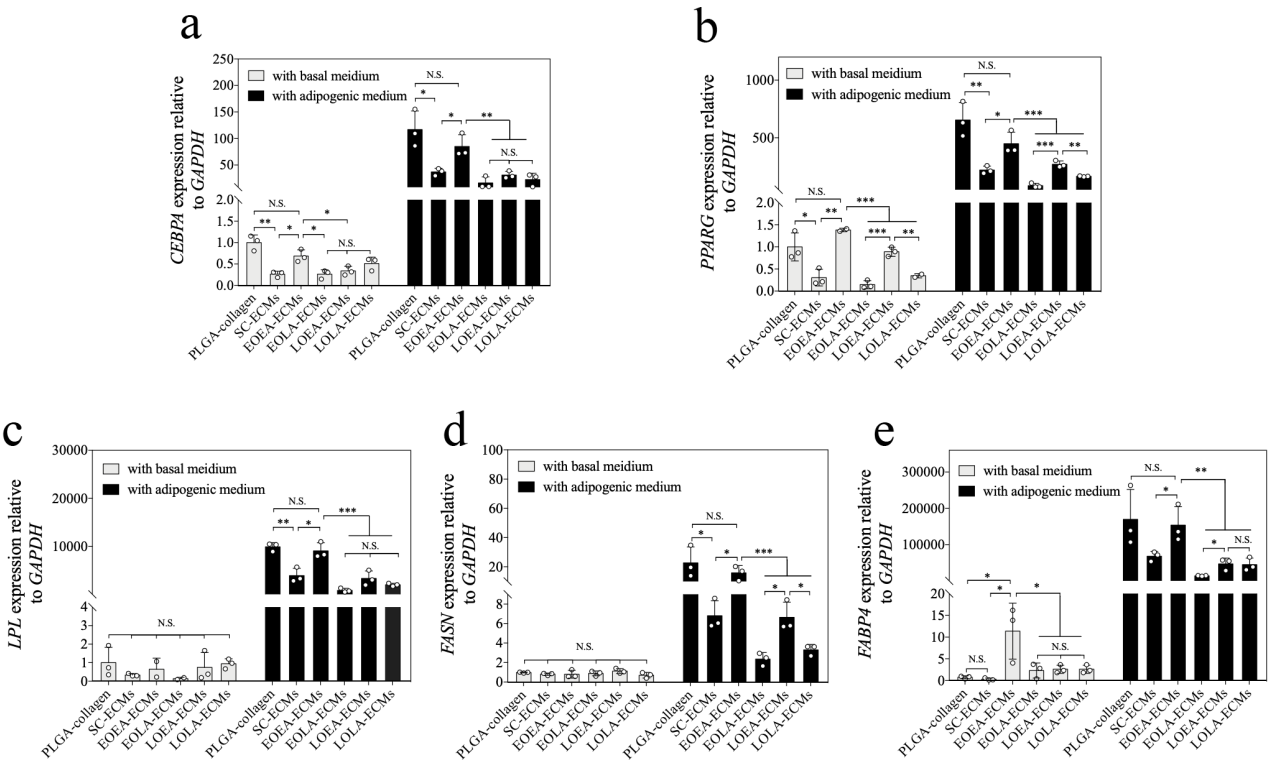


Figure 4.12. RT-PCR analysis of adipogenesis-related genes in the cells/ECMs-scaffold and cells/PLGA-collagen constructs after culture in basal medium or adipogenic medium, including CEBPA (a), PPARG (b), LPL (C), FASN (d) and FABP4 (e). Date represent means ± S.D. (n = 3). *, $P < 0.05$; **, $P < 0.01$; ***, $P < 0.001$. N.S., no significant difference.

The influence of the ECM scaffolds on the osteogenic differentiation of hMSCs was evaluated by culturing hMSCs in ECM scaffolds with basal medium or osteogenic medium for 21 days. Calcium

deposition was detected by alizarin red S staining. The expression levels of osteogenesis-related genes were investigated by RT-PCR analysis.

When hMSCs were cultured in basal medium, alizarin red S staining showed no obvious calcium deposition in the scaffolds except for slight staining in LOEA–ECMs and LOLA–ECMs scaffolds (Figure 4.13a). Quantification of calcium deposition showed very low levels of calcium depositions in all scaffolds (Figure 4.13b).

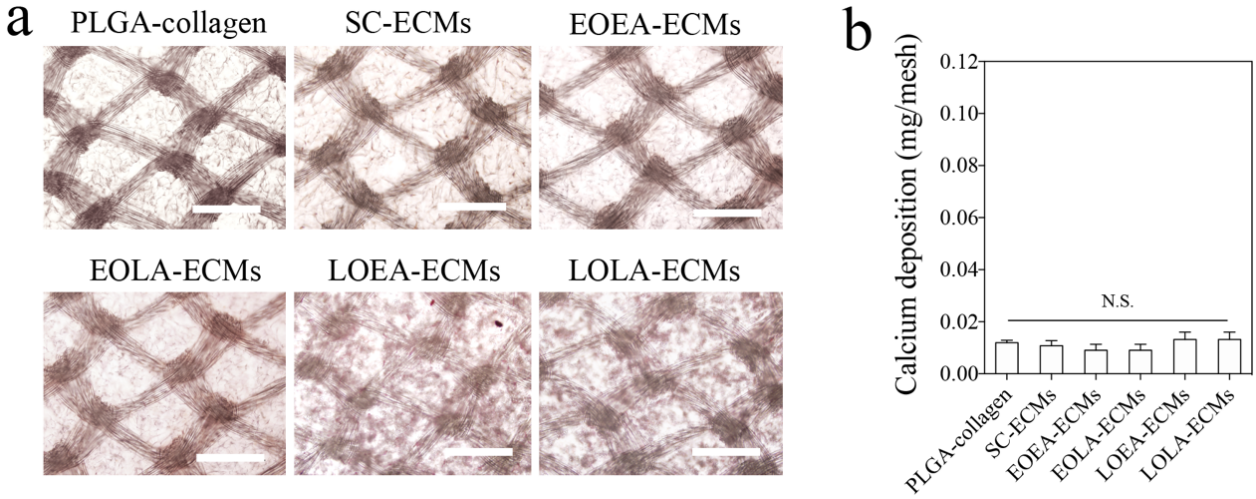


Figure 4.13. Measurement of the calcium deposition in the cells/ECMs-scaffold and cells/PLGA-collagen constructs when being cultured in basal medium. Qualitative analysis of the constructs by alizarin red S after culture in basal medium (a), and quantitative analysis of the calcium deposits after culture in basal medium (b). Date represent means ± S.D. (n = 3). *, $P < 0.05$; N.S., no significant difference. Scale bar: 500 μm.

When hMScs were cultured in osteogenic induction medium, positive alizarin red S staining was observed in all scaffolds (Figure 4.14a). LOEA–ECMs and LOLA–ECMs had higher levels of calcium deposition than did the other scaffolds (Figure 4.14b).

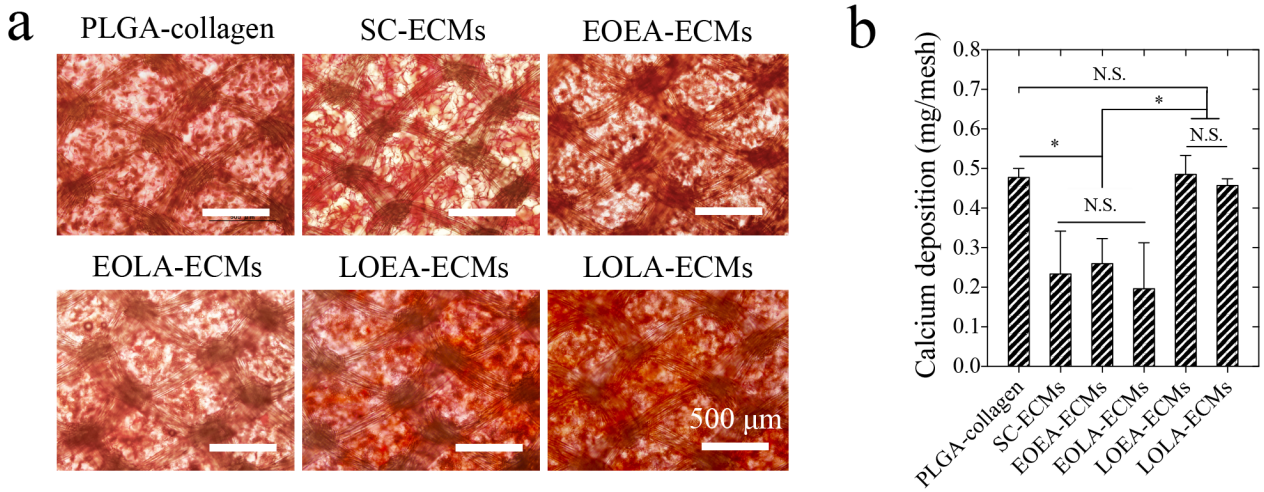


Figure 4.14. Measurement of the calcium deposition in the cells/ECMs-scaffold and cells/PLGA-collagen constructs after culture in osteogenic medium. Qualitative analysis of the constructs by alizarin red S after 21 days of culture (a), and quantitative analysis of the calcium deposits after 21 days of culture (b). n = 3. Scale bar: 500 μm.

Gene expression results showed that very significantly higher expression of osteogenesis-related marker genes was detected in hMSCs cultured in osteogenic induction medium compared to the culture in basal medium (Figure 4.15). hMSCs cultured in LOEA–ECMs and LOLA–ECMs scaffolds showed a higher expression level of genes encoding RUNX2, SP7, OCN and SPP1. The cells cultured in PLGA–collagen, SC–ECMs and EOEA–ECMs scaffolds showed higher expression of IBSP than did the cells cultured in other ECM scaffolds (Figure 4.15c). The calcium deposition and gene expression results indicated that LOEA–ECM and LOLA–ECM scaffolds had a promotive effect on the osteogenic differentiation of hMSCs.

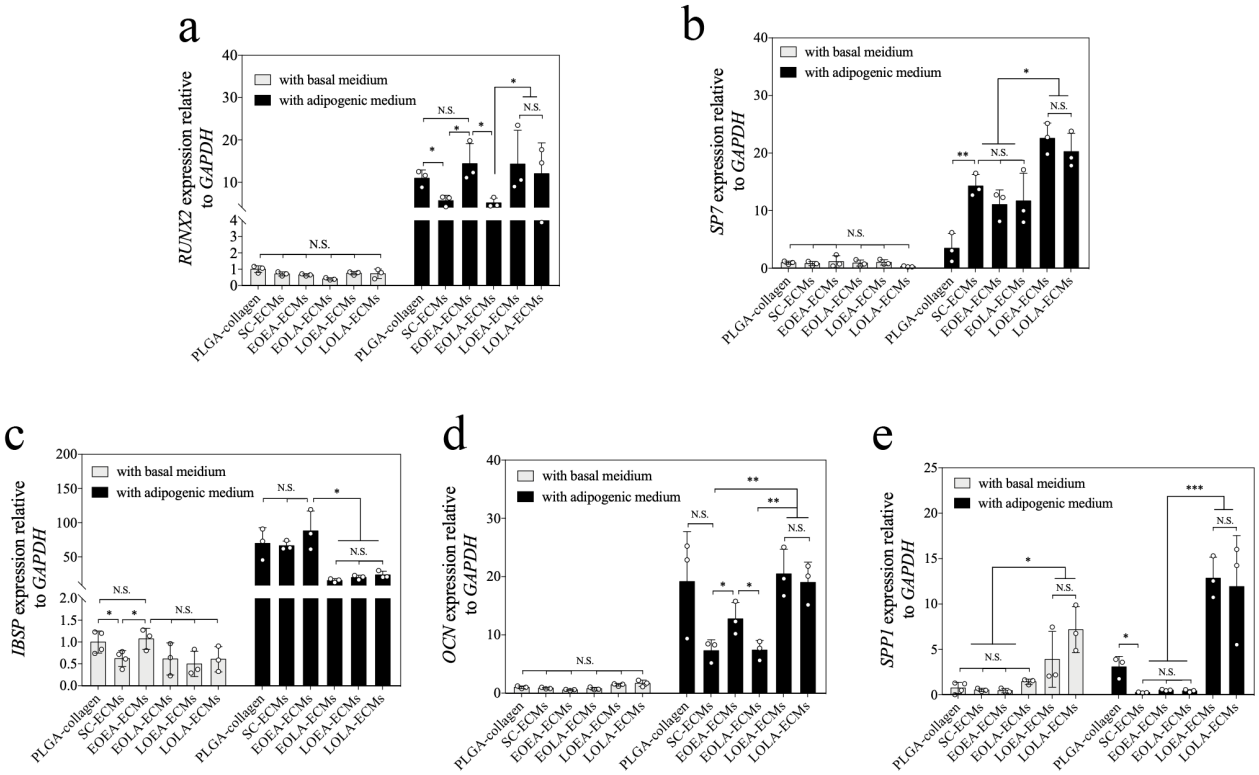


Figure 4.15. RT-PCR analysis of osteogenesis-related genes in the cells/ECMs-scaffold and cells/PLGA-collagen constructs after culture in basal medium or osteogenic medium, including RUNX2 (a), SP7 (b), IBSP (C), OCN (d) and SPP1 (e). n = 3.

## 4.5 Discussion

Bone marrow-derived hMSCs are the most widely used stem cells for osteoporosis research baecause of their potential to differentiate into osteoblasts, easy expansion culture and easy manipulation for in vivo application.[45, 46] Stem cell fates are known to be affected by their surrounding ECMs microenvironment.[47, 48] To elucidate the role of matrices from osteoporosis microenvironments in balancing osteogenic and adipogenic differentiation of hMSCs, a suitable cell culture model that mimics the dynamic ECMs change in osteoporosis microenvironments is desirable for in vitro osteoporosis studies. In the present study, such dynamically changing ECMs were prepared from simultaneous osteogenic and adipogenic differentiation of hMSCs at different differentiation stages in PLGA-collagen hybrid mesh. The dynamically remodeling ECMs were in situ deposited in the PLGA-collagen hybrid mesh. Four types of dynamically remodelling ECM scaffolds, EOEA-

ECMs, EOLA-ECMs, LOEA-ECMs and LOLA-ECMs, were prepared and used for investigation of their influence on hMSCs adhesion, proliferation and adipogenic and osteogenic differentiation.

Depending on the stage of osteogenesis-co-adipogenesis of hMSCs, the ECMs scaffolds had different composition. Their components were not simple mixtures of stepwise osteogenic matrices[49] and adipogenic matrices.[50] The results suggested dynamic remodelling of ECMs in the PLGA-collagen-ECMs hybrid meshes, which might reflect the dynamic changing ECMs in osteoporosis microenvironments. The ECMs scaffolds supported the stem cells adhesion. Influence of ECMs scaffolds on hMSCs proliferation was dependent on ECMs type. After culture for 7 days, cell proliferatio in EOLA ECMs scaffolds was higher than that in EOEA, LOEA and LOLA ECMs scaffolds.

The influence of ECMs scaffolds on adipogenic and osteogenic differentiation of hMSCs was also dependent on ECMs type. EOEA-ECMs scaffold had a high effect on promotion of adipogenesis while a low effect on promotion of osteogenesis of hMSCs. EOLA-ECMs scaffold had a low effect on promotion of both adipogenesis and osteogenesis of hMSCs. LOEA-ECM and LOLA-ECM scaffolds showed a high effect on promotion of osteogenesis while a moderate effect on promotion of adipogenesis of hMSCs. By a comparison of their effects on both proliferation and differentiation, EOLA-ECM scaffold promoted proliferation while suppressed adipogenic and osteogenic differentiation of hMSCs. EOEA-, LOEA- and LOLA-ECM scaffolds had a promotive effect on either adipogenic or osteogenic diffrentiaion or both differentiation of hMSCs, while slightly suppressed hMSCs proliferation.

The different effects of ECMs scaffolds on adipogenic and osteogenic differentiation should be due to their compositional characteristics. Previous studies have reported that ECMs components can affect stem cells fates during their differentiation and fibronectin can inhibit adipogenesis by activating signal pathway through interaction with integrin α5β1, which is highly expressed on cell surface in preadipocytes.[51, 52] In the present research, fibronectin was highly detected in EOLA-ECMs, LOEA-ECMs and LOLA-ECMs scaffolds but weakly detected in EOEA-ECMs scaffold. That could be one of the reasons for suppressive effect of EOLA-ECMs, LOEA-ECMs and LOLA-ECMs and promotive effect of EOEA-ECMs scaffold on adipogenesis. Collagen I and fibronectin can trigger focal adhesion phosphatase signaling pathway and further promote osteogenesis of hMSCs.[53] The low expression of collagen type I in EOLA-ECMs scaffold and fibronectin in EOEA-ECMs scaffold might be one of the reasons for suppression effect on osteogenesis of hMSCs. LOEA-ECMs and LOLA-ECMs had high expression levels of collagen type I and fibronectin that contributed to the promotive effect on osteogenesis of hMSCs.

## 4.6 Conclusions

In this study, four types of biomimetic 3D PLGA-collagen-ECMs hybrid scaffolds were prepared by depositing ECMs from simultaneous osteogenic-co-adipogenic differentiation of hMSCs on PLGA-collagen hybrid mesh. The four types of ECMs scaffolds, EOEA-ECMs, EOLA-ECM, LOEA-ECMs and LOLA-ECMs scaffolds, had different composion that was dependent on the simultaneous differentiation stages. They supported the stem cells adhesion and proliferation and showed different influence on adipogenic and osteogenic differentiation of hMSCs. EOEA-ECMs scaffold showed promotive effect on adipogenic differentiation of hMSCs. EOLA-ECM scaffold had suppression effect on both adipogenic and osteogenic differentiation of hMSCs, while promitive effect on hMSCs proliferation. LOEA-ECMs and LOLA-ECMs scaffolds exhibited promotive effect on osteogenic

differentiation and a moderate effect on adipogenic differentiation of hMSCs. The 3D PLGA-collagen-ECMs hybrid meshes should provide useful 3D cell culture models for investigation of cell-ECMs interaction.

## 4.7 Reference

[1] N.R. Fuggle, E.M. Curtis, K.A. Ward, N.C. Harvey, E.M. Dennison, C. Cooper, Fracture prediction, imaging and screening in osteoporosis, Nature Reviews Endocrinology (2019).
[2] J. Luu, K. Palczewski, Human aging and disease: Lessons from age-related macular degeneration, Proceedings of the National Academy of Sciences 115(12) (2018) 2866-2872.
[3] R. Eastell, T.W. O'Neill, L.C. Hofbauer, B. Langdahl, I.R. Reid, D.T. Gold, S.R. Cummings, Postmenopausal osteoporosis, Nature Reviews Disease Primers 2 (2016) 16069.
[4] J. Tan, X. Xu, Z. Tong, J. lin, Q. Yu, Y. Lin, W. Kuang, Decreased osteogenesis of adult mesenchymal stem cells by reactive oxygen species under cyclic stretch: a possible mechanism of age related osteoporosis, Bone Research 3 (2015) 15003.
[5] S. Khosla, L.C. Hofbauer, Osteoporosis treatment: recent developments and ongoing challenges, The Lancet Diabetes & Endocrinology 5(11) (2017) 898-907.
[6] A. Infante, C.I. Rodriguez, Osteogenesis and aging: lessons from mesenchymal stem cells, Stem Cell Res Ther 9(1) (2018) 244.
[7] G. Lacava, F. Laus, A. Amaroli, A. Marchegiani, R. Censi, P. Di Martino, T. Yanagawa, M.G. Sabbieti, D. Agas, P62 deficiency shifts mesenchymal/stromal stem cell commitment toward adipogenesis and disrupts bone marrow homeostasis in aged mice, J Cell Physiol (2019).
[8] Y. Yang, X. Wang, T.-C. Huang, X. Hu, N. Kawazoe, W.-B. Tsai, Y. Yang, G. Chen, Regulation of mesenchymal stem cell functions by micro–nano hybrid patterned surfaces, Journal of Materials Chemistry B 6(34) (2018) 5424-5434.
[9] M. Bao, J. Xie, W.T.S. Huck, Recent Advances in Engineering the Stem Cell Microniche in 3D, Advanced Science 5(8) (2018) 1800448.
[10] H.A. Fink, R. MacDonald, M.L. Forte, C.E. Rosebush, K.E. Ensrud, J.T. Schousboe, V.A. Nelson, K. Ullman, M. Butler, C.M. Olson, B.C. Taylor, M. Brasure, T.J. Wilt, Long-Term Drug Therapy and Drug Discontinuations and Holidays for Osteoporosis Fracture Prevention: A Systematic Review, Annals of internal medicine (2019).
[11] A. Pispati, V. Pandey, R. Patel, Oral Bisphosphonate Induced Recurrent Osteonecrosis of Jaw with Atypical Femoral Fracture and Subsequent Mandible Fracture in the Same Patient: A Case Report, Journal of orthopaedic case reports 8(3) (2018) 85-88.
[12] N.B. Watts, Long-term risks of bisphosphonate therapy, Arquivos brasileiros de endocrinologia e metabologia 58(5) (2014) 523-9.
[13] B. Antebi, G. Pelled, D. Gazit, Stem cell therapy for osteoporosis, Current osteoporosis reports 12(1) (2014) 41-7.
[14] Y. Li, D. Jin, W. Xie, L. Wen, W. Chen, J. Xu, J. Ding, D. Ren, Z. Xiao, Mesenchymal Stem Cells-Derived Exosomes: A Possible Therapeutic Strategy for Osteoporosis, Current stem cell research & therapy 13(5) (2018) 362-368.
[15] B. Nyambat, C.-H. Chen, P.-C. Wong, C.-W. Chiang, M.K. Satapathy, E.-Y. Chuang, Genipin-crosslinked adipose stem cell derived extracellular matrix-nano graphene oxide composite sponge for skin tissue

engineering, Journal of Materials Chemistry B 6(6) (2018) 979-990.
[16] M. Wang, J.P. Hinton, J.M.C. Gard, J.G.N. Garcia, B.S. Knudsen, R.B. Nagle, A.E. Cress, Integrin α6β4E variant is associated with actin and CD9 structures and modifies the biophysical properties of cell–cell and cell–extracellular matrix interactions, Molecular Biology of the Cell 30(7) (2019) 838-850.
[17] C. Loebel, R.L. Mauck, J.A. Burdick, Local nascent protein deposition and remodelling guide mesenchymal stromal cell mechanosensing and fate in three-dimensional hydrogels, Nature Materials (2019).
[18] C.M. Madl, B.L. LeSavage, R.E. Dewi, K.J. Lampe, S.C. Heilshorn, Matrix Remodeling Enhances the Differentiation Capacity of Neural Progenitor Cells in 3D Hydrogels, Advanced Science 6(4) (2019) 1801716.
[19] E. Ko, S.J. Yu, G.J. Pagan-Diaz, Z. Mahmassani, M.D. Boppart, S.G. Im, R. Bashir, H. Kong, Matrix Topography Regulates Synaptic Transmission at the Neuromuscular Junction, Advanced Science 6(6) (2019) 1801521.
[20] S. Muduli, H.H.-C. Lee, J.-S. Yang, T.-Y. Chen, A. Higuchi, S.S. Kumar, A.A. Alarfaj, M.A. Munusamy, G. Benelli, K. Murugan, C.-Y. Liu, Y.-F. Chen, Y. Chang, B. Moorthy, H.-C. Wang, S.-T. Hsu, Q.-D. Ling, Proliferation and osteogenic differentiation of amniotic fluid-derived stem cells, Journal of Materials Chemistry B 5(27) (2017) 5345-5354.
[21] A. Higuchi, Q.D. Ling, Y.A. Ko, Y. Chang, A. Umezawa, Biomaterials for the feeder-free culture of human embryonic stem cells and induced pluripotent stem cells, Chem Rev 111(5) (2011) 3021-35.
[22] P.E. Bourgine, B.E. Pippenger, A. Todorov, L. Tchang, I. Martin, Tissue decellularization by activation of programmed cell death, Biomaterials 34(26) (2013) 6099-6108.
[23] L. He, J. Zhou, M. Chen, C.-S. Lin, S.G. Kim, Y. Zhou, L. Xiang, M. Xie, H. Bai, H. Yao, C. Shi, P.G. Coelho, T.G. Bromage, B. Hu, N. Tovar, L. Witek, J. Wu, K. Chen, W. Gu, J. Zheng, T.-J. Sheu, J. Zhong, J. Wen, Y. Niu, B. Cheng, Q. Gong, D.M. Owens, M. Stanislauskas, J. Pei, G. Chotkowski, S. Wang, G. Yang, D.J. Zegarelli, X. Shi, M. Finkel, W. Zhang, J. Li, J. Cheng, D.P. Tarnow, X. Zhou, Z. Wang, X. Jiang, A. Romanov, D.W. Rowe, S. Wang, L. Ye, J. Ling, J. Mao, Parenchymal and stromal tissue regeneration of tooth organ by pivotal signals reinstated in decellularized matrix, Nature Materials 18(6) (2019) 627-637.
[24] D. Bejleri, M.E. Davis, Decellularized Extracellular Matrix Materials for Cardiac Repair and Regeneration, Advanced healthcare materials 8(5) (2019) 1801217.
[25] R. Cai, T. Nakamoto, N. Kawazoe, G. Chen, Influence of stepwise chondrogenesis-mimicking 3D extracellular matrix on chondrogenic differentiation of mesenchymal stem cells, Biomaterials 52 (2015) 199-207.
[26] G.S. Hussey, J.L. Dziki, S.F. Badylak, Extracellular matrix-based materials for regenerative medicine, Nature Reviews Materials 3(7) (2018) 159-173.
[27] A. Higuchi, Q.D. Ling, S.T. Hsu, A. Umezawa, Biomimetic cell culture proteins as extracellular matrices for stem cell differentiation, Chem Rev 112(8) (2012) 4507-40.
[28] L. Ching-yi, C. She-Hung, L. Hung-Yi, L. Shih-Tseng, A method to develop an in vitro osteoporosis model of porcine vertebrae: histological and biomechanical study, Journal of Neurosurgery: Spine SPI 14(6) (2011) 789-798.
[29] J. Compston, Management of glucocorticoid-induced osteoporosis, Nature Reviews Rheumatology 6 (2010) 82.
[30] Y. Yang, H. Lin, H. Shen, B. Wang, G. Lei, R.S. Tuan, Mesenchymal stem cell-derived extracellular matrix enhances chondrogenic phenotype of and cartilage formation by encapsulated chondrocytes in vitro and in vivo, Acta biomaterialia 69 (2018) 71-82.
[31] M. Yuan, P.-J. Pai, X. Liu, H. Lam, B.P. Chan, Proteomic Analysis of Nucleus Pulposus Cell-derived Extracellular Matrix Niche and Its Effect on Phenotypic Alteration of Dermal Fibroblasts, Scientific reports 8(1) (2018) 1512.

[32] R. Kaukonen, G. Jacquemet, H. Hamidi, J. Ivaska, Cell-derived matrices for studying cell proliferation and directional migration in a complex 3D microenvironment, Nature Protocols 12 (2017) 2376.
[33] W. Wei, J. Li, S. Chen, M. Chen, Q. Xie, H. Sun, J. Ruan, H. Zhou, X. Bi, A. Zhuang, Z. You, P. Gu, X. Fan, In vitro osteogenic induction of bone marrow mesenchymal stem cells with a decellularized matrix derived from human adipose stem cells and in vivo implantation for bone regeneration, Journal of Materials Chemistry B 5(13) (2017) 2468-2482.
[34] Y. Teng, X. Li, Y. Chen, H. Cai, W. Cao, X. Chen, Y. Sun, J. Liang, Y. Fan, X. Zhang, Extracellular matrix powder from cultured cartilage-like tissue as cell carrier for cartilage repair, Journal of Materials Chemistry B 5(18) (2017) 3283-3292.
[35] R. Cai, T. Nakamoto, T. Hoshiba, N. Kawazoe, G. Chen, Matrices secreted during simultaneous osteogenesis and adipogenesis of mesenchymal stem cells affect stem cells differentiation, Acta biomaterialia 35 (2016) 185-93.
[36] H. Lu, H.H. Oh, N. Kawazoe, K. Yamagishi, G. Chen, PLLA-collagen and PLLA-gelatin hybrid scaffolds with funnel-like porous structure for skin tissue engineering, Science and technology of advanced materials 13(6) (2012) 064210.
[37] X. He, H. Lu, N. Kawazoe, T. Tateishi, G. Chen, A novel cylinder-type poly(L-lactic acid)-collagen hybrid sponge for cartilage tissue engineering, Tissue engineering. Part C, Methods 16(3) (2010) 329-38.
[38] G. Chen, T. Ushida, T. Tateishi, Hybrid Biomaterials for Tissue Engineering: A Preparative Method for PLA or PLGA–Collagen Hybrid Sponges, Advanced Materials 12(6) (2000) 455-457.
[39] H. Lu, N. Kawazoe, T. Kitajima, Y. Myoken, M. Tomita, A. Umezawa, G. Chen, Y. Ito, Spatial immobilization of bone morphogenetic protein-4 in a collagen-PLGA hybrid scaffold for enhanced osteoinductivity, Biomaterials 33(26) (2012) 6140-6.
[40] G. Chen, T. Ushida, T. Tateishi, A hybrid network of synthetic polymer mesh and collagen sponge, Chemical Communications (16) (2000) 1505-1506.
[41] T.N. Rong Cai, Takashi Hoshiba, Naoki Kawazoe and Guoping Chen, Control of Simultaneous Osteogenic and Adipogenic Differentiation of Mesenchymal Stem Cells, Journal of Stem Cell Research & Therapy 4(8) (2014) 223.
[42] N. Kawazoe, C. Inoue, T. Tateishi, G. Chen, A cell leakproof PLGA-collagen hybrid scaffold for cartilage tissue engineering, Biotechnology progress 26(3) (2010) 819-26.
[43] H. Lu, T. Hoshiba, N. Kawazoe, G. Chen, Autologous extracellular matrix scaffolds for tissue engineering, Biomaterials 32(10) (2011) 2489-99.
[44] Y. Chen, K. Lee, Y. Chen, Y. Yang, N. Kawazoe, G. Chen, Preparation of Stepwise Adipogenesis-Mimicking ECM-Deposited PLGA–Collagen Hybrid Meshes and Their Influence on Adipogenic Differentiation of hMSCs, ACS Biomaterials Science & Engineering (2019).
[45] C. Zhang, L. Li, Y. Jiang, C. Wang, B. Geng, Y. Wang, J. Chen, F. Liu, P. Qiu, G. Zhai, P. Chen, R. Quan, J. Wang, Space microgravity drives transdifferentiation of human bone marrow–derived mesenchymal stem cells from osteogenesis to adipogenesis, The FASEB Journal 32(8) (2018) 4444-4458.
[46] K. Zheng, Y. Chen, W. Huang, Y. Lin, D.L. Kaplan, Y. Fan, Chemically Functionalized Silk for Human Bone Marrow-Derived Mesenchymal Stem Cells Proliferation and Differentiation, ACS applied materials & interfaces 8(23) (2016) 14406-14413.
[47] P.E. Bourgine, T. Klein, A.M. Paczulla, T. Shimizu, L. Kunz, K.D. Kokkaliaris, D.L. Coutu, C. Lengerke, R. Skoda, T. Schroeder, I. Martin, In vitro biomimetic engineering of a human hematopoietic niche with functional properties, Proceedings of the National Academy of Sciences 115(25) (2018) E5688-E5695.
[48] G. Chen, N. Kawazoe, Biomimetic Extracellular Matrices and Scaffolds Prepared from Cultured Cells, Advances in experimental medicine and biology 1078 (2018) 465-474.

[49] T. Hoshiba, N. Kawazoe, T. Tateishi, G. Chen, Development of stepwise osteogenesis-mimicking matrices for the regulation of mesenchymal stem cell functions, The Journal of biological chemistry 284(45) (2009) 31164-73.
[50] T. Hoshiba, N. Kawazoe, T. Tateishi, G. Chen, Development of extracellular matrices mimicking stepwise adipogenesis of mesenchymal stem cells, Advanced materials (Deerfield Beach, Fla.) 22(28) (2010) 3042-7.
[51] B.M. Spiegelman, C.A. Ginty, Fibronectin modulation of cell shape and lipogenic gene expression in 3T3-adipocytes, Cell 35(3 Pt 2) (1983) 657-66.
[52] Y. Wang, L. Zhao, C. Smas, H.S. Sul, Pref-1 Interacts with Fibronectin To Inhibit Adipocyte Differentiation, Molecular and Cellular Biology 30(14) (2010) 3480.
[53] R.M. Salasznyk, R.F. Klees, W.A. Williams, A. Boskey, G.E. Plopper, Focal adhesion kinase signaling pathways regulate the osteogenic differentiation of human mesenchymal stem cells, Experimental cell research 313(1) (2007) 22-37.

# Chapter 5

# Conclusions and future perspective

## 5.1 Conclusions

In this thesis, the study introduced a method to prepare 3D ECM scaffolds. A PLGA-collagen hybrid mesh was used as a template, the ECMs secreted by hMSCs that went through stepwise osteogenesis, adipogenesis and osteogenesis-co-adipogenesis were in situ deposited in PLGA-collagen hybrid meshes to mimic the 3D ECM microenvironment. Their influences on stem cell functions were investigated.

In chapter 1, a general introduction is presented to describe how important of understanding the precise roles of ECM on stem cells functions. The commonly used ECM based materials are introduced. As for mimicking stepwise changed ECM microenvironment, cell-derived ECM has showed a huge advantage. The limitations of 2D system and the requirement of preparation of 3D ECM scaffold are discussed. The currently used decellularization methods are compared and the motivation and innovation of this work are explained.

In chapter 2, a preparation of stepwise adipogenesis-mimicking ECMs-deposited PLGA-collagen hybrid meshes was introduced. These biomimatic ECM scaffolds were prepared by culturing hMSCs in PLGA-collagen hybrid mesh and by controlling their adipogenic differentiation degree at stem cell stage, early and late stages. The ECMs were deposited in the PLGA-collagen hybrid mesh during cell culture. After removal of cellular components, the ECM scaffolds were analyzed by immunohistological staining. Their components were dependent on the differentiation stage of hMSCs. They also had different influence on adipogenic differentiation of hMSCs. The ECMs scaffold mimicking the early stage of adipogenesis enhanced the adipogenic differentiation of MSCs, while the ECMs scaffold mimicking the stem cell stage of MSCs or late stage of adipogenesis showed an inhibitory effect.

In chapter 3, we prepared ECM deposited PLGA-collagen hybrid meshes mimicking stepwise osteogenesis by culturing hMSCs in PLGA-collagen hybrid meshes and controlling the degree of their osteogenic differentiation at the stem cell stage and the early stage and late stage of osteogenesis. The stepwise ECM scaffolds exhibited different compositions depending on the stage of osteogenesis, and they also showed different influences on the osteogenic differentiation of the hMSCs. The ECM scaffold mimicking the early stage of osteogenesis promoted the osteogenic differentiation of hMSCs, and the ECM scaffold mimicking the late stage of osteogenesis showed a moderate effect on the promotion of the osteogenic differentiation of hMSCs. However, the ECM scaffold mimicking the stem cell stage of hMSCs exhibited an inhibitory effect.

In chapter 4, four types of biomimetic 3D PLGA-collagen-ECMs hybrid scaffolds were prepared by depositing ECMs from simultaneous osteogenic-co-adipogenic differentiation of hMSCs on PLGA-collagen hybrid mesh. The four types of ECMs scaffolds, EOEA-ECMs, EOLA-ECM, LOEA-ECMs and LOLA-ECMs scaffolds, had different components that were dependent on the simultaneous differentiation stages. They supported the stem cells adhesion and proliferation and showed different influence on adipogenic and osteogenic differentiation of hMSCs. EOEA-ECMs scaffold showed promotive effect on adipogenic differentiation of hMSCs. EOLA-ECM scaffold had suppression effect on both adipogenic and osteogenic differentiation of hMSCs, while promitive effect on hMSCs proliferation. LOEA-ECMs and LOLA-ECMs scaffolds exhibited promotive effect on osteogenic differentiation and a moderate effect on adipogenic differentiation of hMSCs. The 3D PLGA-collagen-ECMs hybrid meshes should provide useful 3D cell culture models for investigation of cell-ECMs interaction.

In conclusions, the 3D PLGA-collagen-ECM hybrid meshes were demonstrated as ECM models to mimic the dynamic ECM variation during adipogenesis, osteogenesis and osteogenesis-co-adipogenesis. Depending on the stage of osteogenesis-co-adipogenesis of hMSCs, the ECM had different compositions. The ECM composition of osteogenesis-co-adipogenesis is not simple mixtures of stepwise osteogenic matrix and adipogenic matrix. EA-ECM scaffold had a promotive effect on adipogenic differentiation of hMSCs. EO-ECM scaffold was favorable for osteogenic differentiation of hMSCs. Four new types of osteogenesis-co-adipogenesis-mimicking ECM scaffolds had different influences on balancing osteogenic and adipogenic differentiation of hMSCs. The EOEA-ECM scaffold showed a promotive effect on the adipogenic differentiation of hMSCs. The EOLA-ECM scaffold suppressed both adipogenic and osteogenic differentiation of hMSCs. LOEA-ECM and LOLA-ECM scaffolds exhibited a promotive effect on osteogenic differentiation. These 3D PLGA-collagen-ECM hybrid meshes provided well controlled ECM models for mimicking the extracellular microenvironment of stem cells during their differentiation process and a novel tool for investigating the cell-ECM interactions.

## 5.2. Future perspective

The work described in this dissertation is focused on preparation of a 3D ECM system that mimic the stepwise differentiation of hMSCs. Mimicking the tissue or organ development process and their ECM microenvironment is still remained challenge. For instance, osteogenesis is a process of development and formation of bony tissue, which involves the differentiation of hMSCs. There are two ways of bone formation, one is intramembranous ossification (IMO) another is endochondral ossification (ECO). Among them, mimicking the developmental course of IMO is a widely used approach for bone tissue regeneration. In this case, hMSCs are directly guided to osteoblasts. One of the main obstacles for direct osteogenesis is the provision of a sufficient supply of nutrients and oxygen for the survival of the stem cells during directly osteogenic differentiation. However, when the cells were cultured on the large 3D scaffolds, limited diffusion of nutrients and oxygen can cause the problems in cell survival, proliferation and differentiation. ECO is another mechanism during bone development, which involves the formation of a hypertrophic cartilage template where the hMSCs undergoes a cartilaginous hypertrophy, and subsequent formation of bone tissue. Cartilage based constructs can withstand lower oxygen concentrations than bone-mimicking scaffolds containing osteoblasts, and this advantage of cartilage ensured the culture of large grafts, and the better survival of cells after in vivo implantation. Cartilage contains the required extracellular

matrices (ECMs), and subsequently initiates a semi-autonomous ECO as it occurs during bone development. Hence, it is a potential but as of yet not largely explored pathway for bone repair.

In vitro mimicking the development process of ECO can advance their application as an alternative approach for bone regeneration. It has demonstrated that ECM components can affect stem cells fate. While, it is still unclear that the different influences of ECM from the cells during ECO or IMO on stem cells functions. Mimicking the dynamic microenvironment of ECM should be helpful for understanding the ECM roles.

# List of publications

1. **Yazhou Chen,** K. Lee, Y. Chen, Y. Yang, N. Kawazoe, G. Chen. Preparation of stepwise adipogenesis-mimicking ECMs-deposited PLGA-collagen hybrid meshes and their influence on adipogenic differentiation of hMSCs. ACS Biomaterials Science & Engineering 2019,5,11,6099-6108.

2. **Yazhou Chen,** Lee, K.; Yang, Y.; Kawazoe, N.; Chen, G. PLGA-collagen-ECM hybrid scaffolds functionalized with biomimetic extracellular matrices secreted by mesenchymal stem cells during stepwise osteogenesis-co-adipogenesis. Journal of Materials Chemistry B 2019, 7, 7195-7206.

3. **Yazhou Chen,** Lee, K.; Yang, Y.; Kawazoe, N.; Chen, G. PLGA-collagen-ECM hybrid meshes mimicking stepwise osteogenesis and their influence on the osteogenic differentiation of hMSCs. (Biofabrication) (Accept). doi.org/10.1088/1758-5090/ab782b.

4. Lee, K.; **Yazhou Chen,** Yang, Y.; Kawazoe, N.; Chen, G. Solution viscosity regulates chondrocyte proliferation and phenotype during 3D culture. Journal of Materials Chemistry B 2019, doi: 10.1039/c9tb02204j.

5. X. Wang.; J, Zhang.; J. Li.; Y. Chen.; **Yazhou Chen**, Y.; Kawazoe, N.; Chen, G. Bifunctional scaffolds for the photothermal therapy of breast tumor cells and adipose tissue regeneration.

# Acknowledgements

This thesis would never have materialized if I have not received the help from my supervisor, teachers and all the member from our group.

First and foremost, I wish to express my sincere gratitude to my supervisor Prof. Guoping Chen for his invaluable instruction, incessant inspiration and constant encouragement. He provided me with abundant suggestions and priceless criticisms, which have let me know how to be a real scientific researcher. His energy and passion for knowledge and education have had such a great influence on me that I am sure they always remain a beacon in my future career. I always made some mistakes about my research and some problems that I cannot solve, Prof. Chen always gave me very good advices for my research. Prof. Chen also revise my publications and dissertation very carefully. It is my great honor to study in Prof. Chen's lab for the three years.

Special thanks should be given to Prof. Yingnan Yang. I was an exchange student in Prof. Yang's group in Aug. 2014. Prof. Yang not only provide me a wide range of opportunities for practicing experiment skills and becoming independent thinking, but also as a guider who educate, guide and encourage me to be more self-confidence in academic research. Prof. Yang also introduced me to study in NIMS. Because of this opportunity, I got a chance to continue my Ph.D. in NIMS. Without Prof. Yang's help, I cannot get a chance to become a Ph.D. candidate.

Special thanks also should be given to Dr. Naoki Kawazoe and Dr. Toru Yoshitomi for their patient help and warm encouragement in my research. I can remember many details about the discussion with Kawazoe sensei, his wide scope of knowledge and rigorous attitude about science impressed me a lot. I am so lucky to get the chance to know and work with Kawazoe sensei. Dr. Toru Yoshitomi gave me a lot of very good advices about how to be a good presenter when I introduced my research. Yoshitomi have a full of ideas and opinions that nourishes my soul.

I really appreciate the valuable suggestion and assistance from Dr. Rong Cai, Dr. Xiaomeng Li, Dr. Ying Chen, Dr. Yingjun Yang and Dr. Xiuhui Wang. They gave me a lot of advices and shared their truthful and illuminating views on my research. Moreover, I would like to give my thanks to all my colleagues in Tissue Regeneration Materials Unit who have provided me great help and support, including Mr. Kyubae Lee, Mr. Yongtao Wang, Ms. Yan Xie, Ms. Linawati, Mr. Jing Zhang and Mr. Jianhua Chen.

I would like to express my warm thanks to Mrs. Akiyama Haruyo and Mrs. Akiko Ito. They help me a lot for the matters and procedures involved in the University of Tsukuba and NIMS. Their great efforts made my life in Japan much easier and enjoyable.

I also would like to give my sincere thanks to the rest of my dissertation committee, Prof. Mitsuhiro Ebara, Prof. Tetsushi Taguchi and Prof. Tsujimura Seiya, thank you very much for all of your comments and suggestion.

This work was carried out at Tissue Regeneration Materials Unit, National Institute for Materials Science and Graduate School of Pure and Applied Science of University of Tsukuba. I appreciate the financial support

from NIMS (Junior Research Assistantship) during 3-year research in NIMS.